

Regulation of Planar Cell Polarity by *Protein tyrosine kinase 7* in the mammalian  
Auditory Sensory Epithelium.

Jianyi Lee  
Kuala Lumpur, Malaysia

B.S., University of Virginia, 2008

A Dissertation presented to the Graduate Faculty  
of the University of Virginia in Candidacy for the Degree of  
Doctor of Philosophy

Department of Cell Biology

University of Virginia  
December 2013

## **Abstract**

Planar cell polarity (PCP) is a common feature of all tissues, and refers to the coordinated orientation of cells and/or cellular structures in an axis parallel to the plane of a tissue. Diverse morphogenetic and physiological processes depend on the proper establishment of PCP. In vertebrates, the genetic factors that regulate PCP include the conserved core PCP pathway genes and ciliary genes. In addition, the elucidation of a number of distinct PCP components suggests that vertebrates have adapted additional mechanisms to control PCP in diverse cellular processes. Our lab has previously identified *Protein tyrosine kinase 7 (Ptk7)*, encoding an atypical receptor tyrosine kinase, as a novel vertebrate-specific regulator of PCP [1]. The underlying mechanisms by which *Ptk7* regulates PCP are poorly understood. The clear morphological manifestations of PCP in the mouse auditory sensory epithelium or organ of Corti (OC) make it a powerful model system to study PCP signaling in mammals. In the OC, PCP is defined by the V-shaped structure of the stereociliary bundle that sits atop each sensory hair cell and by the uniform orientation of stereociliary bundles across the epithelium. The precise establishment of these features is critical for the proper hearing functions of the cochlea. The goal of this dissertation was to dissect the cellular and molecular mechanisms by which *Ptk7* regulates PCP in the OC. We have discovered that *Ptk7* functions in parallel with the noncanonical Wnt/PCP pathway to regulate actomyosin contractility and orient hair cell PCP. For the first time, we demonstrate an active role for nonsensory supporting cells in hair cell PCP where an apical contractile myosin II

network assembles and is proposed to exert polarized contractile tension on hair cells. We also determined a pathway for actomyosin regulation in the OC where Ptk7 promotes planar polarized Src signaling at cell-cell contacts to spatially regulate actomyosin contractility. These studies have led us to propose a new model for PCP regulation in the OC where Ptk7 mediates anisotropic myosin II based contractile tension between hair cell and supporting cell contacts to orient hair cell PCP. Together, my work provides novel mechanistic insights into hair cell PCP regulation.

## **Acknowledgements**

Completing this dissertation marks a major milestone in my career. I would not have accomplished this feat without the help and support of many intelligent and inspiring individuals. You have all made an indelible mark on me and I am forever indebted to you.

First and foremost, I would like to express my sincerest gratitude to my PhD mentor, Dr. Xiaowei Lu, whose expertise, immeasurable guidance and unyielding patience has carried me far in my graduate career. Her enthusiasm for science and optimism embodies admirable qualities of a leader and teacher that I draw inspiration from whenever I am met with a challenge. Furthermore, her contributions with time, ideas and funding have made my Ph.D. experience a highly productive and stimulating one. For that, it truly has been a great honor to be your student and I thank you for giving me this rare opportunity to develop my scientific independence under your wing.

I would also like to thank my committee members, Drs. Jeffrey Corwin, Douglas DeSimone, Barry Gumbiner and Ian Macara for their support, insightful discussions and advice throughout my years in graduate school. It has served me well and I owe them my heartfelt appreciation.

I extend my appreciation for my former and current colleagues at the Lu lab who have fostered an excellent environment to develop my passion in science. I especially thank Drs. Anna Andreeva, Conor Sipe, and Cynthia Grimsley-Myers, I could not have asked for a better team of people to work with. I would also like to acknowledge the Yu and Dwyer labs for giving me the

opportunity share my work with you and for the valuable feedback I have received at our joint lab meetings. I also thank all members of the Department of Cell Biology, especially Mary Hall and Dr. David Castle, for considering me to be a part of the graduate program.

I must not forget the mentors who have been instrumental in sparking my interest in the sciences from the beginning when I arrived at the University of Virginia as an undergraduate. Thank you Dean Sandra Seidel, Dr. Lynn Hedrick and Dr. Claire Cronmiller for serving as great women role models for me. I also thank Dr. Dan Engel for the opportunity to do research in his lab.

To all friends whom I have known during my time at UVa, your continued friendship and emotional support have further enriched my experiences and you have given me so many good memories to cherish. I especially thank Cammy and Erwen Tang, LaToya Roker, Kazusa Edamura, Yong Han Yeong, Michelle Ko and Eugene Lin.

Finally, the basis for the success of reaching this milestone comes from the unconditional love and support that I have received from my parents, Loy Lee and Soon Chun Boey. Pa and Mum, thank you for your hard work and all the sacrifices you have made to make it possible for me to pursue my education in the US. Your faith and confidence in me are constant reminders of why I am here and that I can accomplish anything I set my mind on. I am also grateful for my siblings, Suyin Lee and Ken Thye Lee and cousin Priscilla Lee for their care and support. To my best friend and my partner in life, Sheung Yin Kevin Mo, thank you for your love and always putting my interests above yours, I can't imagine

going through this without you. I can always count on you to keep me grounded and motivated to see my dreams come to fruition. Your presence in my life has brought me much peace and joy, and I look forward to our lives finally converging.

Everyone, I am extremely delighted to celebrate this success with you and I am eternally grateful for your help and support. We did it! From the bottom of my heart, thank you.

## **Table of Contents**

<b>Abstract</b> .....	<b>i</b>
<b>Acknowledgements</b> .....	<b>iii</b>
<b>Table of Contents</b> .....	<b>vi</b>
<b>List of Figures</b> .....	<b>xi</b>
<b>List of Tables</b> .....	<b>xiii</b>
<b>Abbreviations</b> .....	<b>xiv</b>

## **Chapter 1: Background**

### **Section 1.1 Planar Cell Polarity (PCP)**

1.1.1 Basic principles of PCP establishment.....	3
1.1.2 The core PCP system .....	4
1.1.3 Fat/Dachsous System .....	6
1.1.4 PCP pathways independent of core PCP or Ft/Ds systems.....	8
1.1.5 PCP signaling in vertebrates.....	9
1.1.6 Downstream effectors of PCP signaling.....	12
1.1.7 Vertebrate specific regulators .....	14

### **Section 1.2 Development of the mammalian Cochlea**

1.2.1 The organ of Corti (OC) .....	16
1.2.2 Specification and Differentiation of the OC .....	19
1.2.3 Morphogenesis of the Cochlea I: Cochlear Duct Extension .....	21
1.2.4 Morphogenesis of the Cochlea: Stereociliary bundle development...	24
1.2.5 Hair cell PCP in the OC.....	25
1.2.6 Noncanonical Wnt/core PCP signaling in the OC .....	29

### **Section 1.3 Protein Tyrosine Kinase 7 (*Ptk7*)**

1.3.1 Overview .....	31
1.3.2 Expression and Structure of PTK7.....	31
1.3.3 Functional aspects of PTK7 .....	34

## **Section 1.4 Mechanical Forces and Tissue Morphogenesis**

1.4.1 Overview .....	37
1.4.2 Generation of Cortical Forces .....	39
1.4.3 Mechanotransduction and Force Transmission .....	41
1.4.4 Role of forces in tissue morphogenesis .....	42
<b>Section 1.5 Scope of Dissertation .....</b>	<b>44</b>

## **CHAPTER 2: PTK7 Regulates Myosin II Activity to Orient Planar Polarity in the Mammalian Auditory Epithelium**

<b>2.1 Introduction.....</b>	<b>48</b>
<b>2.2 Results.....</b>	<b>50</b>
2.2.1 <i>Ptk7</i> Is Not Required for Asymmetric Membrane Localization of Dishevelled-2 in the OC .....	50
2.2.2 PTK7 and Fz3/6 Receptors Act in Parallel and Have Opposing Effects on Hair Cell PCP .....	51
2.2.3 <i>Ptk7</i> Is Required in Supporting Cells to Regulate Hair Cell PCP .....	52
2.2.4 JNK Signaling Is Unlikely to Mediate PTK7 Function in the OC .....	53
2.2.5 <i>Ptk7</i> and the Noncanonical Wnt Pathway Differentially Regulate a Contractile Apical Myosin II Network in Supporting Cells.....	55
2.2.6 <i>Ptk7</i> Regulates Myosin II Activity to Orient Hair Cell PCP .....	57
2.2.7 <i>Ptk7</i> Promotes Planar Asymmetry of Junctional Vinculin.....	58
2.2.8 Planar Asymmetry of Junctional Vinculin Is Restored in <i>Fz3<sup>-/-</sup>; Ptk7<sup>-/-</sup></i> Mutants .....	60
2.2.9 Vangl2 and <i>Ptk7</i> differentially regulate Planar Asymmetry of Vinculin (unpublished) .....	60
2.2.10 Inefficient deletion of <i>Ptk7</i> in hair cells in <i>Math1<sup>Cre</sup>; Ptk7<sup>CO</sup></i> cochlea (unpublished) .....	61
<b>2.3 Discussion.....</b>	<b>62</b>
<b>2.4 Figures.....</b>	<b>67</b>

## CHAPTER 3: PTK7-Src signaling at epithelial cell contacts mediates spatial organization of actomyosin and planar cell polarity

<b>3.1 Introduction</b> .....	<b>90</b>
<b>3.2 Results</b> .....	<b>93</b>
3.2.1 PTK7 positively regulates Src signaling and ROCK2 phosphorylation in the mouse auditory sensory epithelium .....	93
3.2.2 Src inhibition and hyperactivation both result in PCP defects in the OC.....	94
3.2.3 Src signaling mediates ROCK2 phosphorylation at intercellular junctions in the OC.....	96
3.2.4 Identification of vinculin and cortactin as potential targets of PTK7-Src signaling in the organ of Corti (unpublished).....	97
3.2.5 Vinculin is required for hair cell PCP and regulates apical myosin IIB foci assembly in the OC (unpublished).....	98
<b>3.3 Discussion</b> .....	<b>99</b>
<b>3.4 Figures</b> .....	<b>104</b>

### APPENDIX I: The Role of EphrinB ligands in Cochlear Morphogenesis

<b>I.1 Introduction</b> .....	<b>118</b>
<b>I.2 Results</b> .....	<b>120</b>
I.2.1 Expression of EphrinB1 and EphrinB2 in the developing OC .....	120
I.2.2 EphrinB1 is not required for hair cell PCP.....	122
I.2.3 Genetic Interaction between <i>EphrinB1</i> and <i>Fz3/Fz6</i> in the OC.....	123
<b>I.3 Discussion</b> .....	<b>124</b>
<b>I.4 Figures</b> .....	<b>127</b>

### APPENDIX II: Dynamics of the myosin II network in the developing OC

<b>II.1 Introduction</b> .....	<b>133</b>
<b>II.2 Results</b> .....	<b>134</b>
II.2.1 Live imaging set up.....	134

II.2.2	Myosin II is recruited to medial borders of hair cells .....	135
II.2.3	Dynamics of the myosin II network is disrupted in <i>Ptk7</i> <sup>-/-</sup> OC .....	136
<b>II.3</b>	<b>Discussion .....</b>	<b>136</b>
<b>II.4</b>	<b>Figures.....</b>	<b>139</b>

### **APPENDIX III: Crosstalk between *Ptk7*-mediated pathway and hair cell intrinsic polarity pathways**

<b>III.1</b>	<b>Introduction .....</b>	<b>144</b>
<b>III.2</b>	<b>Results .....</b>	<b>145</b>
III.2.1	<i>Ptk7</i> regulates cortical localization of Par-3 in the OC .....	145
III.2.2	GEFs and GAPs for Rac.....	147
III.2.3	Gpsm2 localization is misoriented <i>Ptk7</i> <sup>-/-</sup> OC.....	149
<b>III.3</b>	<b>Discussion .....</b>	<b>149</b>
<b>III.4</b>	<b>Figures .....</b>	<b>152</b>

### **CHAPTER 4: Summary and Future Work**

<b>4.1</b>	<b>Summary .....</b>	<b>157</b>
<b>4.2</b>	<b>Future Directions .....</b>	<b>161</b>
4.2.1	Does polarized tension regulate basal body positioning in the OC? .....	161
4.2.2	Does polarized contractile tension mediated by PTK7-Src signaling pathway spatially regulate cortical Rac-PAK activity? .....	162
4.2.3	How does PTK7-Src signaling regulate actomyosin contractility?... ..	163
4.2.4	Does proteolytic cleavage of PTK7 regulate planar polarized Src signaling in the OC?.....	164
4.2.5	How does the noncanonical Wnt/PCP pathway regulate actomyosin contractility in the OC? .....	166

**CHAPTER 5: Materials and Methods**

<b>5.1 Mice and Genotyping .....</b>	<b>169</b>
<b>5.2 Generation of a floxed <i>Ptk7</i> allele .....</b>	<b>169</b>
<b>5.3 <i>Ptk7</i> genotyping in mosaic analysis .....</b>	<b>170</b>
<b>5.4 Immunohistochemistry .....</b>	<b>170</b>
<b>5.5 Cell culture and Western Blotting .....</b>	<b>171</b>
<b>5.6 Organotypic cochlear explant cultures .....</b>	<b>172</b>
<b>5.7 Image acquisition .....</b>	<b>173</b>
<b>5.8 Analysis of stereociliary bundle orientation/kinocilium position ...</b>	<b>173</b>
<b>5.9 Quantification of pY416-Src and pY722-ROCK2 localization.....</b>	<b>174</b>
<b>5.10 Live imaging of MIIB-GFP.....</b>	<b>175</b>

**CHAPTER 6: Bibliography**

## **List of Figures**

Figure 1	PCP signaling systems	8
Figure 2	Organization of the organ of Corti	18
Figure 3	Cochlear duct outgrowth	23
Figure 4	<i>Ptk7</i> Regulates Fz3 Localization but Is Not Required for Asymmetric Localization of Dvl2 in the OC	67
Figure 5	Localization of Dvl2 in <i>Fz3<sup>-/-</sup></i> ; <i>Fz6<sup>-/-</sup></i> cochleae	69
Figure 6	Epistasis Analysis of <i>Ptk7</i> and <i>Fz3/Fz6</i> in Hair Cell PCP	70
Figure 7	Quantification of stereociliary bundle orientation for OHC1 and OHC2	72
Figure 8	Mosaic Analysis of <i>Ptk7</i> in Hair Cell PCP	73
Figure 9	Conditional inactivation of <i>Ptk7</i> using the Cre-loxP technology	75
Figure 10	JNK Signaling Is Unlikely to Mediate PTK7 Function in the OC	77
Figure 11	<i>Ptk7</i> and the Noncanonical Wnt Pathway Differentially Regulate a Contractile Myosin IIB Network in Supporting Cells	79
Figure 12	<i>Ptk7</i> Regulates Myosin II Activity to Orient Hair Cell PCP	81
Figure 13	Planar Asymmetry of Junctional Vinculin Is Abolished in <i>Ptk7<sup>-/-</sup></i> OC and Restored in <i>Fz3<sup>-/-</sup></i> ; <i>Ptk7<sup>-/-</sup></i> OC	83
Figure 14	E-cadherin and $\beta$ -catenin localization in <i>Ptk7<sup>-/-</sup></i> cochleae and myosin IIB and vinculin localization in <i>Fz3<sup>-/-</sup></i> ; <i>Ptk7<sup>-/-</sup></i> cochleae.	85
Figure 15	Vinculin planar asymmetry is differentially regulated by <i>Ptk7</i> and the non-canonical Wnt/PCP pathway	87

Figure 16	Analysis of <i>Math1<sup>Cre</sup>; Ptk7<sup>CO/-</sup></i> cochleae	88
Figure 17	PTK7 regulates planar polarized Src signaling and ROCK2 phosphorylation at intercellular junctions in the mouse OC	104
Figure 18	ROCK2 is still localized to intercellular junctions in <i>Ptk7<sup>-/-</sup></i> cochleae	106
Figure 19	Src inhibition and hyperactivation both result in PCP defects in the OC	107
Figure 20	Localization of core PCP proteins Dvl2 and Fz3 in Src-inhibited and <i>Csk<sup>CKO</sup></i> cochleae	109
Figure 21	Src inhibition and hyperactivation have opposing effects on pY416-Src and pY722-ROCK2 localization in the OC	111
Figure 22	Cortactin localization in the OC	113
Figure 23	<i>Ptk7</i> promotes phosphorylation of junctional vinculin in the OC.	114
Figure 24	Vinculin is required for hair cell PCP.	115
Figure 25	Vinculin regulates the assembly of apical myosin II foci in supporting cells	117
Figure 26	EphrinB1 forms a complex with Fz3 <i>in vitro</i> .	127
Figure 27	EphrinB1 expression in the developing OC	128
Figure 28	EphrinB2 expression in the cochlea	130
Figure 29	EphrinB1 is not required for hair cell PCP	131
Figure 30	Genetic interaction between <i>EphrinB1</i> and <i>Fz3/Fz6</i>	132
Figure 31	Comparison of Myosin IIB-GFP expression in live cochlear explants with Myosin IIB immunostaining in fixed cochlear tissues.	139

Figure 32	Myosin II is recruited to medial borders of hair cells in control OC	140
Figure 33	Dynamics of the myosin II network is disrupted in <i>Ptk7</i> <sup>-/-</sup> OC	142
Figure 34	Asymmetric localization of Par-3 is regulated by <i>Ptk7</i>	152
Figure 35	FilGAP localization in the OC	153
Figure 36	srGAP2 localization in the OC	154
Figure 37	Gpsm2 asymmetric localization is regulated by <i>Ptk7</i>	155
Figure 38	Model proposed for hair cell PCP regulation by <i>Ptk7</i>	160

### **List of Tables**

Table 1	Primers used for PCR genotyping	176
Table 2	Primary antibodies used for immunostaining	177

## **Abbreviations**

A-P	Anterior-Posterior
ADAM	A Disintegrin And Metalloproteinase
AJ	Adherens Junctions
Arp2/3	Actin-related protein 2/3
ATP	Adenosine Triphosphate
BMP	Bone morphogenetic protein
BSA	Bovine Serum Albumin
CE	Convergent extension
Csk	C-terminal Src Kinase
D-V	Dorsoventral
DC	Deiter cells
DMEM	Dulbecco's modified Eagle's medium
DMF	Dimethylformamide
DMSO	Dimethyl
DN	Dominant negative
Dsh/Dvl	Dishevelled
DTT	Dithiothreitol
EDTA	Ethylenediaminetetraacetic acid
Efnb1/2	EphrinB1/B2
Eph	Ephrin Receptor
ES Cells	Embryonic Stem Cells
FBS	Fetal Bovine Serum
Fj	Four-jointed
FL	Floxed allele
FRT	FLP recognition target
Ft/Ds	Fat/Dachsous
Fz	Frizzled receptor
GAP	GTPase activated protein
GAPDH	Glyceraldehyde 3-phosphate dehydrogenase
GBE	Germband extension
GEF	Guanine nucleotide exchange factor
HBSS	Hanks' Balanced Salt Solution
HEPES	4-(2-hydroxyethyl)-1-piperazineethanesulfonic acid
HRP	Horseradish Peroxidase
Ig	Immunoglobulin
IHC	Inner Hair Cells
IPC	Inner Pillar Cells
IPhC	Inner Phallangeal Cells
JNK	c-Jun N-terminal Kinase

MIIB	Myosin II Heavy Chain B
MIIB-GFP	Myosin IIB-Green Fluorescent Protein
ML	Mediolateral
MLC	Myosin light chain
MMP	Matrix Metalloproteinases
NaN <sub>3</sub>	Sodium Azide
NaOH	Sodium Hydroxide
NMII	Non-muscle myosin II
NTD	Neural Tube Defect
OC	Organ of Corti
OHC	Outer Hair Cell
OPC	Outer Pillar Cells
PAK	p21-Activated Kinase
PBST	Phosphate Buffered Saline with Tween-20
PC	Pillar Cell
PCP	Planar Cell Polarity
PCR	Polymerase Chain Reaction
PFA	Paraformaldehyde
pPAK	phosphorylated PAK
PTK7	Protein Tyrosine Kinase 7
RLC	Regulatory light chain
ROCK	Rho Kinase
ROI	Region of Interest
RTK	Receptor Tyrosine Kinase
SC	Supporting Cell
SFK	Src Family Kinases
Src	Src
TCA	Trichloroacetic acid
Tris-HCl	Trisaminomethane hydrochloride
Vangl2	Van Gogh-Like 2
Vcl	Vinculin
WB	Western Blot
Wg	Wingless
WT	Wild-type
ADAM	A Disintegrin And Metalloproteinase
ATP	Adenosine Triphosphate
CE	Convergent extension
CSK	C-terminal Src Kinase
DMSO	Dimethyl
DN	Dominant negative
Dsh/Dvl	Dishevelled
D-V	Dorsoventral
Efnb1/2	EphrinB1/B2

Eph	Ephrin Receptor
FBS	Fetal Bovine Serum
FL	Floxed allele
Fz	Frizzled receptor
GAP	GTPase activated protein
GAPDH	Glyceraldehyde 3-phosphate dehydrogenase
GEF	Guanine exchange factor
HBSS	Hanks' Balanced Salt Solution
HEPES	4-(2-hydroxyethyl)-1-piperazineethanesulfonic acid
Ig	Immunoglobulin
IHC	Inner Hair Cells
JNK	c-Jun N-terminal Kinase
MIIB	Myosin II Heavy Chain B
MIIB-GFP	Myosin IIB-Green Fluorescent Protein
ML	Mediolateral
MLC	Myosin light chain
MMP	Matrix Metalloproteinases
NaN <sub>3</sub>	Sodium Azide
NMII	Non-muscle myosin II
NTD	Neural Tube Defect
OC	Organ of Corti
OHC	Outer Hair Cell
PAK	p21-Activated Kinase
PC	Pillar Cell
PCP	Planar Cell Polarity
PFA	Paraformaldehyde
PTK7	Protein Tyrosine Kinase 7
RLC	Regulatory light chain
ROCK	Rho Kinase
RTK	Receptor Tyrosine Kinase
SC	Supporting Cell
SFK	Src Family Kinases
Src	cellular Src
TCA	Trichloroacetic acid
Vangl2	Van Gogh-Like Protein 2
Vcl	Vinculin
WB	Western Blot
WT	Wild-type

## Chapter 1: Background

Planar cell polarity (PCP) is a common feature of tissues and refers to the coordination of cells and/or cellular structures across the plane of a two-dimensional cell sheet. It was first discovered in *Drosophila*, where PCP is manifested by the uniform alignment of sensory bristles and cellular hairs (trichomes) in the wing and abdomen, and by the orientation of ommatidia in the compound eye. In vertebrates, the organization of scales in fish, alignment of hair follicles in skin and stereociliary bundles of the inner ear epithelium in mammals represent clear examples of PCP [2–4]. Although most evident in epithelial tissues, PCP has also been observed in mesenchymal tissues undergoing collective and directional cell migration [5].

Diverse morphogenetic and physiological processes across the animal kingdom are dependent on the proper establishment of PCP. PCP defects are associated with developmental abnormalities such as deafness, polycystic kidney disease, neural tube defects and congenital heart disease [6]. Over the past 30 years, extensive efforts have been made towards elucidating the genetic factors that regulate PCP. A “core” cassette of PCP genes were originally identified in *Drosophila* and subsequently shown to share conserved functions for PCP in vertebrates. Interestingly, a number of distinct components operate exclusively in vertebrate PCP processes. Our lab has previously identified *Protein tyrosine kinase 7 (Ptk7)* as a novel regulator of PCP in vertebrate development [1]. *Ptk7* mouse mutants display characteristic PCP defects such as craniorachischisis (open neural tube) and stereociliary bundle misorientation in the inner ear.

However, the mechanisms by which *Ptk7* regulates PCP in mammals remain poorly understood.

The cochlea exhibits one of the most distinctive forms of PCP in mammals and is defined by two main features: the asymmetric V-shaped stereociliary bundle at the apical surfaces of each sensory hair cell and the uniform orientation of these bundles across the sensory epithelium of the cochlea. These features are established during embryonic development and are critical for the normal perception of sound as stereociliary bundles are directionally sensitive to mechanical stimuli. These striking morphological manifestations of PCP make the cochlea a powerful model system to dissect the cellular and molecular underpinnings of PCP signaling in vertebrates. Therefore, we have taken advantage of this model system to gain mechanistic insights to *Ptk7*-mediated establishment of PCP in the cochlea.

## **Section 1.1 Planar Cell Polarity (PCP)**

### **1.1.1 Basic principles of PCP establishment**

For tissues to display PCP, individual cells have to adopt intrinsic polarity and the orientation of intrinsic polarity has to be coordinated with respect to neighboring cells across the tissue. Achieving these two levels of organization requires (1) global directional information to coordinate PCP across the tissue, (2) cellular factors which integrate both local and global signals to establish the primary PCP axis and (3) tissue-specific effector modules that impinge on

cytoskeletal regulation to polarize individual cells in coordination with neighboring cells (reviewed in [7–10]).

The molecular framework for understanding PCP establishment has been provided by rigorous genetic studies in *Drosophila*, and is best characterized in the wing epithelium [11]. Presently, two signaling systems are known to regulate PCP: the core PCP system and the Fat/Dachsous (Ft/Ds) system. The underlying principle of both these systems is cell-cell communication. Components of these modules display subcellular asymmetries in their distributions and/or activities via heterophilic cell-surface protein interactions. Interestingly, a number of manifestations of PCP have been identified in *Drosophila* and are not regulated by either of these systems, suggesting that additional PCP signaling systems exist.

### **1.1.2 The core PCP system**

Based on defects in the uniform orientation of hairs on the wing, a “core” network of genes were found to be required for PCP [11]. The core PCP signaling module consists of six components: transmembrane proteins such as seven-membrane domain Frizzled receptors (Fz), tetraspanin Van Gogh/Strabismus (Vang/Stbm), atypical cadherin Starry Night/Flamingo (Stan/Fmi), and cytoplasmic adaptor proteins Dishevelled (Dsh/Dvl), Diego (Dgo) and Prickle (Pk) (Figure 1).

A hallmark feature of the core PCP proteins is that they asymmetrically localize at the adherens junctions prior to morphological polarization events.

These proteins normally segregate into two groups to demarcate complementary proximal (Vang and Pk) and distal (Fz, Dsh and Dgo) domains in each cell. Furthermore, disrupting any one of the core PCP gene function affects the asymmetric localization of all core PCP proteins. It is thought that the asymmetric localization of core PCP components arise from intracellular feedback interactions between proximal and distal PCP proteins while the local propagation of this asymmetry to neighboring cells requires the assembly of asymmetric intercellular complexes. Stan forms homodimers and facilitates intercellular interactions between Fz and Vang to set up the initial polarity bias of Fz activity. Subsequently, intracellular interactions between Dsh, Pk and Dgo enhance and propagate the directionality of Fz-Vang binding, hence creating a self-organizing feedback loop to stabilize a Fz-PCP signaling axis. A proposed mechanism for polarized distribution of the core PCP components implicates directional microtubule-transport of Fz, Dsh and Fmi [12, 13].

In the wing, core PCP mutations do not cause randomization of hair orientation. They exhibit a phenomenon known as 'domineering non-autonomy', where the polarity of wild-type cells adjacent to mutant clones is strongly perturbed such that their wing hairs either orient toward or away from the mutant clone [14]. For instance, clones of cells lacking Fz induces surrounding wing hairs to point toward the *fz* mutant clone [15]. In contrast, *Stbm* mutant clones directs wild-type hairs to orient away from it [16]. These directional non-autonomous effects on hair polarity support the instructive role of the core PCP

pathway in PCP establishment. Moreover, it has been shown that this phenomenon is conserved in all *Drosophila* tissues.

It still remains unclear how asymmetric core PCP protein localization aligns with the axes of the wing. The concept of a morphogen gradient has been proposed to encode long-range directional information for the core PCP system. One of the proposed candidates for a morphogen is the *Wnt* family of glycoproteins, which serve as ligands for Fz receptors. Until recently, *Drosophila* Wnts were thought to function as permissive rather than instructive cues for Fz as both over-expression and loss of function of multiple Wnts did not produce PCP phenotypes [17–19]. Newly reported evidence has demonstrated that Wingless (Wg) and dWnt4 function redundantly to support instructive roles in PCP in the *Drosophila* wing [20]. An alternative model posits that the Fat/Dachsous system provides global polarity signals to the core PCP pathway, but recent genetic evidence is not consistent with this model (See Section 1.1.3).

### 1.1.3 Fat/Dachsous System

In addition to the noncanonical Wnt/PCP pathway, a second signaling system regulates PCP and involves the protocadherins Fat (Ft) and Dachsous (Ds) (Figure 1) (reviewed in [21–24]). The Ft/Ds system is also known as the global module. Ft and Ds preferentially form intercellular bridges between adjacent cells and Ds binding negatively regulates Ft activity. The strength of the Ft/Ds interaction is further modulated by Four-jointed (Fj), a Golgi kinase that phosphorylates the extracellular cadherin domains of both Ft and Ds. Similar to

the core PCP components, loss of Ft or Ds leads to non-autonomous PCP defects [25–28].

Unlike the core PCP pathway, these components do not exhibit obvious asymmetric subcellular localizations. Instead, Fj and Ds are expressed in opposing gradients in the wing and eye, resulting in a gradient of Ft/Ds binding and activity [26, 29, 30]. The alignment of the Ft/Ds pathway to the body axes is regulated by upstream morphogens such as Wingless (Wg), Decapentaplegic (Dpp) and Hedgehog (Hh) that control the transcription of *ds* and *fj* and create opposite gradients of Ft/Ds binding interactions.

The relationship between the Ft/Ds and the core PCP signaling modules is not clear. The observed gradient of Ft/Ds in polarized tissues was initially proposed to set up global polarity signals for the core PCP system and hence was placed upstream of the core PCP pathway. However, those views were challenged by evidence from genetic mosaic studies. Casal *et al.* demonstrated that in the *Drosophila* abdomen, directional non-autonomous effects of wild type cells by Ft or Ds mutant clones occur even in the absence of Fz [18]. Furthermore, planar polarity defects in Ds mutant flies are exacerbated by the loss of Fmi activity [18]. In the wing, reversing Ds and Fj expression gradients reverses hair polarity while abolishing these gradients appears to have no effect on wing hair polarity [26, 30, 31]. This observation suggests that Ds and Fj are not essential components that provide spatial information in the wing. Together, these studies suggest that these two systems function in parallel and reinforce PCP using independent inputs.

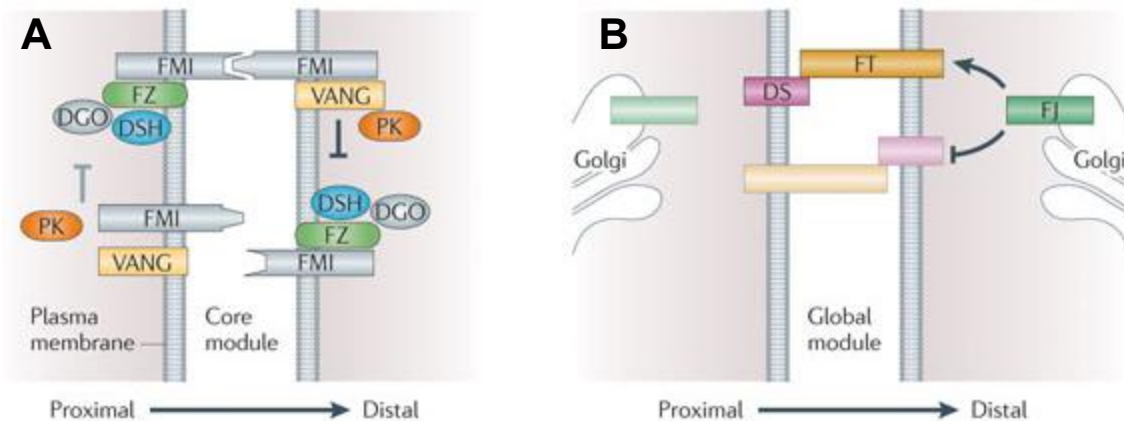


**Figure 1. PCP signaling systems.** (A) The core PCP system consists of Frizzled (Fz), Dishevelled (Dsh), Van Gogh (Vang), Prickle (Pk) and Flamingo (Fmi). Prior to morphological polarization, core PCP components adopt asymmetric subcellular localizations at the adherens junctions and segregate into two distinct subsets on the proximal (Fz/Dsh/Dgo) and distal (Vang/Pk) domains of opposing cell-cell junctions to communicate polarity information between neighboring cells. Polarized subcellular distributions are modulated by intercellular and intracellular feedback interactions. (B) The second Fat/Dachsous signaling module involves atypical cadherins Fat (Ft) and Dachsous (Ds) which interact heterophilically. This binding is further modulated by a Golgi kinase, Four-jointed (Fj). Fj phosphorylates both Ft and Ds to make Ft a stronger ligand for Ds. In polarized tissues, Fj and Ds are expressed in opposing gradients, resulting in a bias in the orientation of the Ft-Ds heterodimer.

(Figure was adapted from Bayly & Axelrod, 2011 [7])

#### 1.1.4 PCP pathways independent of core PCP or Ft/Ds systems

In *Drosophila*, several manifestations of PCP are regulated by mechanisms that are independent of the core PCP or Ft/Ds systems. One of the most well studied examples occurs during germband extension, where planar polarized junctional rearrangements causes the germband epithelium to double in length along the anterior-posterior (AP) axis and narrow along the dorsal-

ventral (DV) axis [32–35]. This polarized cell behavior relies on planar polarized actomyosin contractility and adhesion, and requires the patterned expression of transcription factors Even-skipped (Eve) and Runt [32, 34, 36]. Of note, another pathway is responsible for mediating planar polarized cell behaviors during elongation of the egg chamber during oogenesis. Critical to this process is the alignment of basal actin filaments along the DV axis in follicle cells, in perpendicular to the axis of elongation [37–40]. In this context, Fat2, a Fat homolog and the receptor tyrosine phosphatase DLar exhibit planar polarized distributions and regulates the planar polarized orientation of actin filaments [34, 41, 42].

### 1.1.5 PCP signaling in vertebrates

Components of the *Drosophila* core PCP pathway are highly conserved in vertebrates. In mammals, at least 10 genes encode Frizzled receptors (Fz1-10), 2 genes for Van Gogh-like (Vangl1-2), 3 genes for Dishevelled (Dvl1-3), 3 genes for Celsr (homolog of Flamingo, Celsr1-3) and 2 genes for Prickle (Pk1-2). The existence of multiple vertebrate isoforms of each core PCP component presents added complexity and challenges to understanding how these systems function in vertebrates. Nevertheless, analyses of loss of function mutants have implicated the core PCP pathway in diverse developmental processes in vertebrates.

Analogous to the alignment of hairs and sensory bristles in *Drosophila*, PCP signaling in vertebrates regulates the coordinated polarization of epithelial

cells such as the posterior positioning of motile cilia in cells of the embryonic node, hair follicle orientation in the skin and stereocilia orientation in the inner ear (See section 1.2.6). In the embryonic node, motile cilia beat in a clockwise motion to generate leftward flow of nodal fluid and biases the accumulation of an unidentified signal that is critical for establishing left-right (LR) asymmetry in the body [43]. Asymmetric distribution of core PCP proteins have been observed in nodal cells, and defects in LR asymmetry are found in multiple organisms when *Vangl* and *Dvl* functions are disrupted [44–47]. Another phenomenon that requires PCP signaling is the orientation of hair follicles in the skin. Each hair follicle is a collection of hundreds of cells that becomes organized into an asymmetric structure such that the associated hair makes an acute angle with respect to the skin epithelium. Disorganization of hairs in the skin are found in *Celsr1*, *Vangl2* and *Fz6* mutant mice, marked by the appearance of whorls and ridges in their fur [3, 48, 49]. Chimeric experiments also revealed the nonautonomous component of PCP signaling in hair follicle orientation, evidenced by the observation that *Vangl2*<sup>Lp/Lp</sup> mutant cells affected the proper polarization of adjacent wild-type hair follicles [3]. In the inner ear, PCP signaling regulates the uniform orientation of stereociliary bundles in the sensory epithelium and has been the one of the most widely used model systems for studying PCP (see Section 1.2.5-1.2.6) [50].

While PCP signaling plays a crucial role in polarizing cells in epithelial sheets, vertebrate PCP genes are required for coordinating collective cell movements. Forward genetic screens in *Xenopus* and zebrafish demonstrated

that orthologs of *Drosophila* PCP genes are critical for the process of convergent extension during embryogenesis [51–53]. Convergent extension (CE) describes the narrowing of a tissue in one axis (convergence) and its subsequent elongation in a perpendicular axis (extension) [54]. At the cellular level, mediolateral elongation and polarized cellular extensions allow intercalation of mesodermal cells between each other, facilitating the convergence of cells towards the midline and extension along the anterior-posterior (AP) axis [55–57]. In fish, frogs and mice, CE provides the driving force for two important developmental processes: neural tube closure and axis elongation. During neurulation, cells in the neural plate undergo CE, causing the neural plate curl and eventually fuse to form a hollow tube known as the neural tube. Single mutations in *Vangl2*, *Celsr1* or the combinatorial loss of either *Dvl1* and *Dvl2* or *Fz3* and *Fz6* function result in phenotypes characterized by open neural tube and a shortened body axis [2, 58–60]. Although PCP genes are clearly involved, there is little evidence for asymmetric distribution of PCP proteins in tissues undergoing CE, possibly because cells are actively shifting around and have transient cell-cell interactions. In addition to axis elongation and neural tube closure, PCP signaling also regulates CE in mouse cochlea, kidney, heart and eye [4, 61–63].

PCP genes have also been implicated in the development of the nervous system, where it regulates processes such as neuronal migration, axon guidance and dendritic patterning (Reviewed in [64, 65]). Studies in mice and zebrafish provide evidence for the role of PCP signaling in the caudal migration of facial

branchiomotor (FBM) neurons from rhombomere 4 (where they are generated) to rhombomere 6. For instance, loss of *vangl2* (*trilobite*), *fzd3a* and *celsr2* in zebrafish and *Vangl2<sup>LP</sup>* mutations in mice results in disrupted FBM migration [66, 67]. Conditional inactivation of *Celsr1* in FBM neurons randomizes the direction of FBM migration [68]. In addition to aberrant FBM neuron migration, *Fz3*, *Celsr3*, *Vangl2<sup>LP</sup>* mutant mice also exhibit loss of major axon tracts that connect the thalamus and cortex and defects in rostral turning of spinal cord sensory axons [69, 70]. In mammals and flies, *Celsr/Fmi* proteins are required for dendritic development where it prevents overgrowth of dendrites [71, 72]. *Dvl1<sup>-/-</sup>* hippocampal neurons have reduced dendritic growth and arborization [73].

### 1.1.6 Downstream effectors of PCP signaling

Downstream of the core PCP system, effectors regulate diverse cellular outcomes such as reorganizing the cytoskeleton, modifying cell adhesion/movement, affecting nuclear signaling and orientation of the mitotic spindle. In the *Drosophila* wing, tissue specific effectors affect the growth and/or positioning of hairs (trichomes) and bristles in individual cells. A small group of proteins function as planar polarity effectors, which include Fuzzy (Fy), Inturned (In) and Fritz (Frtz) [74–76]. In the wing, these proteins regulate the localization of another effector Multiple Wing Hairs (Mwh) to restrict actin polymerization to the distal edge of the cell [23]. Disruptions of vertebrate homologs of these proteins produce mild gastrulation defects and its functions in the OC are currently unknown [77].

Several conserved effectors of the core PCP pathway have functions in all tissues and were identified from studies in *Drosophila*, *Xenopus* and cultured cells. These proteins function as regulators of the actin cytoskeleton and include the Rho small GTPases (RhoA, Rac, and Cdc42), Jun N-terminal Kinase (JNK) and formin protein Daam1 [78]. These proteins are well-known regulators of cell polarity, cytoskeletal remodeling, adhesion and motility. Due to their broad cellular functions and expression of multiple forms, determining their specific functions in mammalian PCP requires the generation of conditional mutants. Our lab has previously examined the role of Rac GTPases in inner ear PCP. Rac1 and Rac3 function redundantly in cochlear CE and have a maintenance function in hair cell PCP in the developing OC. Specifically, p21-activated kinase (PAK), a downstream effector of Rac regulates the orientation and maintenance of hair cell PCP [79, 80].

The c-Jun N-terminal Kinase (JNK) signaling cascade has been generally considered as a key effector of the PCP pathway in vertebrates and lies downstream of Rac [81, 82]. JNK signaling regulates CE during *Xenopus* gastrulation, and later shown to act on other PCP-dependent processes such as neuronal migration and axon guidance [82, 83]. Pharmacological inhibition of JNK signaling in the cochlea contributes to bundle structural defects and cellular disorganization. Conditional deletion of *Jnk1* and *Jnk2* exhibit supernumerary rows throughout the OC without obvious cochlear length/width defects (unpublished).

Elucidating the effectors of the Ft/DS system has been challenging, as they are involved in the regulation of both planar polarity and tissue growth. Under certain circumstances, Ft/Ds signaling can affect the asymmetric distribution of core PCP proteins indirectly by regulating oriented cell division, cell dynamics and alignment and polarity of microtubules involved in Fz transport [12, 84, 85]. In addition, Ft/Ds activity has been proposed to regulate oriented cell divisions by polarizing the distribution of a downstream atypical myosin Dachs to promote anisotropy in junctional tension [86]. In vertebrates, the effectors of the Ft/Ds system remain unknown.

### **1.1.7 Vertebrate specific regulators**

A number of genes have been exclusively associated with vertebrate PCP processes. Mutations of genes encoding these proteins produce characteristic PCP phenotypes and display genetic interactions with the core PCP components. These proteins are proposed to refine and mediate PCP signaling in a context-specific manner. Proteins such as Ror2 and Ryk function as co-receptors for PCP and are Wnt responsive. Other proteins such as Scribble, Smurf ubiquitin ligases and Sec24b participate in PCP by regulating the trafficking, transport and turnover of core PCP proteins. In addition, *Protein tyrosine kinase 7 (Ptk7)* encodes an atypical receptor tyrosine kinase for which its *Drosophila* counterpart Off-track (Otk) has no role in PCP in flies (see Section 1.3). Its functions are still not well understood and the major goal of this

dissertation is aimed at dissecting its role in the regulation of PCP in the inner ear.

Ror2 belongs to a family of transmembrane receptors that interact with noncanonical Wnt5a and mediate its effects on PCP signaling [87]. In fact, *Ror2* mutant mice display similar phenotypes with *Wnt5a* mutants. This interaction attenuates canonical Wnt signaling and promotes JNK activity through Vangl2 phosphorylation. In the developing limb, a gradient of Wnt5a generates PCP gradient of Vangl2 activity to direct proper limb elongation [88]. In the inner ear, Ror2 mutants have a relatively mild PCP phenotype and complexes with Cthrc1 to stabilize Wnt-Fz receptor complexes [89].

Receptor-like tyrosine kinase (Ryk), an atypical receptor tyrosine kinase, is the mammalian homolog for *derailed* and functions in axon guidance and neurite outgrowth in flies and mammals. While *Ryk*<sup>-/-</sup> mice do not have PCP phenotypes, it genetically interacts with *Vangl2* and complexes together with Wnt5a acts to modulate Vangl2 stability [90].

Scribble (*Scrb*), a well-known determinant of apical-basal polarity was initially identified as a novel PCP regulator from studies of the *Circletail* mouse mutant. *Scrb* regulates asymmetric localization of Vangl2 [91] and was proposed to be required for targeting and restricting Vangl2 to the apical domain of hair cells.

*Sec24b* encodes for a cargo-sorting member of the COPII endoplasmic reticulum-Golgi transport vesicle. Loss of function *Sec24b* mutants exhibit PCP phenotypes in the neural tube, heart and inner ear and genetically interacts with

Vangl2 and Scrb [92]. Sec24b regulates the proper trafficking of Vangl2 to the membrane [93].

Smad ubiquitination regulatory factors, Smurf1 and Smurf2 have also been implicated in vertebrate PCP regulation. Loss of function of these two E3 ubiquitin ligases in mice produce PCP phenotypes in the cochlea and neural tube defects. These proteins were found to be recruited into a complex with phosphorylated Dvl and Par-6 and target Pk for degradation [94].

## **Section 1.2 Development of the mammalian Cochlea**

### **1.2.1 The organ of Corti (OC)**

The snail-shaped coiled cochlea is the primary auditory sensory organ that resides in the bony labyrinth of the inner ear. It houses a unique sensory epithelium that is exquisitely patterned for converting mechanical sound stimuli into electrical impulses. This epithelium also known as the organ of Corti (OC) rests on the basilar membrane and consists of a finite number of specialized epithelial cells that are divided into two groups: sensory hair cells (HC) and nonsensory supporting cells (SC). In the mature OC, these epithelial cells are organized into a stereotypical mosaic pattern where supporting cells interdigitate between hair cells (Figure 2). Along the medial-to-lateral axis of the cochlear duct, sensory hair cells are further arranged into a single row of inner hair cells (IHCs) and three rows of outer hair cells (OHCs). Supporting cells include the

inner and outer pillar cells (IPC and OPC), Border/Inner Phalangeal cells (IPhC) and Deiter Cells (DC).

Sensory hair cells assemble the V-shaped actin-rich stereociliary bundle, apical specializations that serve as the primary sensory receptors for hearing. In response to changes in sound pressure waves, the basilar membrane vibrates and causes the stereociliary bundle to pivot towards the lateral edge of the cochlear duct. This directionally biased deflection triggers the opening of mechanically gated ion channels in the stereocilia and induces a depolarizing inward current in hair cells. Synaptic vesicles carrying neurotransmitter molecules fuse at the basolateral surfaces of hair cells to transmit electrical signals through afferent neurons to the brainstem. Moreover, the cochlea is tonotopically mapped whereby sensory hair cells at each location along the cochlear duct are tuned to respond to sounds of a specific frequency. It is thought that the IHCs primarily serve to detect basilar membrane vibrations and OHCs serve in amplifying and conferring higher sensitivity to IHCs.

As its name suggests, non-sensory supporting cells provide structural support for the OC. Hair cells do not interface the basilar membrane directly. Instead, they rest on the cell bodies of supporting cells, which contact the basilar membrane. Cross-sections of the OC reveal high structural complexity of supporting cells. Supporting cells project finger-like phalangeal processes to fill the gaps between hair cells and form a tight ion impermeable epithelium, critical for maintaining the ionic compositions between the fluid-filled chambers in the cochlea.

Evidently, development of the elaborate structural features of the OC is tightly linked to the proper hearing functions of the cochlea. Majority of sensorineural hearing loss stems from damage to and loss of sensory hair cells in the cochlea. In mammals, these aberrations are irreversible as we lack the natural capacity to regenerate hair cells. Substantial progress needs to be made towards understanding the mechanisms that underlie cochlear development with the ultimate goal of designing effective diagnostics and identifying targets for regenerative therapies for hearing loss.

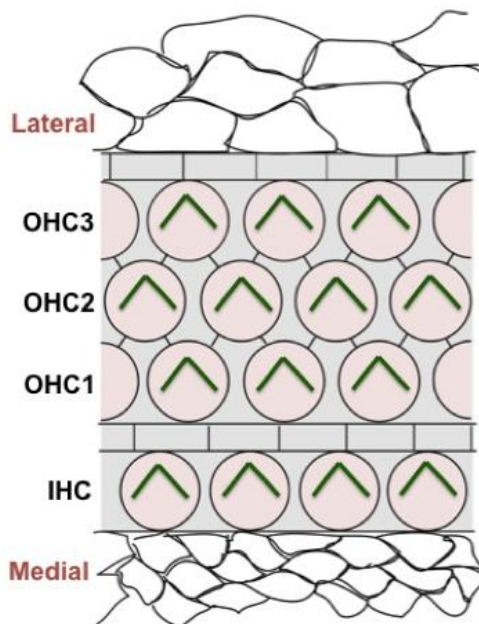


**Figure 2. Organization of the organ of Corti (En face view).** Hair cells (pink) are arranged into four rows along the medial lateral axis of the cochlear duct. Supporting cells (gray) interdigitate between hair cells. Juxtaposing the lateral and medial edges of the OC are the cells of the lesser epithelial ridge (LER) and the greater epithelial ridge (GER), respectively. Each hair cell assembles a V-shaped stereociliary bundle (green) that is oriented towards the lateral edge of the OC

### 1.2.2 Specification and Differentiation of the OC

The mammalian inner ear comprising the vestibular and auditory sensory organs arises from the otic placode, a region of thickened ectoderm that develops adjacent to the hindbrain and is present at embryonic day (E) 8.5 in the mouse [95]. Over the next 24 hours, the otic placode undergoes invagination and pinches off from the ectoderm to form the fluid-filled otocyst. Multi-potent epithelial progenitor cells in the otocyst further develop into three major lineages, prosensory cells (which contribute to hair cells and supporting cells), proneural cells (which become auditory or vestibular neurons) and nonsensory cells (which give rise to all other cells derived from the otocyst).

At E11, the cochlear duct emerges from the ventral portion of the otocyst [96, 97] and the initial outgrowth process is regulated by several genes such as *Gata3*, *Pax2* and *Eya1* (Figure 3). Epithelial-mesenchymal interactions in the developing otocyst direct the coiling of the duct [98]. Specification of the prosensory domain occurs concurrently with the growth of the cochlear duct. Multiple factors and signaling pathways cooperate to specify and restrict the prosensory domain to a narrow region bounded by two non-sensory domains; the greater epithelial ridge (GER) on its medial side and the lesser epithelial ridge (LER) on its lateral side. Broad expression of Notch regulators such as *Hes1* and *Hey1/2*, *Lunatic Fringe (Lfng)* and the Notch ligand *Jagged1 (Jag1)* in the early otocyst stage suggests a requirement for Notch signaling in restricting and/or specifying prosensory fate. This hypothesis was further validated by studies

where loss-of-function of Notch signaling in mice led to a significant loss of hair cell and supporting cell numbers [99–101].

In contrast, Hedgehog signaling functions as a negative regulator of prosensory cell fates in non-sensory cells within the cochlear duct to restrict the size and position of the OC. Deletion of *Gli3*, a downstream target of hedgehog signaling, produced shortened cochlear ducts with expanded and ectopic sensory patches [102]. Interestingly, spiral ganglia located medial to the developing OC strongly express a hedgehog ligand, Sonic Hedgehog (Shh). Bone Morphogenetic Protein 4 (Bmp4) is also one of the earliest molecular players involved in prosensory specification. High expression of BMP4 was observed in the region lateral to the OC known as the Lesser Epithelial Ridge (LER) [103]. The observed opposing expression gradients of BMP and Hedgehog ligands suggests that these two signaling pathways may antagonize each other to further restrict and pattern the prosensory domain. The prosensory domain is also demarcated by the expression of SRY-related high mobility-group (HMG)-box transcription factor, *Sox2*. Loss of function *Sox2* mutants inhibits prosensory domain formation, implicating it as another molecular player in the specification of the sensory primodium in the OC [104, 105].

At E13, expression of a cyclin-dependent kinase inhibitor p27<sup>Kip1</sup> is upregulated in the prosensory domain in a graded fashion from the apex to base of the cochlea [106]. This molecular event overlaps with terminal mitoses of multipotent prosensory cells and precedes the first signs of hair cell differentiation. Between E13 and E15, prosensory cells differentiate into inner

and outer hair cells (IHC, OHC) and between five to seven different types of supporting cells (SC) (Figure 1). Hair cell differentiation occurs along two axes in the cochlea; first, along a base-to-apex gradient and a second medial-to-lateral gradient where inner hair cell differentiation precedes outer hair cell differentiation. Multiple lines of evidence implicate Atoh1 or Math1, a basic Helix-Loop-Helix (bHLH) transcription factor, as a master regulator of hair cell differentiation [107–109]. At this developmental time point, Atoh1 is upregulated. In response to Atoh1, hair cells express specific Notch ligands to activate Notch1 receptors in neighboring prosensory cells and repress hair cell fate by inhibiting Atoh1 expression [110, 111]. Together with other regulators such as Inhibitor of Differentiation (Id), Prox1 and Sox2, the Notch signaling pathway plays an essential role in singling out hair cell fates from supporting cell fates. What remains elusive is how different types of hair cells and supporting cells are specified during development.

### **1.2.3 Morphogenesis of the Cochlea I: Cochlear Duct Extension**

Concomitant with differentiation of the post-mitotic prosensory cells, the cochlear duct continues to extend and coil, doubling in length to approximately 1.75 turns by P0 (Figure 3) [112, 113]. Cochlear duct extension and coiling appears to be an evolutionary adaptation of the basilar papilla in tetrapod species, and confers the ability to discriminate a wider range of sound frequencies [97]. During terminal morphogenesis, the four to five cell layers thick prosensory domain unidirectionally thins out into a two-cell layer thick epithelium

where hair cells rest on the cell bodies of supporting cells [9]. Cochlear extension occurs in the absence of any cell death or proliferation indicating that dynamic cellular rearrangements provide the main driving force for this process. Another by-product of these movements is the highly ordered pattern of hair cells and supporting cells (Figure 2).

The cellular movements underlying these rearrangements are highly reminiscent of convergent extension (CE) movements where cells actively narrow along one axis (convergence) and extend along a perpendicular axis (extension) [54, 114]. In vertebrates, the noncanonical Wnt/core PCP pathway regulates CE during neural tube closure. Mutations in core PCP genes such as *Vangl2* and *Dishevelled* often exhibit shorter and widened cochleae, implicating core PCP signaling in cochlear extension [61, 115]. A recent study showed that disruption of p120-catenin, a component of the adherens junction, leads to CE defects but not hair cell PCP defects in the cochlea. Altered distribution of cadherins in core PCP mutants reveal that cadherin-dependent mechanisms are involved in cochlear CE and that the core PCP pathway regulates cochlear CE and hair cell planar polarity independently [116].

Downstream of the PCP signaling pathway, our lab has demonstrated that Rho family of small GTPases *Rac1* and *Rac3* function redundantly to regulate cochlear extension [80]. Conditional *Rac1* single mutants have shortened cochlear ducts while *Rac1; Rac3* double mutants display exacerbated cochlear duct defects. Upon closer examination, epithelial cells in the floor region of E14.5 *Rac1; Rac3* double mutant cochleae revealed a loss of epithelial cohesion and

were accompanied by formation cyst-like sensory patches in the cochlea. These findings are consistent with a role for Rac GTPases in coupling actin dynamics and E-cadherin cell adhesion to regulate mediolateral and radial cell intercalations during cochlear extension. Another study has proposed that PCP signaling may regulate cell adhesion by recruiting Rac1 to the adherens junctions [117].

Non-muscle myosin II (NMII) is a key player that regulates CE in both *Drosophila* and vertebrates through modulation of junctional remodeling and cell shape change [32, 118]. Genetic and pharmacological perturbations of myosin II activity disrupts cochlear outgrowth and causes cellular disorganization in the OC, hence implicating myosin II in cochlear extension and cellular patterning [114].

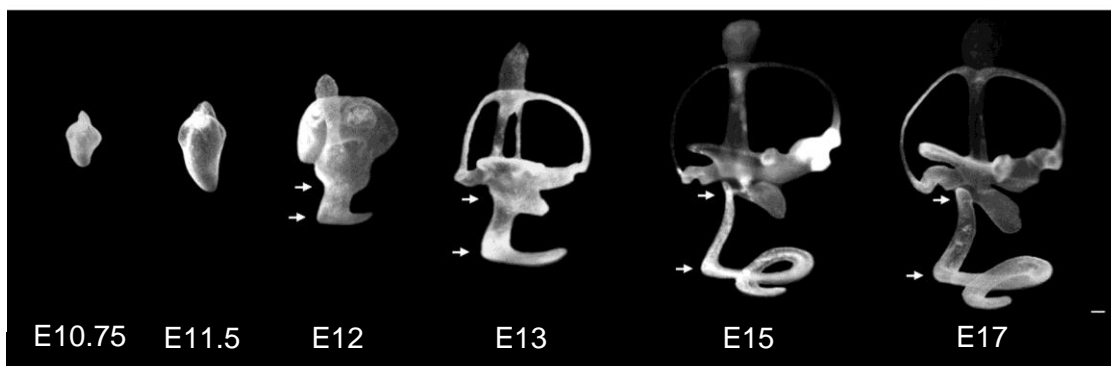


**Figure 3. Cochlear duct outgrowth.** Paint filled mouse inner ears illustrating the outgrowth of the cochlear duct over the course of embryonic development between E10.75 and E17. The cochlear duct emerges from the ventral portion of the inner ear (indicated by arrows), subsequently elongates and coils to form approximately 1.75 turns. D, Dorsal, V, Ventral

(Adapted and modified from Morsli *et al.*, 1998 [112])

#### **1.2.4 Morphogenesis of the Cochlea: Stereociliary bundle development**

As the cochlear duct extends, polarized actin-rich stereociliary bundles assemble on the luminal surfaces of sensory hair cells, and are uniformly oriented across the OC. In addition, cells in the OC become mono-ciliated containing a single microtubule based primary cilium known as the kinocilium.

Stereociliary bundle development follows similar hair cell differentiation gradients and PCP in hair cells is accomplished in two phases: establishment and refinement [119]. Initially, short microvilli of uniform size and length cover the luminal surfaces of nascent hair cells at E12.5 [120]. At E15, the axonemal kinocilium templated by the basal body elongates and projects out into the luminal space from the center of each hair cell. Subsequently, the kinocilium migrates non-randomly towards the lateral pole of the hair cell by E16.5 and triggers neighboring microvilli to elongate in a controlled manner.

Each microvillus thickens to become a more tightly bundled paracrystalline array of rigid actin filaments that define the stereocilia. The current model for the transformation of microvillus to stereocilium follows one where new actin filaments are added on the periphery of the stereocilium as existing filaments migrate towards the core of the stereocilium [121, 122]. Regulated actin assembly directs stereocilia growth to specific lengths, leading to the formation of the staircase-like array such that the tallest row of stereocilia lies next to the kinocilium. To promote bundle cohesion, a number of proteinaceous filaments link individual stereocilia with each other and the tallest row of stereocilia with the kinocilium. As the stereocilia elongates, a proportion of actin filaments project

into the apical cytoplasm to form rootlets which anchor into the cuticular plate, a dense meshwork of cross-linked actin and cytoskeletal proteins located just below the apical surface of hair cells. Excess microvilli that fail to incorporate into the rows of the stereociliary bundle will be resorbed. Once assembled, the stereocilia continue to grow, mature and renew but the kinocilium will degenerate postnatally.

Between late embryonic and early postnatal developmental stages, hair cells undergo a critical period of refinement to correct any deviations of their stereociliary bundle and achieve uniform orientation [123]. Outer hair cells also remodel their apical surfaces to ensure optimal mechanotransduction prior to the onset of hearing at P10 [124]. Beyond this critical reorientation period, stereociliary bundle orientation defects otherwise uncorrected remain misaligned through adulthood. This may be attributed to the progressive stiffening of the intercellular junctions and thickening of the actin belts that physically restrict rearrangements of the stereociliary bundle [125, 126]. Hair cells with misoriented stereociliary bundles do not undergo cell death but perturbed PCP signaling in the OC affects the cellular architecture of neighboring supporting cells [127]. These morphological disruptions may alter the general biomechanical properties of the OC and interrupt the amplification function of OHCs, hence decreasing their sensitivity to sound.

### **1.2.5 Hair cell PCP in the OC**

PCP in hair cells in the OC is defined at two levels. In individual hair cells, planar polarity is defined by the V-shape structure of the stereociliary bundle. At the tissue level, hair cells across the OC uniformly align their stereociliary bundles towards the lateral edge of the cochlear duct.

The uniform orientation of stereociliary bundles across the OC is regulated by the noncanonical Wnt/core PCP signaling pathway (see Section 1.1 and Section 1.2.6). Perturbations in core PCP signaling result in mild to severe randomizations of stereociliary bundle orientation that are dependent on the genetic background, hair cell subset and/or specific region of the OC [59, 61, 115]. However, in all cases, the structural polarity of individual stereociliary bundles remains intact. Therefore, core PCP signaling is dispensable for the intrinsic polarity of hair cells but is required to coordinate planar polarity at the tissue level.

The transient nature of the kinocilium suggests a developmental role and it has been thought to function as a guidepost for hair bundle morphogenesis and orientation. During establishment of PCP, migration of the kinocilium marks a critical step in polarizing the orientation of the stereociliary bundle. The link between kinocilium and hair cell PCP has been shown by analyses of mouse mutants of ciliary/basal body associated proteins, which exhibit complete loss or mispositioning of the kinocilium [128–130]. In the cochleae of these mutant mice, stereociliary bundle structure and bundle orientation are disrupted, therefore highlighting the pivotal role of the kinocilium in the polarization of the hair bundle.

A few groups including ours have shed light on the mechanisms that regulate hair cell-intrinsic polarity in the OC. Our lab has previously identified that cortical Rac-PAK activity is normally localized to the lateral domain of hair cells and tightly correlates with basal body positioning and bundle orientation. Therefore, localized Rac-PAK activity may serve as cell intrinsic polarity cues [79, 128, 131]. Disruption in the functions of two microtubule motor associated proteins, Lissencephaly 1 (Lis1) and Kinesin Family protein 3A (Kif3a), result in hair bundle morphology and orientation defects. These observations supports the idea that microtubule-mediated process are involved regulating hair cell PCP. Furthermore, these proteins also regulate cortical Rac-PAK localization. At postnatal stages, Lis1 functions to maintain planar polarity by recruiting cytoplasmic dynein to generate pulling forces on the microtubule array and microtubule organization. In the absence of these proteins, core PCP asymmetric localizations are maintained suggesting that they could operate independent of tissue PCP signaling. We therefore propose that microtubule capture at the lateral hair cell cortex establishes a cortical domain of Rac-PAK signaling creating a positive feedback loop, which subsequent microtubule-cortical attachments are strengthened to position the basal body at the lateral side of the hair cell. Microtubule capture at the lateral cortex may be mediated by mechanisms analogous to spindle orientation.

A newly published study has revealed a role for the aPKC/Par-3/Par-6 polarity complex in planar polarization of hair cells [132]. This polarity complex has conserved functions during asymmetric cell division, where they localize

asymmetrically at the apical cortex and recruit a scaffolding protein mammalian Inscuteable (mInsc), G protein Gai and LGN/Gpsm2 (homolog of Pins). This complex of proteins subsequently recruits effectors such as dynein to pull on astral microtubules and orient the mitotic spindle. In the OC, Par-3 localizes at the lateral apical surface of hair cells and recruits mInsc/LGN/Gai complex to exclude aPKC medially, creating a molecular blueprint on the hair cell apical surface that defines the V-shape of the developing stereociliary bundle. In addition to localizing on the apical surface, Par-3 and aPKC were both asymmetrically distributed in opposite domains at the adherens junctions, where core PCP proteins are localized. Although the functional significance of aPKC/Par-3 junctional localization has not been defined, this finding raises an interesting possibility that it may link tissue polarity with cell-intrinsic polarity pathways in the OC.

Altogether, the accumulating evidence supports a two-tier hierarchy for hair cell PCP regulation in the OC. Tissue-level PCP signaling generates extrinsic or tissue polarity cues which are then interpreted by the hair cell intrinsic effector machinery to align intrinsic polarity to the tissue polarity axis. Additionally, these cell-intrinsic pathways can function independently of inputs from the tissue polarity pathways to establish planar polarization of individual hair cells. The studies highlighted above have provided critical leads in the potential cell intrinsic mechanisms. Several questions surrounding this model include the nature of the tissue polarity cues and how these cues are transduced to the cell-intrinsic mechanisms.

### 1.2.6 Noncanonical Wnt/core PCP signaling in the OC

Eaton first proposed that PCP signaling regulates stereociliary hair bundles in the inner ear [133]. Subsequent studies confirmed this idea, where core PCP mouse mutants exhibited mild to severe randomizations of stereociliary bundle orientation in the OC [59, 115, 134]. It has also been commonly observed that stereociliary bundles in the outermost OHC rows show heightened sensitivity to PCP perturbations. In the case of *Fz3* and *Fz6* double mutants, stereociliary bundle orientation defects are restricted to the IHCs [59]. Moreover, these mutations are also often associated with a shortened and widened cochlear duct, suggesting the role of CE during cochlear duct extension [61, 115].

Examination of mammalian homologs of core PCP components reveals that they are asymmetrically distributed in the OC [91]. Due to the close juxtaposition of hair cells and supporting cells, it has been difficult to distinguish whether PCP proteins specifically localize to either or both cell types in the OC. Initial studies show that *Vangl2* localized at cell-cell junctions between medial domains of hair cells and lateral domains of supporting cells [91]. High-resolution imaging methods later confirmed that *Vangl2* is enriched at the lateral membrane of supporting cells [135]. *Dvl1* and *Dvl2* both accumulated along the lateral membrane of hair cells [60]. Analysis of two redundant Fz receptors (*Fz3* and *Fz6*) involved in hair cell PCP regulation was asymmetrically localized on the medial side of hair cells and supporting cells, hence colocalizing with *Vangl2* instead of *Dvl1/2* [59].

Similar to the cochlea, sensory epithelia in the vestibular sensory organs also exhibit hair cell PCP and depend on core PCP signaling. In the utricle and saccule, two populations of sensory hair cells show reversed polarities along a line of reversal. Examination of core PCP proteins in these tissues reveal that localizations of Fz6 and Pk2 were not altered across the line of reversal even though the orientation of stereociliary bundles was reversed [136]. Together, these results indicate that although asymmetric distribution of core PCP proteins are conserved in the auditory and vestibular sensory organs, it does not seem to be the absolute determinant of PCP in hair cells.

Wnts have been examined for their role in hair cell PCP. In mammals, there are at least 8 Wnt genes that are expressed in the cochlea [123, 137]. Two Wnt genes, *Wnt5a* and *Wnt7a*, display graded expression patterns at developmental timepoints that coincide with the establishment of hair cell PCP. Application of exogenous Wnt7a or Wnt antagonists such as Sfrp1, Sfrp3 (Frzb) or WIF1 to wild-type cochlear explant cultures causes orientation defects of stereociliary bundles [119, 123, 138]. These results suggest a role for Wnt gradients in hair cell PCP. However, mild PCP phenotypes have been found in *Wnt5a* knockout mice and stereociliary bundle orientation was normal in *Wnt7a*<sup>-/-</sup> mice [123, 138]. Therefore, an instructive role for these molecules has not been defined perhaps due to functional redundancies between multiple Wnts.

Taken together, it remains to be determined the nature of and identity of the cues that encode directional information to establish the PCP axis in the OC. Most enigmatic are the downstream signaling mechanisms that impinge on

cytoskeletal rearrangements to regulate stereociliary bundle formation.

Furthermore, the signaling mechanisms that link core PCP signaling to the cell-intrinsic polarity machinery are otherwise unknown.

## **Section 1.3 Protein Tyrosine Kinase 7 (*Ptk7*)**

### **1.3.1 Overview**

*Protein Tyrosine Kinase 7 (Ptk7* and also known as colon carcinoma kinase-4/CCK-4) encodes an atypical receptor tyrosine kinase, which has been implicated as a molecular switch with versatile functions during development and adulthood. Our lab previously identified *Ptk7* as a novel regulator of planar cell polarity in vertebrates. Morpholino knockdown of *Ptk7* leads to CE defects in *Xenopus* and *Ptk7* mutant mice display severe neural tube closure defects and stereocilia misorientation in the inner ear, reminiscent of those found in core PCP mutants [1]. Given the observed developmental abnormalities of *Ptk7* mutants and its presence in various cancers, PTK7 has emerged as an important player during development, cancer progression and metastasis [139, 140]. Studies performed in *Xenopus*, zebrafish and mouse model systems reveal that the mechanisms underlying *Ptk7* function are complex and context-specific.

### **1.3.2 Expression and Structure of PTK7**

PTK7 is ubiquitously expressed in embryonic and adult tissues, undifferentiated human embryonic stem (ES) cells and tumors [141–143].

Analysis of human cDNA from testis and various cancer lines revealed as many as 5 alternatively spliced variants of PTK7 [144]. During embryonic development, *Ptk7* is dynamically expressed in tissues. In the early mouse embryo, *Ptk7* expression is regulated by *Cdx*, a homeodomain transcription factor [145]. Within the mouse OC, *Ptk7* is localized to both hair cells and supporting cells. At E16.5, PTK7 localizes to the apical surfaces of outer hair cells and at the adherens junctions of both developing hair cells and supporting cells. By E18, *Ptk7* becomes restricted to lateral membranes of hair cells and supporting cells [1]. This observation suggests that *Ptk7* function must be tightly regulated to ensure proper tissue morphogenesis.

Polymorphisms in human PTK7 have been identified albeit not associated with any disease. Interestingly, developmental disorders whose symptoms include mental retardation, craniofacial, limb and skeletal abnormalities have been attributed to duplication of chromosome 6p where the *PTK7* gene is located [146]. PTK7's involvement in cancer progression has been well documented suggesting its potential as a therapeutic target and prognostic marker. In fact, the human PTK7 gene was first cloned from melanoma cells and is misexpressed in multiple cancers including colon cancer, esophageal cancer, acute myeloid leukemia and breast cancer. Recently, PTK7 has been associated with resistance to chemotherapeutic drugs [147].

Analysis of the mouse *Ptk7* gene indicates 92.6% sequence identity with the human PTK7 gene. *Ptk7* is homologous to *Hydra Lemon*, chick *kinase-like gene (KLG)* and *Drosophila Offtrack (Otk)*. It is an 118kDa protein consisting of

an extracellular domain with 7 immunoglobulin-like (Ig) repeats, a transmembrane domain and an intracellular kinase domain (Figure 2). It is predicted to be a dead kinase owing to the lack of the conserved 'DFG' triplet motif (replaced with 'ALG') required for binding of magnesium ions that coordinate ATP in the ATP-binding cleft [148]. Despite its predicted lack of catalytic activity, the kinase domain of PTK7 is crucial for regulating diverse biological processes. The intracellular kinase domain has emerged as a critical component of Ptk7. In *Xenopus*, PTK7 mediates Dsh membrane localization through its cytoplasmic domain [149]. Other interaction partners of the cytoplasmic domain include adaptor protein RACK1 and  $\beta$ -catenin. While detectable PTK7 kinase activity has not been reported in literature, data from our lab suggests that PTK7 is both a substrate for and activator of tyrosine kinase Src in epithelial cells (Unpublished).

Ligands for mouse *Ptk7* have yet to be identified. In *Xenopus*, Ptk7 interacts with canonical Wnts, Wnt3a and Wnt8 [150]. PTK7 may participate in sequestering canonical Wnts and attenuating canonical Wnt signaling. Wnt4, a non-canonical Wnt has been shown to interact with *Drosophila* Otk. *In vitro*, the transmembrane domain of PTK7 displays weak propensity for dimer formation [151]. Transmembrane region of PTK7 is critical for stabilizing PTK7 localization at the membrane. The extracellular domain (ECD) functions to coordinate cell-cell communication and adhesion.

A number of posttranslational modifications regulate many aspects of PTK7 function during development and in cancer. For instance, Chuzhoi (*Chz*)

mutant mice carrying an additional cleavage site on PTK7 extracellular domain produce characteristic PCP phenotypes [152]. The membrane type1-matrix metalloproteinase (MT1-MMP) and members of a disintegrin and metalloprotease (ADAM) family mediate proteolytic cleavage of PTK7 ECD. Following MT1-MMP mediate cleavage of the ECD, C-terminal PTK7 fragments are sequentially cleaved by  $\gamma$ -secretase and released into the cytosol [153, 154]. Full length PTK7 has been shown to inhibit actin cytoskeleton contractility while the soluble ECD promotes this activity and cell invasion [154]. The PTK7 gene sequence also contains 10 putative N-glycosylation sites, but functional analyses of this posttranslational modification has not been explored [143]. Since variants of PTK7 are differentially expressed in tissues, posttranslational modifications of the protein may confer cell-type specific functions.

### 1.3.3 Functional aspects of PTK7

Investigations across various organisms reveal that PTK7 has evolved different functions across species with molecular mechanisms that appear to be context specific. Multiple lines of evidence argue that PTK7 is a regulator of vertebrate PCP. For instance, loss-of-function PTK7 mouse mutants primarily cause characteristic PCP phenotypes, PTK7 genetically interacts with a core PCP gene *Vangl2*, and can activate JNK signaling *in vitro* [1, 150]. Dishevelled (Dsh) occupies a key branching point that separates canonical Wnt signaling from non-canonical Wnt/PCP signaling. Membrane recruitment of Dsh is a prerequisite for PCP signaling activity. While translocation of Dsh to the

membrane requires Ptk7 function in *Xenopus*, this requirement is dispensable in the mouse and zebrafish, reflecting mechanistic differences between species [149, 155, 156]. Other context dependent functions that require PTK7 for Dsh membrane recruitment have yet to be identified.

*Ptk7* plays a conserved role in PCP by regulating convergent extension movements during gastrulation and neural tube closure in *Xenopus*, zebrafish and mice. *Ptk7*<sup>-/-</sup> mice exhibit severe neural tube closure defects. PTK7 affects polarized protrusive activity of mesodermal cells during CE [1, 155]. Abnormal CE also occurs in *Xenopus* and zebrafish when PTK7 function is disrupted [1, 156, 157]. During neural tube closure in *Xenopus*, PTK7 is proposed to regulate CE through its interaction with RACK1 and PKCδ1 to further stabilize Dsh at the membrane.

Neural crest migration is another example of a PCP regulated process. Crest cells at the neural plate migrate along defined paths to give rise to diverse cell types that underlie craniofacial structures and the peripheral nervous system. Injection of PTK7 morpholinos in the *Xenopus* embryo blocks neural crest migration due to the failure in localizing Dsh at the membrane [149]. While the downstream mechanisms are unknown, PTK7 is proposed to stabilize the Fz7-Dsh complex and promote Dsh phosphorylation [149]. An interaction between PTK7 and PlexinA is also functionally important in neural crest migration but this interaction does not affect Dsh membrane localization [158]. Therefore, PTK7 can function as a coreceptor for either Fz or Plexin to regulate neural crest migration.

Recently, several groups have proposed that *Ptk7* does not function exclusively in PCP signaling but also affects canonical Wnt/ $\beta$ -catenin signaling [150, 156, 159]. These studies have yielded conflicting results. Two groups reported that PTK7 inactivates canonical Wnt signaling. Ptk7 co-precipitates canonical Wnts, Wnt3a and Wnt8 in the presence of Fz7 but does not interact with noncanonical Wnts [150]. It has been hypothesized that PTK7 functions to sequester canonical Wnt receptor complexes thereby attenuating canonical Wnt signaling. In zebrafish, PTK7 potentiates Wnt5a- and Wnt11-mediated non-canonical Wnt signaling activity [156]. Expression of PTK7 ECD rescued axial CE defects suggesting that PTK7 functions *in vivo* as a canonical Wnt co-receptor. To date, Wnt/ $\beta$ -catenin phenotypes have not been reported in mice. On the contrary, a positive role for PTK7 in canonical Wnt signaling was reported by an independent study. Puppo and colleagues found an interaction between the amino-terminus of  $\beta$ -catenin and the PTK7 intracellular domain [159]. Based on *in vitro* functional assays in mammalian cells and *Xenopus*, PTK7 promotes canonical Wnt signaling by stabilizing a pool of  $\beta$ -catenin at the membrane that is resistant to degradation, thereby allowing subsequent  $\beta$ -catenin target gene transcription. Overall, these results suggest that PTK7 functions as an important molecular switch between the canonical Wnt/ $\beta$ -catenin pathway and the non-canonical Wnt/PCP pathway.

Little evidence supports a PCP role for PTK7 homologs in lower model organisms. Rather, the *Drosophila* homolog of Ptk7, *otk*, associates with PlexinA receptors to mediate Semaphorin-1a (Sema-1a) repulsive signaling in motor

axon guidance at the embryonic stage [160]. Otk is also implicated in layer-specific neuronal connectivity in the fly visual system [161]. A more recent study reported that interaction between Otk and *Drosophila* Wnt4 inhibits canonical Wnt signaling [150]. Interestingly, overexpression but not loss of Otk caused misalignment of wing hairs, suggesting that *otk* can affect non-canonical Wnt signaling.

Few studies offer insights to the downstream signaling mechanisms and effectors of *Ptk7* function in mammalian PCP. Our functional dissection of *Ptk7* in the inner ear provides evidence to suggest that *Ptk7* functions in an alternate pathway separate from the core PCP pathway to regulate anisotropic contractile forces and orient hair cell PCP. Interestingly, polarized cell behaviors during axis elongation in the *Drosophila* germband epithelium are regulated independently of core PCP signaling [32]. Instead, planar polarized myosin II dynamics and activity facilitates localized contraction and local neighbor exchange, allowing the embryo to narrow and elongate [32, 162]. Therefore, mechanical forces may be well suited to be act as spatial cues for globally coordinating PCP. In the next section, we will elaborate on how forces are generated, transmitted and integrated to moderate large-scale tissue morphogenesis.

## **Section 1.4 Mechanical Forces and Tissue Morphogenesis**

### **1.4.1 Overview**

Throughout development, cells in the embryo undergo dynamic shape changes and movements to acquire specialized form and function. In the OC, developing supporting cells and hair cells continuously reshape and rearrange while establishing PCP [113, 116, 124]. Major emphasis has been placed on characterizing the genes and the chemical cues that coordinate these behaviors. However, one must acknowledge that these cellular behaviors are fundamentally a mechanical process and therefore, physical forces provide a critical link in integrating the genetic and biochemical control of morphogenesis. Unlike biochemical intercellular signals, mechanical forces can serve as long-range cues to coordinate polarity and cellular behaviors.

Within the developing embryo, cells generate forces using their cytoskeleton framework of actin filaments and microtubules. These forces can be further regulated in time and space to generate various transformations in cell and tissue shape. Conversely, cells are also exposed to a myriad of external forces in their microenvironments such as hydrostatic pressure, tension and fluid shear stress. These external forces play a role in modulating cell fate specification and differentiation. To maintain cellular and tissue integrity, cells must also be able to balance between extrinsic and intrinsic forces.

Force generation and force transmission are two self-organizing events that drive tissue morphogenesis. The availability of biophysical and advanced imaging has provided opportunities to probe the basis of these forces and the identities of molecular complexes that sense and transduce mechanical signals over long distances. I will summarize key findings of how cell-generated

mechanical forces develop at a local level and how they integrate at a tissue level to drive global changes in tissue morphology.

#### **1.4.2 Generation of Cortical Forces**

Cortical forces underlie the ability of cells to change shapes or rearrange and are produced by the contraction of a meshwork rich in myosin II, cross-linked actin filaments and other actin binding proteins. These individual components assemble into higher order structures and their cooperative associations form a cohesive contractile unit.

Non-muscle myosin II (hereon referred to as Myosin II) is a motor protein that is composed of two heavy chains, two essential light chains and two regulatory light chains (RLCs). Myosin II is a bipartite molecule; the globular head domain crosslinks actin and couples with ATPase activity to generate mechanical energy for the conformational change (the “powerstroke”) while the tail domain participates in the assembly of bipolar minifilaments which exert tension on the actin cytoskeleton [163, 164]. Mammals express 3 isoforms of myosin II heavy chain encoded by separate genes: Myosin IIA (encoded by *Myh9*), Myosin IIB (encoded by *Myh10*) and Myosin IIC (encoded by *Myh14*). Variations in their localization and the differences in their enzymatic and motor activities contribute to different functions but they also have partially overlapping functions.

Myosin II activity can be regulated at several levels but is primarily regulated through phosphorylation of the RLC by kinases such as myosin light chain kinase (MLCK) and Rho-associated protein kinase (ROCK). This event

releases Myosin II head-head associations to promote F-actin binding and ATPase activity, and relieves head-tail interactions to promote their assembly into minifilaments. In contrast, phosphorylation of several sites on the myosin II heavy chain by kinases such as the transient receptor potential melastatin 7 (TRPM7), Protein Kinase C (PKC) proteins and Casein Kinase II (CKII) destabilizes existing minifilaments and inhibits de novo myosin II assembly [163, 165].

In addition to myosin II minifilament assembly and contractile activity, actin assembly at the cell cortex is an important component of force generation. Actin cytoskeleton provides the framework for contractile activity and is regulated through actin assembly and modulating the architecture of actin filament arrays. Free actin monomers that readily assemble into filaments and subsequently grow by monomer addition to the barbed ends of existing filaments. The actin related protein Arp2/3 complex and formins are two well-known regulators of filament nucleation that produce branched and unbranched filaments, respectively. In attached cells, Arp2/3 mediated-formation of branched actin networks at the plasma membrane function to scaffold and concentrate signaling molecules, myosin II or adhesion molecules and maintain stabilize contacts. Furthermore, actin cross-linkers such as fascin,  $\alpha$ -actinin and filamins organize actin filaments into higher order structures and modulate the mechanical properties of the actomyosin network [166, 167]. The extent of crosslinking regulates stiffness of actomyosin networks and influences contractile force generation and transmission.

The actomyosin network exhibits dynamic properties. On a fast timescale, the actomyosin network behaves like a viscoelastic solid that reversibly deforms. At longer timescales, actomyosin networks exhibit fluid-like behaviors and flows. Flows are directed by gradients in actomyosin contractility and this feature of the actomyosin network functions to redistribute and realign forces within cells. To drive different cellular responses, actomyosin flows can be further regulated in terms of the frequency and amplitude of contractions, and the direction of the flow.

### **1.4.3 Mechanotransduction and Force Transmission**

Mechanotransduction describes the process of cells sensing alterations in the mechanical force balance and transducing these cues into changes in biochemical signaling and gene expression. Forces generated by the actomyosin network are transmitted to neighboring cells and the extracellular milieu through two main locations: cell-cell adhesions and cell-extracellular matrix (ECM) adhesions modulated by cadherins and integrins respectively. Although structurally different, these two adhesion molecules function to connect the actin cytoskeleton through adaptor proteins and remodel the actomyosin network in response to force. I will focus on mechanotransduction at cell-cell adhesive contacts, as they are a major means of transmitting cortical tension within tissues.

At epithelial cell-cell contacts, mechanotransduction is primarily mediated by E-cadherin based intercellular junctions. Using their extracellular domains, E-

cadherins participate in homophilic interactions in *trans* and provide the link between adjacent cells. The cytoplasmic domain of E-cadherin connects with the actin cytoskeleton through interactions with p120-catenin,  $\beta$ -catenin and  $\alpha$ -catenin [168, 169]. This linkage is fortified through binding of additional binding proteins such as vinculin and epithelial protein lost in neoplasm (EPLIN) [170–172]. Cadherin/catenin complexes are bona fide mechanotransduction complexes [173]. The current model posits that in response to force, a conformational change is imposed on  $\alpha$ -catenin exposing cryptic binding sites for vinculin [170, 174]. Subsequently, vinculin stabilizes  $\alpha$ -catenin and interacts with other actin regulatory proteins function to reinforce junctions and alter junction mechanics.

Mechanical forces regulate the strength of adhesions to mediate force transmission, and conversely, adhesions modify forces by altering actomyosin organization and dynamics. At initial cell-cell contact formation, tension drives the clustering of E-cadherin molecules at junctions. Progressive recruitment of Arp2/3 by cadherin clusters promotes branched actin networks and induces a wave of actomyosin activity which lead to the maturation and strengthening of E-cadherin junctions [175]. Furthermore, cross talk between cell-cell adhesions and cell-ECM adhesions can further modulate adhesion as they impinge on common biochemical signaling components. During *Xenopus* CE, integrins are capable of modifying cadherin-mediated adhesion [176].

#### **1.4.4 Role of forces in tissue morphogenesis**

Several studies have shed light on how cell-generated forces cooperate to drive tissue morphogenesis (reviewed in [177]). Coupling of local forces through intercellular adhesions exert global spatial and temporal regulation of contractility to transform tissue shape and direct morphogenetic movements.

Tissue bending and invagination is achieved through apical constriction and underlies morphogenetic processes such as gastrulation, tube formation and neurulation [178]. During neural tube closure, apical constriction is mediated by increased contractility of the circumferential actomyosin network at intercellular junctions. As a result, each cell's apical surface reduces in size relative to its base. The coordinated contractility of the apical myosin II network between linked cell populations transforms an initially planar neural plate into a hollow tube. In the case of *Drosophila* mesodermal invagination, apical constriction is driven by the contraction of a medial myosin II network that spans the apical cortex [179].

Tissue elongation can be accomplished by cellular rearrangements, where cells exchange neighbors, allowing the tissue to converge in one direction and extend in the perpendicular direction. During *Drosophila* germband extension, planar polarized junction remodeling mediated by anisotropic myosin II contractility drives cell intercalation. Myosin II is enriched along vertical junctions (parallel to the dorsal-ventral axis) which shrinks to bring four or more cells in contact and then resolves along the anterior-posterior axis to form new contacts [32]. Contraction of actomyosin cables spanning multiple junctions form rosettes to further promote tissue elongation [33, 180].

The interplay between mechanical forces and PCP has been reported in *Drosophila* tissues. These studies provide evidence for the role of force-mediated cellular rearrangements in coordinating global tissue PCP. Bipolar enrichment of Myosin II in aligned cells of the prospective denticle field mediates cell rearrangements during planar polarization of the *Drosophila* denticle epithelium [181]. In the developing *Drosophila* wing, cells exhibit planar polarized localization of core PCP proteins along the proximal-distal (P-D) axis. It appears that this polarized localization is accomplished in part by contraction of the hinge, which creates anisotropic mechanical stress on the adjacent wing blade region to realign their PCP to the PD axis [84, 182]. Anisotropic tissue tension is proposed to mediate cell neighbor exchanges, cell elongation and oriented cell division and perturbation of *Dachsous* disrupts these cellular rearrangements. The Ft/Ds pathway may function through atypical myosin *Dachs* to allow cells to coordinately respond to mechanical stress. Whether analogous forces influence global PCP in vertebrates awaits further investigation.

### **Section 1.5 Scope of Dissertation**

Establishment of PCP is critical for diverse morphogenetic processes and tissue function. *Ptk7* has been implicated as a novel regulator of PCP in vertebrates, and published studies on *Ptk7* function have yielded important insights with respect to its molecular regulation and how *Ptk7* intersects with the non-canonical Wnt/PCP pathways. Many of these studies have been elucidated in lower vertebrate model systems and we now understand that *Ptk7* has

acquired different functions in a context specific manner. However, few studies have shed light on downstream signaling mechanisms mediated by PTK7. As discussed earlier, *Ptk7* regulates hair cell PCP in the cochlea. The striking manifestation of PCP in the OC offers readout at single cell resolution and makes the mouse cochlea an excellent model system to study PCP signaling. The aim of this work was to dissect the underlying cellular and molecular mechanisms of PTK7 during establishment of PCP in the mouse OC.

Using a genetic approach, we identify *Ptk7* function in supporting cells plays a cell non-autonomous role in hair cell PCP. We have further elucidated that PTK7 functions in parallel with the core PCP signaling pathway to regulate myosin II activity and orient hair cell PCP. These findings are summarized in Chapter 2 of this dissertation.

Chapter 3 offers insights to a downstream signaling mechanism by which PTK7 regulates actomyosin contractility in the OC. In vitro analysis in MDCK II epithelial cells have led to the identification of Src as a novel interaction partner of PTK7. We propose that a PTK7-Src signaling axis spatially regulates myosin II activity by promoting planar polarized ROCK2 phosphorylation at selected boundaries between hair cells and supporting cells. We identify cortactin and vinculin as additional targets of PTK7-Src signaling in the OC.

In addition, this dissertation also contains 3 appendices summarizing preliminary results. Appendix I discusses the role of ephrinB signaling molecules in hair cell PCP, Appendix II describes findings from live imaging studies of myosin II network in the OC and Appendix III explores the potential candidates

involved in cross-talk between *Ptk7* and hair cell intrinsic mechanisms in the OC. Together, my work provides novel insights to the mechanisms that underlie hair cell PCP. In the chapters henceforth, I provide evidence to propose a new model where polarized actomyosin-based contractile forces regulates hair cell PCP.

**CHAPTER 2: PTK7 Regulates Myosin II Activity to Orient Planar Polarity in  
the Mammalian Auditory Epithelium**

This chapter is based on the following publication:

Lee, J, Andreeva, A, Sipe, CW, Liu, L, Cheng, A, Lu, X. "PTK7 Regulates Myosin II Activity to Orient Planar Polarity in the Mammalian Auditory Epithelium"

*Current Biology* June 5, 2012;22(11):956-66.

With permission from Elsevier; license number 3273710487235

## 2.1 Introduction

Epithelial cells are often polarized within the plane of a cell sheet, perpendicular to the apical-basal polarity axis. One of the most prominent examples of epithelial planar cell polarity (PCP) is found in the mammalian auditory sensory epithelium, the organ of Corti (OC). The OC is composed of one row of inner hair cells (IHC) and three rows of outer hair cells (OHC) and non-sensory supporting cells. Hair cells are separated from one another by supporting cells, forming a checkerboard pattern. The stereociliary bundle, the mechanotransduction organelle located on the apical surface of the hair cell, consists of rows of actin-based stereocilia of graded heights in a V-shaped array. This structural asymmetry of the stereociliary bundle defines PCP of an individual hair cell. Across the OC, hair cells display uniform planar polarity, with the vertex of their V-shaped stereociliary bundles all pointing to the lateral edge of the cochlear duct. Uniform bundle orientation is required for normal sound perception [121].

Inner ear PCP is regulated by an evolutionarily conserved noncanonical Wnt pathway, which has emerged as a key regulator of metazoan tissue morphogenesis, including convergent extension (CE) movements during axis elongation, neural tube closure and inner ear morphogenesis [22]. The core components of the noncanonical Wnt pathway are Frizzled (Fz), Dishevelled (Dsh/Dvl), Strabismus (Stbm)/Van Gogh (Vang), Starry night (Stan)/Flamingo (Fmi), Diego (Dgo) and Prickle (Pk). These molecules engage in both intra- and inter-cellular signaling to align PCP in neighboring cells. In other systems,

members of the Rho family small GTPases (RhoA, Rac1 and Cdc42) and their effectors, including Rho-associated kinases (ROCK) and c-Jun N-terminal kinases (JNK), have been implicated in PCP signaling downstream of the core components. In the inner ear, the noncanonical Wnt pathway is required for stereociliary bundle orientation and cochlear convergent extension [183]. Mutations in homologs of Fmi (Celsr1), Vang (Vangl1/Vangl2), Fz (Fz2/Fz3/Fz6) and Dsh (Dvl1/Dvl2/Dvl3) cause misoriented stereociliary bundles and a shortened cochlear duct [22]. The small GTPase Rac1 and its downstream effector p21-activated kinases (PAK) regulate hair cell PCP in the OC [79, 128], while non-muscle myosin II has been implicated in cochlear extension [114].

In addition to the conserved noncanonical Wnt pathway, novel PCP regulators have been identified in mammals, including *Protein tyrosine kinase 7* (*Ptk7*), a receptor tyrosine kinase-like molecule [1, 92–94, 115]. Mouse *Ptk7* mutations cause similar phenotypes to those of noncanonical Wnt pathway mutants, including neural tube and hair cell PCP defects [1, 152]. In *Xenopus*, *Ptk7* has been shown to regulate neural tube closure [1] and neural crest migration [149, 157] by mediating membrane recruitment of Dishevelled through PKC $\delta$  and the adaptor molecule RACK1 [149, 157]. However, it is unclear whether PTK7 regulates mammalian epithelial PCP by a similar mechanism, as PTK7 has been shown to mediate mesodermal CE in mice without affecting Dvl2 membrane localization [155].

To gain insight into the mechanisms by which PTK7 regulates mammalian epithelial PCP, we carried out a functional dissection of *Ptk7* in planar

polarization of hair cells in the OC, where stereociliary bundle orientation provides a robust and quantifiable readout for PCP at single-cell resolution. Our results reveal that *Ptk7* and the noncanonical Wnt pathway differentially regulate myosin II-based contractility to align hair cell PCP. We show that *Ptk7* is required in supporting cells to orient hair cell PCP, likely by exerting contractile tension on neighboring hair cells through an apical myosin II network.

## 2.2 Results

### 2.2.1 *Ptk7* Is Not Required for Asymmetric Membrane Localization of Dishevelled-2 in the OC

Membrane recruitment and asymmetric localization of the cytoplasmic scaffold protein Dishevelled is a conserved readout for PCP signaling [61, 184, 185]. To determine where *Ptk7* intersects with the noncanonical Wnt pathway, we first tested if *Ptk7* is required for membrane recruitment of Dvl2. At E17.5, in the mid-basal region of control OC, endogenous Dvl2 is asymmetrically localized and appears to be enriched on the lateral membranes of hair cells (Figure 4A, C). Dvl2 localization is disrupted in *Vangl2*<sup>Lp/Lp</sup> OC [61] and *Fz3*<sup>-/-</sup>; *Fz6*<sup>-/-</sup> OC (Figure 5), indicating that Dvl2 localization is a functional readout of the noncanonical Wnt pathway activity. By contrast, Dvl2 localization was normal in the *Ptk7*<sup>-/-</sup> OC at E17.5 (Figure 4B, D). Similarly, in the mid-apical region of OC, membrane recruitment of Dvl2 occurred in both control and *Ptk7*<sup>-/-</sup> OC (Figure 4E-H). We also examined Fz3 localization at E17.5, which is normally enriched along the medial poles of hair cells and supporting cells [59, 91] (Figure 4I, K, M, O).

Interestingly, membrane localization of Fz3 was significantly reduced in the *Ptk7*<sup>-/-</sup> OC (Figure 4J, L, N, P). These results indicate that *Ptk7* regulates Fz3 localization but is not required for asymmetric membrane localization of Dvl2 in the OC. Thus, the noncanonical Wnt pathway is at least partially active in the absence of *Ptk7*.

### 2.2.2 PTK7 and Fz3/6 Receptors Act in Parallel and Have Opposing Effects on Hair Cell PCP

The normal Dvl2 membrane localization and reduced Fz3 localization in *Ptk7*<sup>-/-</sup> OC suggests that *Ptk7* is not an obligatory component of the noncanonical Wnt pathway, however it may regulate the strength of noncanonical Wnt signaling. To test this idea, we next sought to determine the epistatic relationship between *Ptk7* and the *Fz3/6* genes. Mouse *Fz3* and *Fz6* regulate PCP signaling in a redundant manner [59]. We used stereociliary bundle orientation as readout for PCP, which is already evident at embryonic day (E) 18.5. In the control, the vertices of the V-shaped stereociliary bundles all point toward the lateral edge of the cochlear duct (Figure 6A, A'). While *Fz3* or *Fz6* single mutants had normal bundle orientation (Figure 6B, B' and data not shown), *Fz3*<sup>-/-</sup>; *Fz6*<sup>-/-</sup> mutants had misoriented stereociliary bundles, affecting primarily IHCs [59] (Figure 6C, C', Figure 5). By contrast, in the *Ptk7*<sup>-/-</sup> OC, bundle misorientation was confined to OHC3 (Figure 6D, D', Figure 7). Surprisingly, bundle misorientation in OHC3 was significantly suppressed in both *Fz3*<sup>-/-</sup>; *Ptk7*<sup>-/-</sup> and *Fz6*<sup>-/-</sup>; *Ptk7*<sup>-/-</sup> mutants (Figure 6E, E', and data not shown). These results indicate that *Ptk7* and *Fz3/Fz6* have

opposing effects on hair cell PCP and suggest that *Ptk7* acts upstream of or in parallel to *Fz3/Fz6*. To distinguish between these two possibilities, we analyzed stereociliary bundle orientation in *Fz3<sup>-/-</sup>; Fz6<sup>-/-</sup>; Ptk7<sup>-/-</sup>* triple mutants. If *Ptk7* acts upstream of *Fz3/Fz6* in a linear genetic pathway, then the *Fz* mutations should be epistatic to *Ptk7*, i.e. the triple mutants should have a phenotype similar to *Fz3/Fz6* double mutants. On the other hand, if *Ptk7* acts in parallel to *Fz3/Fz6*, then neither mutation should be epistatic; instead, the triple mutants may show an additive phenotype. Indeed, the triple mutants displayed a combination of the *Fz3/Fz6* and *Ptk7* mutant phenotypes: both IHC and OHC rows displayed misoriented stereociliary bundles (Figure 6F, F', Figure 7). Taken together, these results indicate that *Ptk7* and *Fz3/Fz6* act in parallel and have opposing effects on hair cell PCP.

### 2.2.3 *Ptk7* Is Required in Supporting Cells to Regulate Hair Cell PCP

Next, we sought to determine the site of action of *Ptk7* in the OC. To this end, we generated a 'floxed' allele of *Ptk7* (*Ptk7<sup>CO</sup>*). A knock-out allele (*Ptk7*) was derived from *Ptk7<sup>CO</sup>* upon germline Cre expression (Figure 9A, B). We first used the *Foxg1<sup>Cre</sup>* line [186] to inactivate *Ptk7* in the entire cochlear epithelium. OHC3s in these mutants displayed misoriented stereociliary bundles similar to *Ptk7<sup>-/-</sup>* mutants (Figure 9C-E), indicating that *Ptk7* acts within the cochlear epithelium to regulate hair cell PCP.

We then carried out genetic mosaic analysis to further determine the cell-type specific requirement of *Ptk7*. PTK7 is expressed in both hair cells and

supporting cells and co-localizes with the adherens junction protein E-cadherin [1]. To generate *Ptk7* mosaics, we took advantage of the *Ella-Cre* line [187], which expresses Cre in all cells but at variable levels. In *Ella-Cre; Ptk7<sup>CO/-</sup>* animals, cells with high Cre expression level would have a genotype of *Ptk7<sup>-/-</sup>*, while cells with low Cre expression level would have a genotype of *Ptk7<sup>CO/-</sup>* thus retaining a functional copy of *Ptk7* (referred to as *Ptk7<sup>+</sup>* thereafter). The genotypes of individual cells in the OC were unambiguously determined by the presence or absence of PTK7 immunostaining (Figure 8B-F). Because only OHC3s were affected in *Ptk7* mutants, we focused on OHC3s and correlated stereociliary bundle orientation with the genotypes of each hair cell and its four immediate supporting cell neighbors (Figure 8A, shaded in blue). Many mosaics had a *Ptk7<sup>+</sup>* hair cell with a misoriented stereociliary bundle surrounded by varying numbers of *Ptk7<sup>-/-</sup>* supporting cells (arrows, Figure 8D-F”). Moreover, as the number of *Ptk7<sup>-/-</sup>* supporting cells surrounding a *Ptk7<sup>+</sup>* hair cell increased (up to 4), both the penetrance and the severity of bundle misorientation defect increased (Figure 8G, H). Together, these results indicate that *Ptk7* function in hair cells alone is insufficient for normal bundle orientation, and that *Ptk7* is required in supporting cells to regulate hair cell PCP.

#### **2.2.4 JNK Signaling Is Unlikely to Mediate PTK7 Function in the OC**

Our results so far are consistent with a model where *Ptk7* and the noncanonical Wnt pathway converge on common effectors to regulate bundle orientation. It has been shown that the noncanonical Wnt pathway activates JNK

signaling in other systems [81, 82]. We therefore considered the possibility that *Ptk7* has an opposing effect on Fz-mediated JNK signaling. To test this, we performed biochemical assays for JNK activation in HEK293T cells (Figure 10A). Using phosphorylation of c-Jun as readout, we found that expression of PTK7 alone had a minimal effect on JNK activation, while expression of Fz3 alone led to JNK activation. Moreover, coexpression of PTK7 and Fz3 did not inhibit JNK activation by Fz3. Thus, in this heterologous system, there was no apparent effect of PTK7 on JNK signaling.

Next, we examined whether PTK7 regulates JNK signaling *in vivo*. By using antibodies that specifically recognize phosphorylated and activated JNK (pJNK), we found that, in E17.5 controls, pJNK localized to cellular junctions and the tips of a subset of stereocilia (Figure 10B-B’), suggesting JNK signaling is active during cochlear morphogenesis. However, in *Ptk7*<sup>-/-</sup> OC, we did not observe any significant changes in pJNK levels or localization (Figure 10C-C’), suggesting that JNK is unlikely to be a downstream effector of PTK7 in the OC.

To more rigorously assess whether PTK7 regulates inner ear PCP through JNK signaling, we next examined genetic interactions between *Ptk7* and the *Jnk* genes using bundle orientation as readout. Among the three mouse homologs of Jnk, *Jnk1* and *Jnk2* are broadly expressed. While single *Jnk* knock-out mice are viable, *Jnk1/2* double mutants display neural tube defects and die at E10.5 [188–190]. We found that *Jnk1* and *Jnk2* single mutants had essentially normal bundle orientation at E18.5 (Figure 10E and data not shown). In the *Jnk1*<sup>-/-</sup>; *Ptk7*<sup>-/-</sup> OC, bundle misorientation persisted in OHC3s, comparable in severity to *Ptk7*<sup>-/-</sup>

mutants (Figure 10F). Similar results were obtained in *Jnk2<sup>-/-</sup>; Ptk7<sup>-/-</sup>* double mutants (data not shown). Therefore, unlike *Fz3/Fz6* mutations, *Jnk1/Jnk2* mutations had no effect on the bundle misorientation phenotype of *Ptk7* mutants, providing further evidence that JNK is unlikely to mediate PTK7 signaling in the OC.

### **2.2.5 *Ptk7* and the Noncanonical Wnt Pathway Differentially Regulate a Contractile Apical Myosin II Network in Supporting Cells**

To further pursue downstream effectors of *Ptk7*, we next investigated a potential role of *Ptk7* in regulating myosin II function in the OC. It has been shown that noncanonical Wnt signaling activates actomyosin contractility in other systems [118, 191, 192]. Moreover, myosin II regulates CE and neural tube closure in *Xenopus* [193, 194] and cochlear extension in mice [114].

We first examined myosin IIB (MIIB, encoded by *Myh10*), one of the three myosin II heavy chain proteins (MIIA, MIIB and MIIC) expressed during cochlear morphogenesis [114]. Hair cell planar polarization and stereociliary bundle formation proceed in a base-to-apex gradient starting at the base of the cochlea around E16.5, as evidenced by migration of the axonemal kinocilium [115] and asymmetric localization of activated PAK [79]. At E16.5, in control tissues, MIIB was localized to cellular junctions [114] (Figure 11A-E). In addition, in the mid-basal region of the cochlea, we also observed an assembly of MIIB foci near the apical surface of supporting cells (pillar and Deiters' cells) (Figure 11A-C, arrows). By contrast, the apical MIIB foci were absent from the supporting cells in

the mid-basal region of the *Ptk7*<sup>-/-</sup> OC and overall junctional localization of MIIB was reduced compared to controls (Figure 11F-J). Western blot analysis of E16.5 whole cochlear lysates showed that total levels of MIIB in *Ptk7*<sup>-/-</sup> cochleae were similar to controls (Figure 11K). These results indicate that *Ptk7* promotes junctional localization of MIIB and is required for the assembly of apical MIIB foci in supporting cells.

To determine if the noncanonical Wnt pathway also regulates MIIB localization, we examined *Fz3*<sup>-/-</sup>; *Fz6*<sup>-/-</sup> and *Vangl2*<sup>Lp/Lp</sup> cochleae at E16.5. In contrast to *Ptk7* mutants, the apical MIIB foci still formed in the supporting cells of *Fz3*<sup>-/-</sup>; *Fz6*<sup>-/-</sup> and *Vangl2*<sup>Lp/Lp</sup> mutants, albeit smaller in size compared to controls (Figure 11L-O). Interestingly, junctional MIIB levels were significantly reduced in *Vangl2*<sup>Lp/Lp</sup> mutants (Figure 11N, O) but only slightly reduced in *Fz3*<sup>-/-</sup>; *Fz6*<sup>-/-</sup> mutants (Figure 11L, M). Thus, *Ptk7* and the noncanonical Wnt pathway differentially regulate MIIB localization in the OC.

We next asked whether the apical MIIB foci in supporting cells were contractile structures. Because force generation by myosin II molecules requires their ATPase activity [163], we reasoned that formation of an active contractile network should be disrupted upon inhibition of the myosin ATPase activity. To test this hypothesis, we took advantage of a Cre-inducible dominant-negative allele of *Myh10* (*Myh10*<sup>DN</sup>) carrying a point mutation (R709C) in MIIB, which retains actin binding but compromises the actin-activated ATPase activity [195]. *Foxg1*<sup>Cre</sup> was used to activate the expression of MIIB (R709C) in the cochlear epithelium, such that *Foxg1*<sup>Cre</sup>; *Myh10*<sup>DN/DN</sup> animals expressed only mutant

(R709C) MIIB in the cochlea. Immunostaining revealed that MIIB (R709C) was still localized to cellular junctions but failed to assemble into apical foci in supporting cells at E16.5 (Figure 11R-S). These observations indicate that assembly of apical MIIB foci requires its ATPase activity and strongly suggest that the apical MIIB foci in supporting cells are contractile structures.

### **2.2.6 *Ptk7* Regulates Myosin II Activity to Orient Hair Cell PCP**

Decreased cortical MIIB level and the absence of apical MIIB foci in the *Ptk7*<sup>-/-</sup> OC suggest compromised myosin II activity. Myosin II is activated by myosin regulatory light chain (RLC) phosphorylation, which is required for actomyosin contractility [163]. We therefore examined the distribution of phosphorylated RLC (pRLC) in the OC. At E16.5, in the mid-basal region of the control OC, pRLC was primarily detected at cellular junctions with higher intensity around pillar cell membranes (Figure 12A, B). In E16.5 *Ptk7*<sup>-/-</sup> OC, pRLC staining appeared to be decreased at cell-cell contacts compared to controls, but, surprisingly, it was highly localized to apical foci in supporting cells (Figure 12C, D, arrows). By Western blot analysis, *Ptk7*<sup>-/-</sup> cochleae showed a ~2-fold increase in total pRLC levels compared to controls (Figure 12M).

The paradox of the absence of MIIB and increased staining of pRLC in apical foci in *Ptk7*<sup>-/-</sup> supporting cells suggests that other myosin II heavy chain molecules may be present in these structures. We therefore examined MIIC and MIIA distribution in *Ptk7*<sup>-/-</sup> OC. In the mid-basal region of the control OC at E16.5, both MIIC and MIIA were detected at apical foci in supporting cells (Figure 12E,

F, I, J). Overall, MIIC appeared to be enriched in supporting cells, whereas MIIA localization was diffused and hardly detectable at cell boundaries. In *Ptk7*<sup>-/-</sup> OC, MIIC staining appeared to be decreased at cell-cell contacts but was still present at apical foci in supporting cells (Figure 12G, H), whereas MIIA staining at apical foci in supporting cells was greatly reduced (Figure 12K, L). Western blot analysis showed that in *Ptk7*<sup>-/-</sup> cochleae, total levels of MIIC were slightly increased (Figure 12N), while total MIIA levels were similar compared to controls (Figure 12O). Taken together, reduced cortical localization of MIIB, MIIC and pRLC and the absence of MIIB and MIIA in apical foci in *Ptk7*<sup>-/-</sup> OC suggest that *Ptk7* regulates myosin II activity.

If compromised myosin II activity caused bundle misorientation in *Ptk7*<sup>-/-</sup> mutants, then blocking myosin II activity should result in similar bundle orientation defects. Because MIIA, MIIB and MIIC are all present and likely function redundantly in the OC, we took a pharmacological approach and applied the myosin II inhibitor blebbistatin to cochlear explant cultures around the time of stereociliary bundle formation (see Chapter 5, Materials & Methods). We found that explants treated with blebbistatin displayed bundle misorientation (arrows, Figure 12Q), whereas bundle orientation in control explants was relatively normal (Figure 12P). Therefore, we conclude that myosin II activity is required for hair cell PCP.

### **2.2.7 *Ptk7* Promotes Planar Asymmetry of Junctional Vinculin**

Defects in myosin II localization suggest that myosin II function is compromised in *Ptk7*<sup>-/-</sup> OC. To evaluate myosin II function, we examined junctional vinculin localization. Vinculin is a tension-sensitive actin-binding protein involved in anchoring actin filaments to adhesion complexes at both focal adhesions and adherens junctions [196–198]. Recent *in vitro* studies demonstrate that recruitment of vinculin to adhesion sites is myosin II-dependent [168, 170, 199, 200]. At E16.5, we observed a base-to-apex gradient of junctional vinculin localization in the control OC that coincides with the gradient of MIIB distribution (see Figure 11A-E). In the mid-basal region of control cochlea, vinculin was asymmetrically localized along cell-cell contacts and enriched on the medial side of hair cell membranes (Figure 13A-C). Strikingly, in the mid-basal region of the *Ptk7*<sup>-/-</sup> OC, planar asymmetry of junctional vinculin was abolished, and overall junctional vinculin staining was reduced compared to controls (Figure 13D-F). On the other hand, localization of resident adherens junction proteins, including E-cadherin and  $\beta$ -catenin, was comparable to controls (Figure 14), suggesting that loss of vinculin planar asymmetry in *Ptk7*<sup>-/-</sup> OC is not a result of disrupted adherens junctions. In the apex, junctional vinculin staining in control and *Ptk7*<sup>-/-</sup> OC was similar and both lacked apparent planar asymmetry (Figure 13G-J). These results indicate that *Ptk7* promotes planar asymmetry of junctional vinculin and strongly support the hypothesis that *Ptk7* regulates myosin II-based polarized contractile forces between OC epithelial cells.

### **2.2.8 Planar Asymmetry of Junctional Vinculin Is Restored in *Fz3*<sup>-/-</sup>; *Ptk7*<sup>-/-</sup> Mutants**

In *Ptk7* mutants, loss of vinculin planar asymmetry correlated with bundle misorientation. To understand the functional significance of vinculin planar asymmetry as well as the basis for the suppression of the *Ptk7* bundle orientation phenotype by *Fz3* (see Figure 6), we examined vinculin localization in *Fz3*<sup>-/-</sup> and *Fz3*<sup>-/-</sup>; *Ptk7*<sup>-/-</sup> mutants at E16.5. In the *Fz3*<sup>-/-</sup> OC, staining intensity of junctional vinculin was similar to controls, though its planar asymmetry appeared less robust (Figure 13K-M). Remarkably, planar asymmetry of junctional vinculin was restored in *Fz3*<sup>-/-</sup>; *Ptk7*<sup>-/-</sup> mutants (Figure 13N-P). Moreover, *Fz3*<sup>-/-</sup>; *Ptk7*<sup>-/-</sup> double mutants showed an increase in junctional MIIB levels and reappearance of apical MIIB foci in supporting cells compared to *Ptk7* single mutants (Figure 14). Taken together, these results demonstrate a strong correlation between vinculin planar asymmetry and hair cell PCP, and further suggest that *Ptk7* and *Fz3* act in an opposing fashion to regulate contractile forces between OC epithelial cells.

### **2.2.9 *Vangl2* and *Ptk7* differentially regulate Planar Asymmetry of Vinculin (unpublished)**

We showed that *Ptk7* and the core PCP pathway differentially regulate myosin IIB. In support of the notion that *Ptk7* regulates tension, vinculin localization in *Ptk7* mutants was reduced and its planar asymmetry was lost. Here we determined whether myosin IIB defects observed in core PCP mutants also correlated with vinculin localization defects. We analyzed the distribution of

vinculin in *Vangl2<sup>Lp/Lp</sup>* mutant OC. In contrast to the loss of planar asymmetry in the mid-basal region of *Ptk7* mutant OC, planar asymmetry of junctional vinculin in *Vangl2<sup>Lp/Lp</sup>* hair cells was misoriented along with a modest reduction in staining intensity (Figure 15G-I) compared to control OC (Figure 15A-C). Therefore, both *Ptk7* and the non-canonical Wnt/PCP pathway act in concert to promote planar asymmetry of vinculin in the OC.

#### **2.2.10 Inefficient deletion of *Ptk7* in hair cells in *Math1<sup>Cre</sup>; Ptk7<sup>/CO</sup>* cochlea (unpublished)**

From our genetic mosaic analysis, we determined that *Ptk7* has a non-autonomous function in supporting cells to regulate hair cell PCP. On the other hand, we were unable to determine cell-autonomous functions of *Ptk7* due to technical difficulties in identifying mosaics with *Ptk7* mutant hair cells surrounded by four neighboring wild-type supporting cells. We therefore inactivated *Ptk7* function in hair cells using a *Math1<sup>Cre</sup>* driver line where Cre is expressed in developing hair cells and a subset of supporting cells as early as E14.5. At E17.5, *Math1<sup>Cre</sup>; Ptk7<sup>/CO</sup>* OC had mild stereociliary bundle orientation defects compared to control OC (Figure 16A, B). Furthermore, upon analysis of *Ptk7* expression in *Math1<sup>Cre</sup>; Ptk7<sup>/CO</sup>* OC, localization of PTK7 at the adherens junction was not significantly altered (Figure 16C, D). In the apex of control OC, we observed expression of PTK7 on apical surfaces of outer hair cells (Figure 16E). This expression pattern was maintained in *Math1<sup>Cre</sup>; Ptk7<sup>/CO</sup>* OC (Figure 16F). These results suggest that *Math1<sup>Cre</sup>*-mediated deletion of *Ptk7* in hair cells may

occur at later stages of development, precluding our elucidation of a cell-autonomous role for *Ptk7* in hair cell PCP.

### 2.3 Discussion

In this study, we present multiple lines of evidence that *Ptk7* is not an obligatory component of the noncanonical Wnt pathway; rather, during PCP signaling in the auditory epithelium, *Ptk7* and the noncanonical Wnt pathway differentially regulate myosin II-based contractile forces to orient PCP. Furthermore, we uncover an active role of supporting cells in this process through a contractile apical myosin II network (Figure 13Q).

In the mouse, *Ptk7* is not required for membrane recruitment of the noncanonical Wnt pathway component Dvl2 either in the inner ear (this study) or in the mesoderm during gastrulation [155]. These results contradict studies in *Xenopus*, where it has been shown that *Ptk7* mediates membrane recruitment of Dishevelled through a PKC $\delta$ -dependent mechanism [149, 157]. A possible explanation is that the *Xenopus* Dishevelled membrane recruitment assay was based on exogenously expressed Dishevelled, while we examined endogenous Dvl2 in the mouse. There is also evidence that PTK7 may have evolved different functions in mice and *Xenopus*. For example, PTK7 has been shown to regulate neural crest migration in *Xenopus*, but not in mice [149, 152]. While it is formally possible that PTK7 might mediate membrane localization of other mouse Dishevelled proteins (Dvl1 and Dvl3), it is unlikely to be the primary function of PTK7 in PCP regulation in the OC. Instead, our results strongly support a function of PTK7 in myosin II regulation to align PCP.

Interestingly, bundle misorientation in *Ptk7* mutants is largely restricted to OHC3 despite broad expression of PTK7 in the cochlea. OHC3s are positioned at the lateral edge of the OC and, as such, are mechanically coupled to a different group of cells than the other hair cell rows. We speculate that their unique mechanical environment may render OHC3s more sensitive to compromised myosin II function in *Ptk7* mutants. Furthermore, normal Dvl2 localization suggests that the noncanonical Wnt pathway is at least partially active in *Ptk7* mutants. We propose that overall PCP signaling is weakened but not disrupted in *Ptk7* mutants, resulting in defects only in OHC3s.

Although we have identified *Ptk7* non-autonomous function in supporting cells, PTK7 may also have a cell-autonomous role in hair cells. However, in this study we could not establish such a role conclusively. Because hair cell and supporting cell membranes are closely juxtaposed, we were unable to identify mosaics where a *Ptk7*<sup>-/-</sup> hair cell was surrounded by four *Ptk7*<sup>+</sup> supporting cells using PTK7 immunostaining. We also lacked a means to perturb *Ptk7* function specifically in hair cells during PCP signaling.

Our genetic analysis revealed, rather surprisingly, opposing effects of *Ptk7* and *Fz3/Fz6* on stereociliary bundle orientation. These findings contrast with our earlier observation that *Ptk7* and *Vangl2*<sup>Lp</sup> mutations showed a positive genetic interaction such that double heterozygous animals displayed spina bifida [1]. It is worth noting that an allelic series of *Vangl2* mutations caused neural tube defects ranging from mild (e.g., spina bifida) to severe (e.g., craniorachischisis) in both mice and humans [201–203]. Thus, reduced *Ptk7* gene dosage may

enhance the dominant effects of the *Looptail* mutation on neural tube closure. *Fz3/Fz6* genes have unique qualities among the noncanonical Wnt pathway components: *Fz3/Fz6* mutations cause bundle misorientation primarily in IHCs, where bundle orientation is frequently reversed. Furthermore, *Fz3/Fz6* and *Dvl2* appear to localize to opposite poles of hair cells, which is at odds with a conserved role of Fz in Dishevelled recruitment through direct binding [204]. Thus, our results add to a growing body of evidence that suggests *Fz3/Fz6* use novel mechanisms to regulate hair cell PCP. We propose that *Fz3/Fz6* and *Ptk7* act in an opposing fashion to modulate actomyosin contractility in the OC and that reduced *Fz3* localization in the *Ptk7*<sup>-/-</sup> OC is probably a secondary effect of altered actomyosin organization rather than the cause for bundle misorientation.

We show that *Ptk7* and the noncanonical Wnt pathway differentially regulate a contractile apical myosin II network in supporting cells. These structures are analogous to those observed during *Drosophila* gastrulation [179, 205] and germ band extension [162, 206, 207], which generate pulsed contractile forces on cell-cell junctions to drive apical constriction and cell intercalation, respectively. We hypothesize that the apical myosin II foci in supporting cells may engage in similar contractile behaviors to exert pulling forces on neighboring hair cells. *Ptk7* modulates myosin-II based contractile tension on hair cells by mediating the assembly of the apical myosin network in supporting cells. *Fz3/Fz6* may modulate contractility in hair cells and/or supporting cells to counterbalance the pulling forces on hair cells (Figure 13Q). In support of this model, we show

that vinculin, a force-sensitive actin binding molecule, is normally enriched along the medial junctions of hair cells, that this planar asymmetry is lost in *Ptk7*<sup>-/-</sup> mutants, and importantly, both vinculin planar asymmetry and bundle orientation were restored in *Fz3*<sup>-/-</sup>; *Ptk7*<sup>-/-</sup> double mutants. Based on the misorientation of vinculin planar asymmetry in *Vangl2*<sup>L<sup>D</sup>/L<sup>D</sup></sup> OC, we further speculate that the noncanonical Wnt/PCP pathway polarize contractile behaviors of myosin II foci to generate tension on selective cell contacts.

The precise mechanisms by which PTK7 regulates myosin II activity remain to be determined. Paradoxically, in spite of reduced cortical myosin II staining, pRLC level was increased in *Ptk7*<sup>-/-</sup> OC. Therefore, it is unlikely that PTK7 regulates myosin II activity through RLC phosphorylation *per se*. These results are consistent with a role of PTK7 in myosin II heavy chain regulation. Different myosin II isoforms are regulated by distinct upstream signals [208]. *Ptk7* deficiency affected the localization of all three heavy chain isoforms, with the strongest impact on MIIB, which has properties best suited to exert tension [163]. These results are consistent with a role of PTK7 in myosin II heavy chain regulation. We suspect that the increased level of pRLC in *Ptk7*<sup>-/-</sup> OC may reflect a compensatory response to compromised myosin II heavy chain function.

How might contractile tension orient hair cell PCP? We showed previously that hair cell PCP is controlled by Rac-PAK signaling [79, 128]. Interestingly, several *in vitro* studies suggest that tension and myosin II can inhibit Rac activity through GEFs and GAPs for Rac [209–212]. Consistent with this idea, activated PAK and vinculin exhibit complementary patterns of planar asymmetry in hair

cells. We propose that polarized contractile tension between OC epithelial cells regulates the spatial pattern of Rac-PAK activity to orient hair cell PCP (Figure 13Q).

## 2.4 Figures

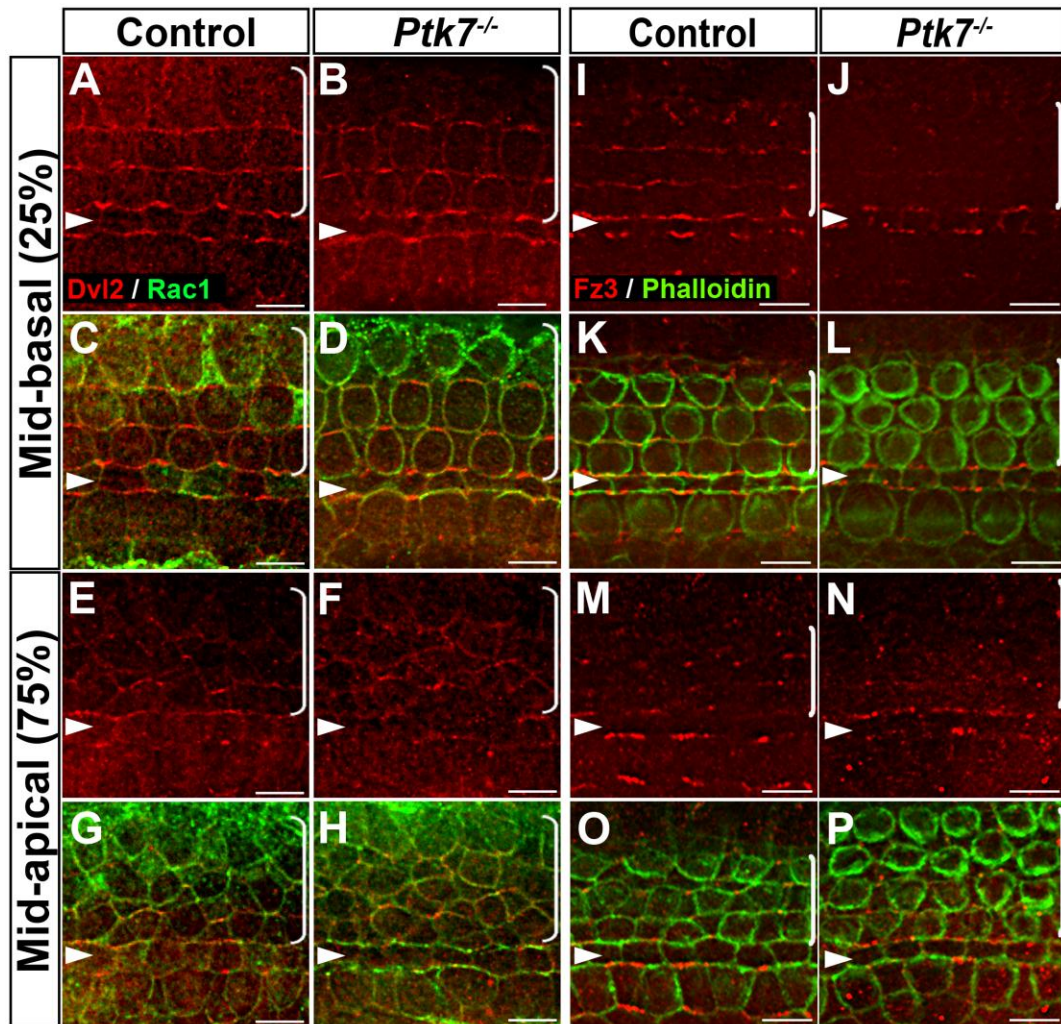


**Figure 4. *Ptk7* Regulates Fz3 Localization but Is Not Required for Asymmetric Localization of Dvl2 in the OC.**

(A–D) In the mid-basal region of the OC at E17.5, Dvl2 (red) was enriched on the lateral membranes of hair cells in both control (A, C) and *Ptk7*<sup>-/-</sup> (B, D) cochleae.

(E–H) In the mid-apical region of the OC at E17.5, similar membrane localization of Dvl2 was observed in control (E, G) and *Ptk7*<sup>-/-</sup> (F, H) cochleae. Cell

boundaries were labeled with Rac1 immunostaining (green). (I–L) In the mid-

basal region of OC at E17.5, Fz3 (red) was enriched on the medial membranes of hair cells and supporting cells in the control (I, K). This localization was

disrupted in *Ptk7*<sup>-/-</sup> cochleae (J, L). (M–P) In the mid-apical region of the OC at

E17.5, asymmetric localization of Fz3 was not apparent in either control (M, O)

or *Ptk7*<sup>-/-</sup> (N, P) cochleae. Green, phalloidin staining. Percentages indicate the

distance of the positions analyzed from the base relative to the length of the

cochlea. Arrowheads indicate the row of pillar cells. Brackets indicate OHC rows.

Lateral is up in all micrographs. Scale bars represent 6 μm.

(Panels A-D were contributed by Sipe CW.)

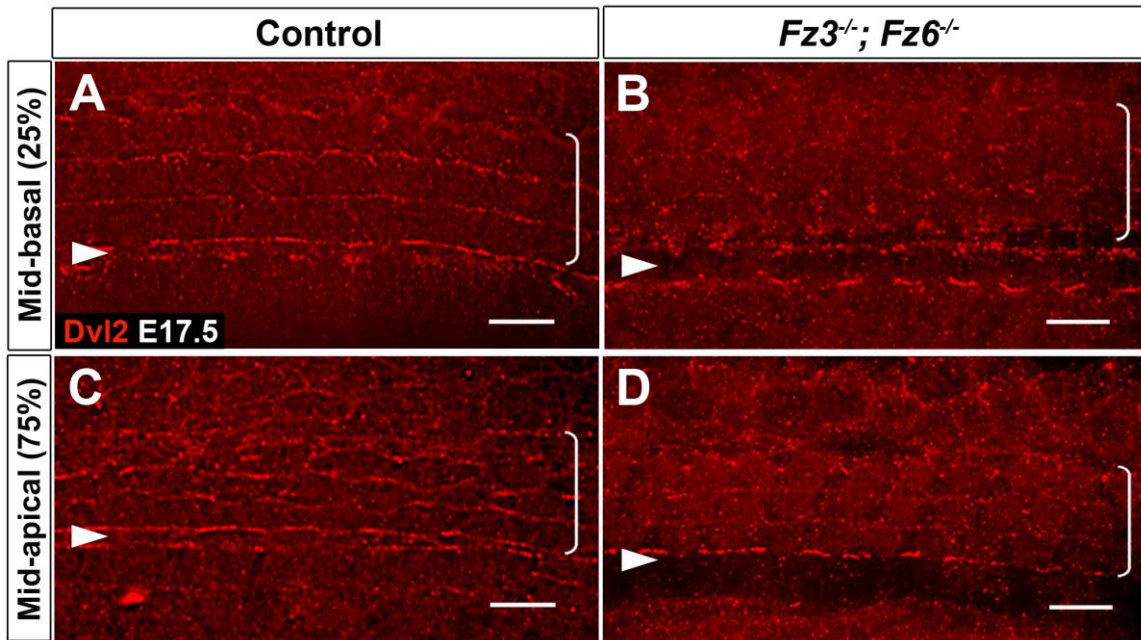


**Figure 5. Localization of Dvl2 in  $Fz3^{-/-}; Fz6^{-/-}$  cochleae.**

(A-D) E17.5 cochlear whole-mounts stained with Dvl2 (red). (A, C) In the control, Dvl2 is enriched on the lateral membrane of hair cells. (B, D) Membrane localization of Dvl2 was abolished in  $Fz3^{-/-}; Fz6^{-/-}$  OC. Percentages indicate the distance of the positions analyzed from the base relative to the length of the cochlea. Arrowheads indicate the row of pillar cells. Brackets indicate OHC rows. Lateral is up in all micrographs. Scale bars, 10  $\mu$ m.

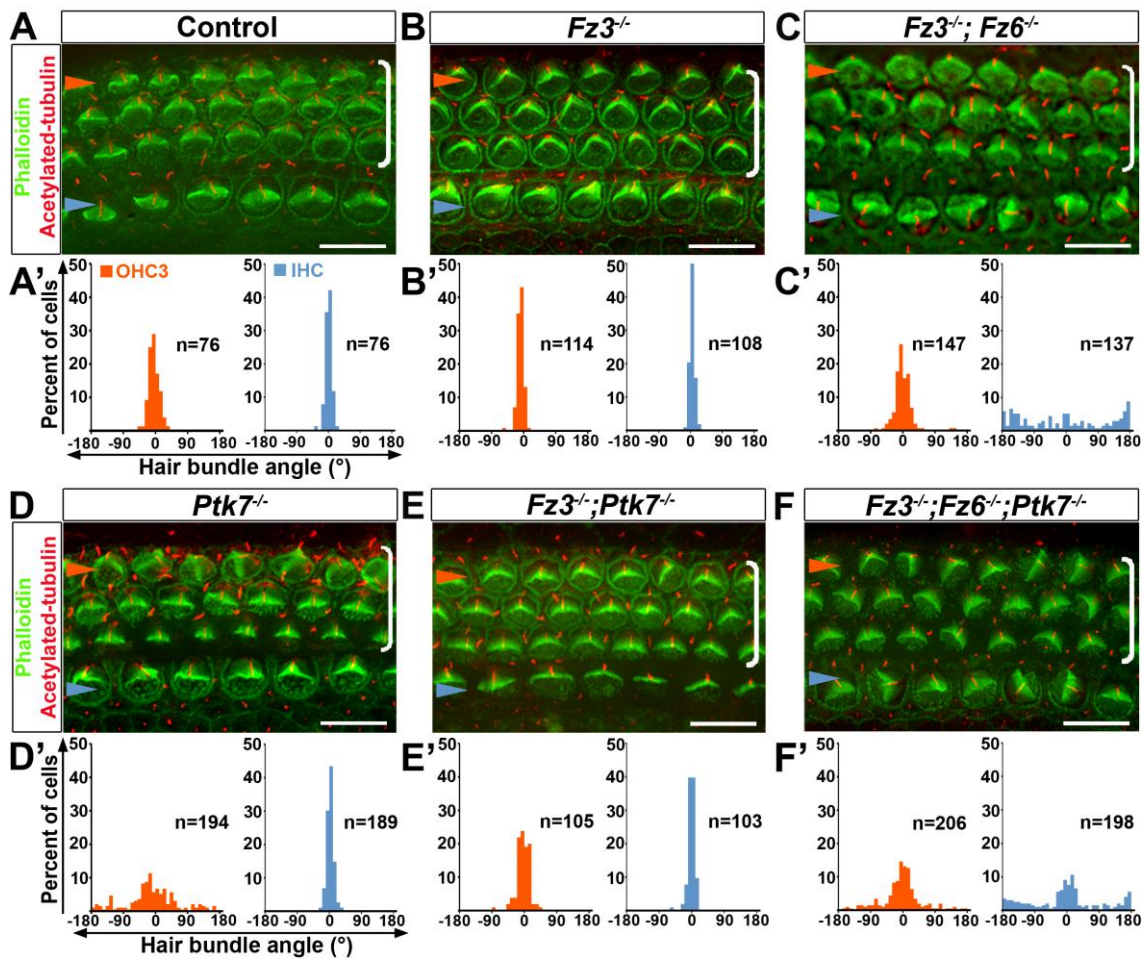


### Figure 6. Epistasis Analysis of *Ptk7* and *Fz3/Fz6* in Hair Cell PCP

(A–F) Basal region (15% cochlear length) of E18.5 cochleae stained with phalloidin (green) and acetylated tubulin (red) to visualize the stereocilia and the kinocilium, respectively. Genotypes are indicated above the panels. (A'–F')

Quantification of bundle orientation in OHC3 (orange bars) and IHC (blue bars) rows for the indicated genotypes. (A and B) In control (A, A') and *Fz3*<sup>-/-</sup> (B, B') cochleae, OHC3 and IHC bundle orientation do not deviate beyond 30° from the medial-lateral axis. (C and C') In *Fz3*<sup>-/-</sup>; *Fz6*<sup>-/-</sup> mutants, the bundle orientation defect was most pronounced in IHCs. (D and D') In *Ptk7*<sup>-/-</sup> mutants, bundle orientation defects were most pronounced in OHC3s. (E and E') In *Fz3*<sup>-/-</sup>; *Ptk7*<sup>-/-</sup> mutants, bundle orientation in OHC3s was significantly improved compared to *Ptk7*<sup>-/-</sup> mutants. (F and F') *Fz3*<sup>-/-</sup>; *Fz6*<sup>-/-</sup>; *Ptk7*<sup>-/-</sup> triple mutants displayed an additive defect in bundle orientation. Blue arrowheads indicate the row of IHCs, orange arrowheads indicate the OHC3 row, and brackets indicate all OHC rows. Lateral is up in all micrographs. Scale bars represent 10 μm.

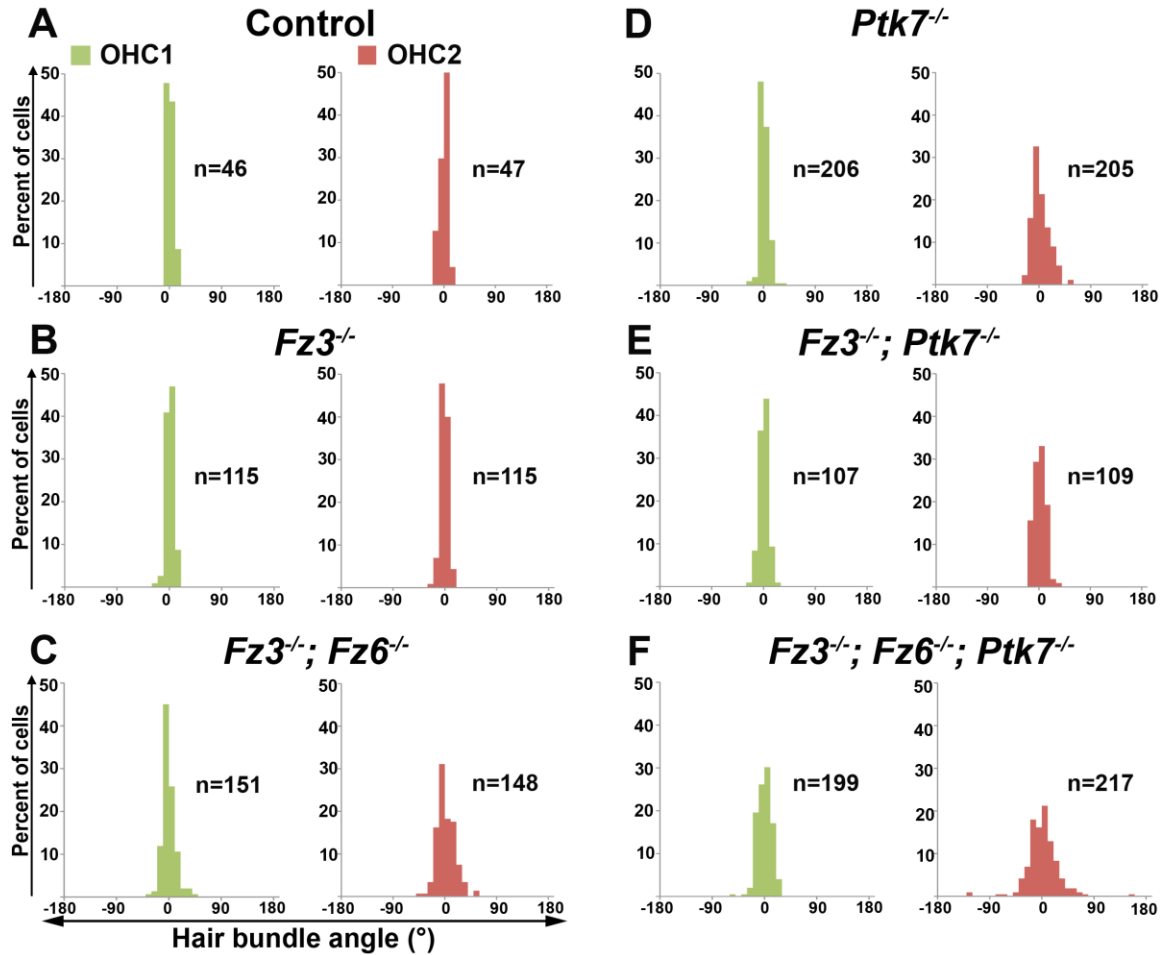


**Figure 7. Quantification of stereociliary bundle orientation for OHC1 and OHC2.**

(A-F) Quantification of stereociliary bundle orientation for rows OHC1 (green bars) and OHC2 (red bars) for the indicated genotypes. Cells were scored in the same manner as in Figure 4. Overall bundle orientation defect in OHC1 and OHC2 showed a consistent pattern of genetic interactions compared to other hair cell rows.

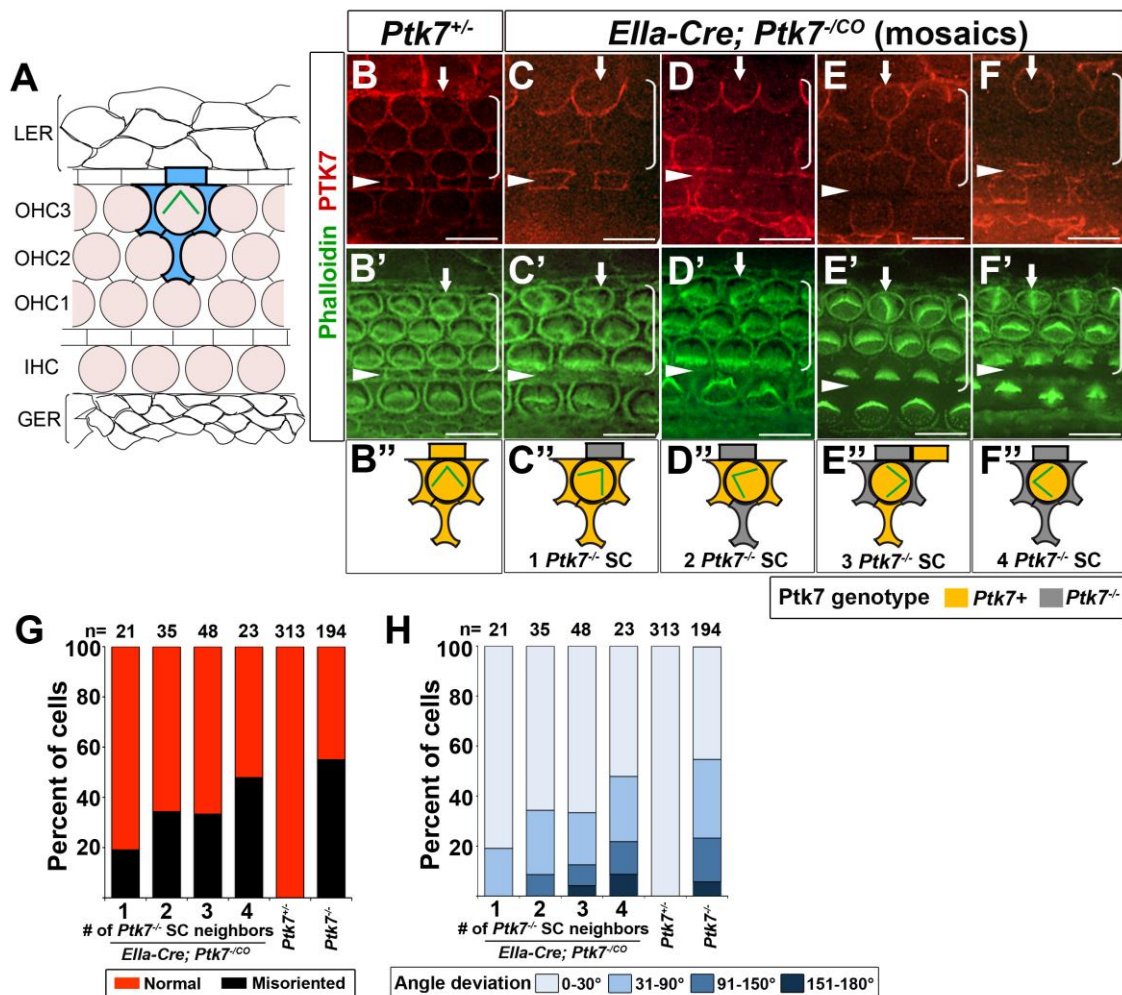


### Figure 8. Mosaic Analysis of *Ptk7* in Hair Cell PCP

(A) Schematic diagram of cellular organization in the OC. Hair cells (shaded light pink) are separated from one another by intervening supporting cells. Each hair cell in OHC3 is immediately surrounded by four supporting cells (shaded in blue). Flanking the OC are cells of the lesser epithelial ridge (LER) and the greater epithelial ridge (GER). (B–F") Midbasal region (25% cochlear length) of E18.5 cochleae stained with PTK7 antibodies (red) and phalloidin (green). (B and B') In controls, PTK7 is expressed in both hair cells and supporting cells and localized to cell-cell contacts. (C–F") Examples of *Ptk7* mosaics in *Ella-Cre; Ptk7<sup>+/CO</sup>* cochleae. *Ptk7<sup>+</sup>* hair cells with misoriented stereociliary bundles (arrows) surrounded by different numbers of *Ptk7<sup>-/-</sup>* supporting cells (SC) are shown and schematized. (G and H) In *Ella-Cre; Ptk7<sup>-/CO</sup>* mosaic cochleae, both the penetrance (G) and the severity (H) of bundle orientation defects in *Ptk7<sup>+</sup>* OHC3 positively correlates with the number of *Ptk7<sup>-/-</sup>* supporting cell neighbors. Arrowheads indicate the row of pillar cells. Brackets indicate OHC rows. Lateral is up in all micrographs. Scale bars represent 10  $\mu\text{m}$ .

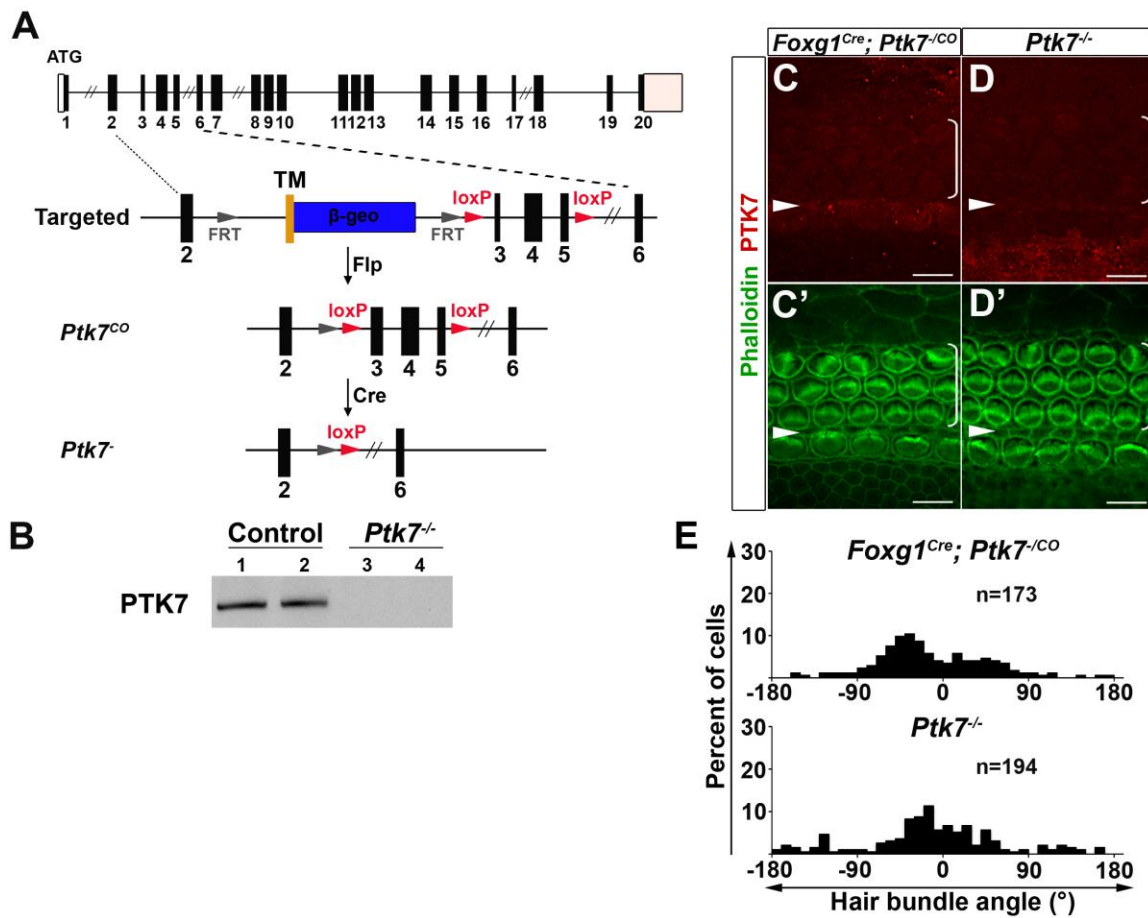


**Figure 9. Conditional inactivation of *Ptk7* using the Cre-loxP technology.**

(A) Generation of the *Ptk7*<sup>CO</sup> allele. A gene-trap strategy was used to target loxP sites into the *Ptk7* locus. The FRT-flanked “secretory gene-trap” cassette contains a transmembrane domain (TM) followed by  $\beta$ geo, a fusion of  $\beta$ -galactosidase and neomycin phosphotransferase. The *Ptk7*<sup>CO</sup> allele was generated by Flp-mediated removal of the gene-trap cassette. In the *Ptk7*<sup>CO</sup> allele, exons 3-5 were flanked by loxP sites (red triangles). The *Ptk7*<sup>-</sup> allele was generated by Cre-mediated deletion of exons 3-5, predicted to cause out-of-frame splicing. (B) Western blot of E16.5 brain lysates showed absence of PTK7 protein from *Ptk7*<sup>-</sup> mutants, indicating that *Ptk7* is a null allele. (C-D') E18.5 cochlear whole-mounts from the mid-basal region (25% of cochlear length) of *Foxg1*<sup>Cre</sup>; *Ptk7*<sup>CO</sup> (C, C') and *Ptk7*<sup>-</sup> cochleae (D, D') stained with PTK7 (red) and phalloidin (green). Arrowheads indicate the row of pillar cells. Brackets indicate OHC rows. Lateral is up in all micrographs. Scale bars, 10  $\mu$ m. (E) OHC3 bundle orientation defects in E18.5 *Foxg1*<sup>Cre</sup>; *Ptk7*<sup>CO</sup> mutants were similar to *Ptk7*<sup>-</sup> cochleae, indicating that *Ptk7* is required in cochlear epithelial cells.

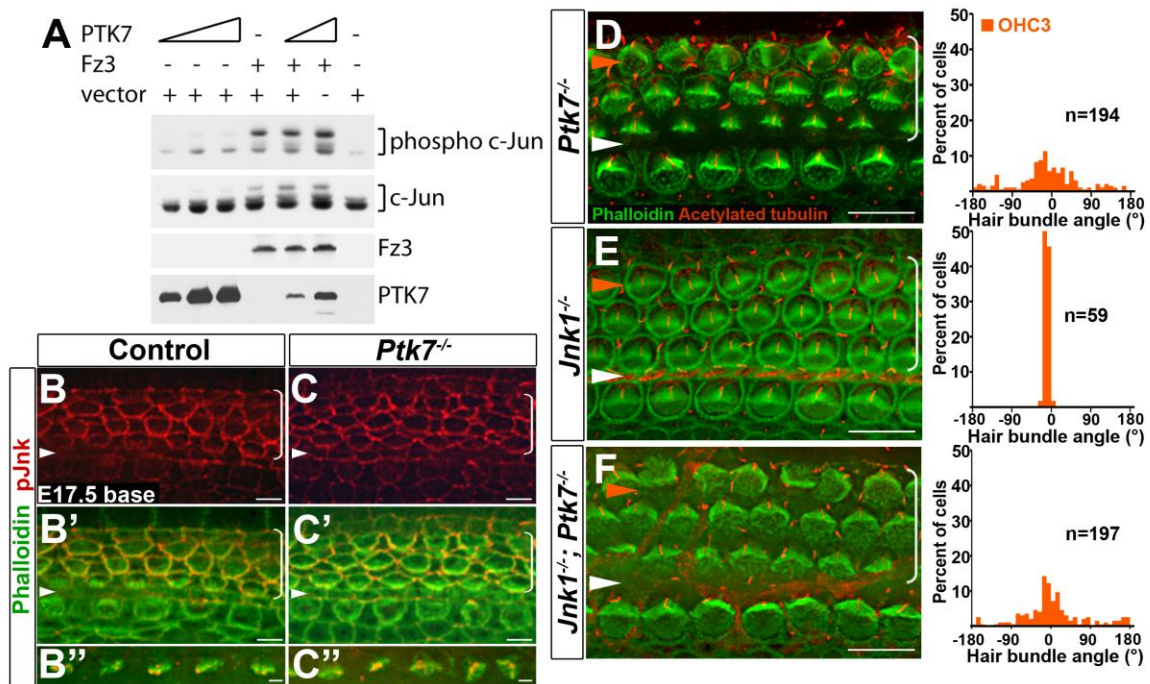


**Figure 10. JNK Signaling Is Unlikely to Mediate PTK7 Function in the OC**

(A) PTK7 expression has no effect on JNK activation in vitro. HEK293T cells were transfected either with PTK7, Fz3, or both and assayed for c-Jun phosphorylation. (B–C'') In the middle turn of E17.5 OC (50% cochlear length), pJNK localization (red) in the *Ptk7*<sup>-/-</sup> OC (C–C'') was similar to the control (B–B''). Green, phalloidin staining. (D–F) Basal region (15% cochlear length) of E18.5 *Ptk7*<sup>-/-</sup> (D), *Jnk1*<sup>-/-</sup> (E), and *Jnk1*<sup>-/-</sup>;*Ptk7*<sup>-/-</sup> (F) cochleae stained with phalloidin (green) and acetylated tubulin (red). Quantifications of bundle orientation of OHC3s are shown to the right. White arrowheads indicate the row of pillar cells; orange arrowheads indicate the OHC3 row. Brackets indicate OHC rows. Lateral is up in all micrographs. Scale bars represent 6µm in (B)–(C'), 2µm in (B'') and (C''), and 10µm in (D)–(F).

(Panel A was contributed by Andreeva A, Panels B-C'' were contributed by Sipe CW)

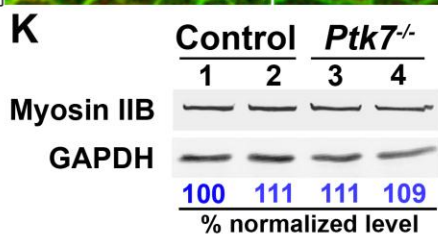
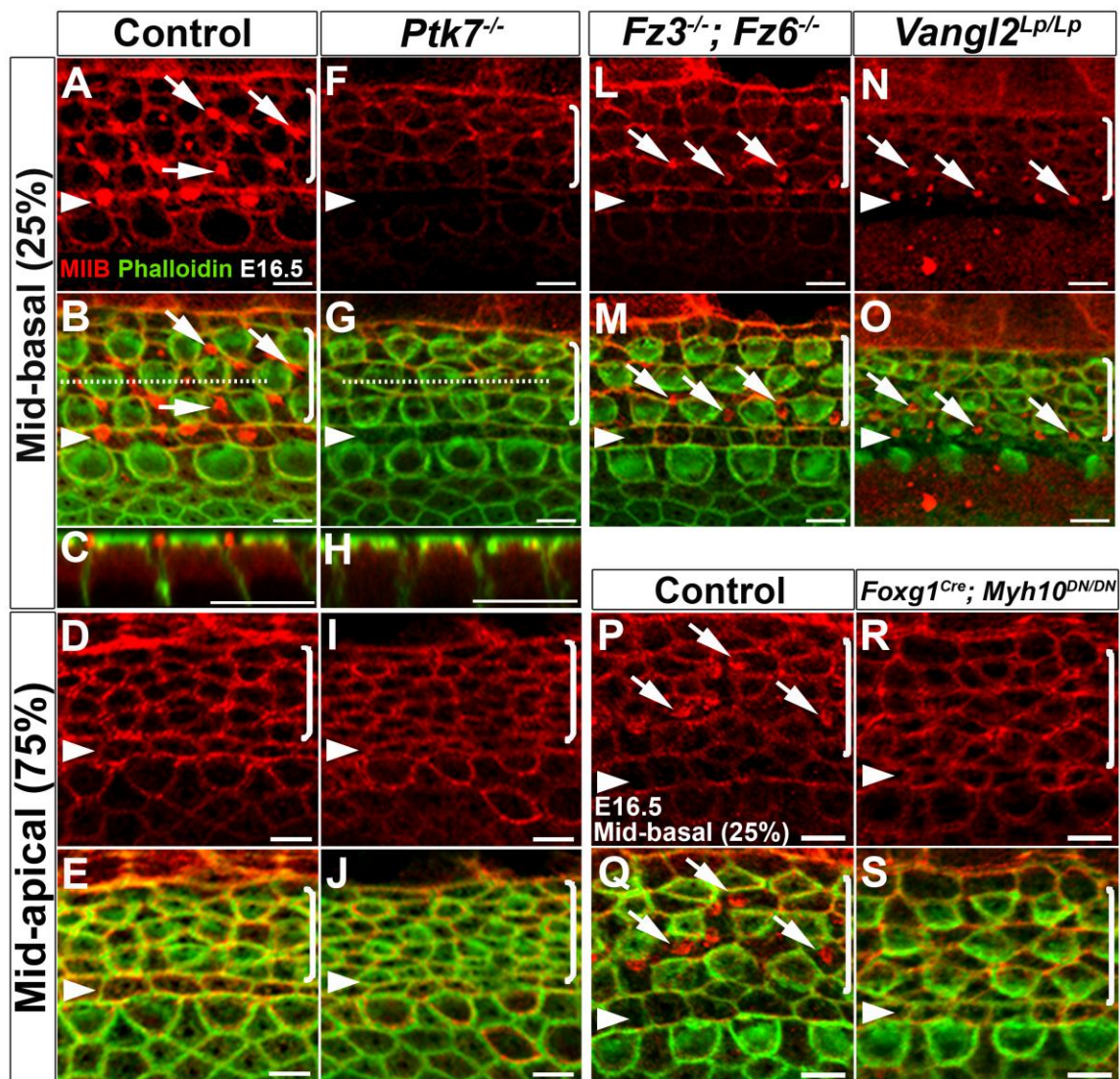


**Figure 11. *Ptk7* and the Noncanonical Wnt Pathway Differentially Regulate a Contractile Myosin IIB Network in Supporting Cells**

(A–J, L–S) Confocal images of MIIB (red) and phalloidin (green) staining in the OC at E16.5. (A–E) In the control OC, MIIB is localized to cell-cell contacts and to apical foci in the supporting cells in the midbasal region of the OC (A–C). (F–J) In *Ptk7*<sup>-/-</sup> OC, apical MIIB foci were absent from supporting cells (F–H) and overall junctional MIIB staining was reduced. (C and H) Z projections along the dashed lines in (B) and (G), respectively, showing the apical position of the MIIB foci in supporting cells. (K) Total levels of MIIB in E16.5 *Ptk7*<sup>-/-</sup> cochleae were comparable to controls. Lysates from four cochleae of the same genotype were pooled and loaded in each lane. GAPDH served as loading control. Numbers on the bottom indicate percentage of normalized levels. (L–O) Apical MIIB foci (arrows) were still present in the supporting cells of *Fz3*<sup>-/-</sup>; *Fz6*<sup>-/-</sup> (L, M) and *Vangl2*<sup>Lp/Lp</sup> (N, O) mutants, albeit smaller in size. (P and Q) Wild-type MIIB is localized to cell-cell contacts and apical foci in supporting cells (arrows). (R and S) ATPase-deficient MIIB (R709C) was localized to cell-cell contacts but failed to assemble into apical foci in supporting cells. Percentages indicate the distance of the positions analyzed from the base relative to the length of the cochlea. Arrowheads indicate the row of pillar cells. Brackets indicate OHC rows. Lateral is up in all micrographs. Scale bars represent 5 μm.

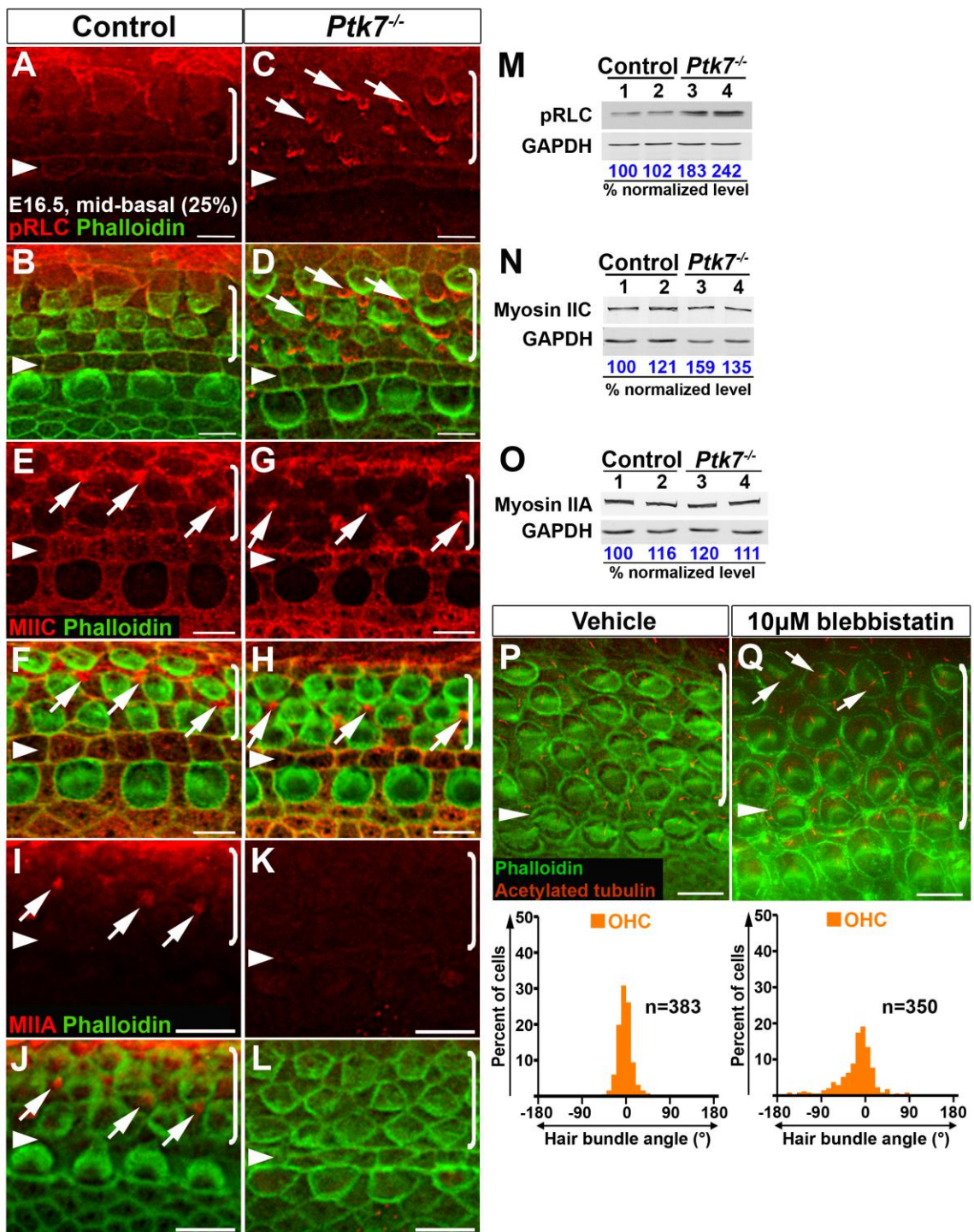


### Figure 12. *Ptk7* Regulates Myosin II Activity to Orient Hair Cell PCP

(A–L) Localization of pRLC (A–D), MIIC (E–H), and MIIA (I–L) in the midbasal region of OC (25% cochlear length) at E16.5. Green, phalloidin staining. (A and B) In the control, pRLC (red) is localized to cell-cell contacts. (C and D) In *Ptk7*<sup>-/-</sup> OC, pRLC staining was decreased at cell boundaries but increased in apical foci in supporting cells (arrows). (E and F) In the control, MIIC (red) localizes to cell-cell contacts and apical foci in supporting cells (arrows). (G and H) In *Ptk7*<sup>-/-</sup> OC, MIIC staining was reduced at cell boundaries but still localized to apical foci in supporting cells (arrows). (I and J) In the control, MIIA (red) is localized to apical foci in supporting cells (arrows). (K and L) In *Ptk7*<sup>-/-</sup> OC, MIIA staining was undetectable. (M–O) Western blot analysis of total levels of pRLC, MIIC, and MIIA in E16.5 *Ptk7*<sup>-/-</sup> cochleae. Lysates from four cochleae of the same genotype were pooled and loaded in each lane. GAPDH served as loading control. Numbers on the bottom indicate percentage of normalized levels. (P and Q) Phalloidin (green) and acetylated-tubulin (red) staining of cochlear explants treated with either vehicle (P) or 10μM blebbistatin (Q), with quantification of bundle orientation shown beneath. Arrows indicate examples of misoriented stereociliary bundles in blebbistatin-treated explants. Arrowheads indicate the row of pillar cells. Brackets indicate OHC rows. Lateral is up in all micrographs. Scale bars represent 5 μm in (A–H) and 6μm in (I–L) and (P)–(Q).

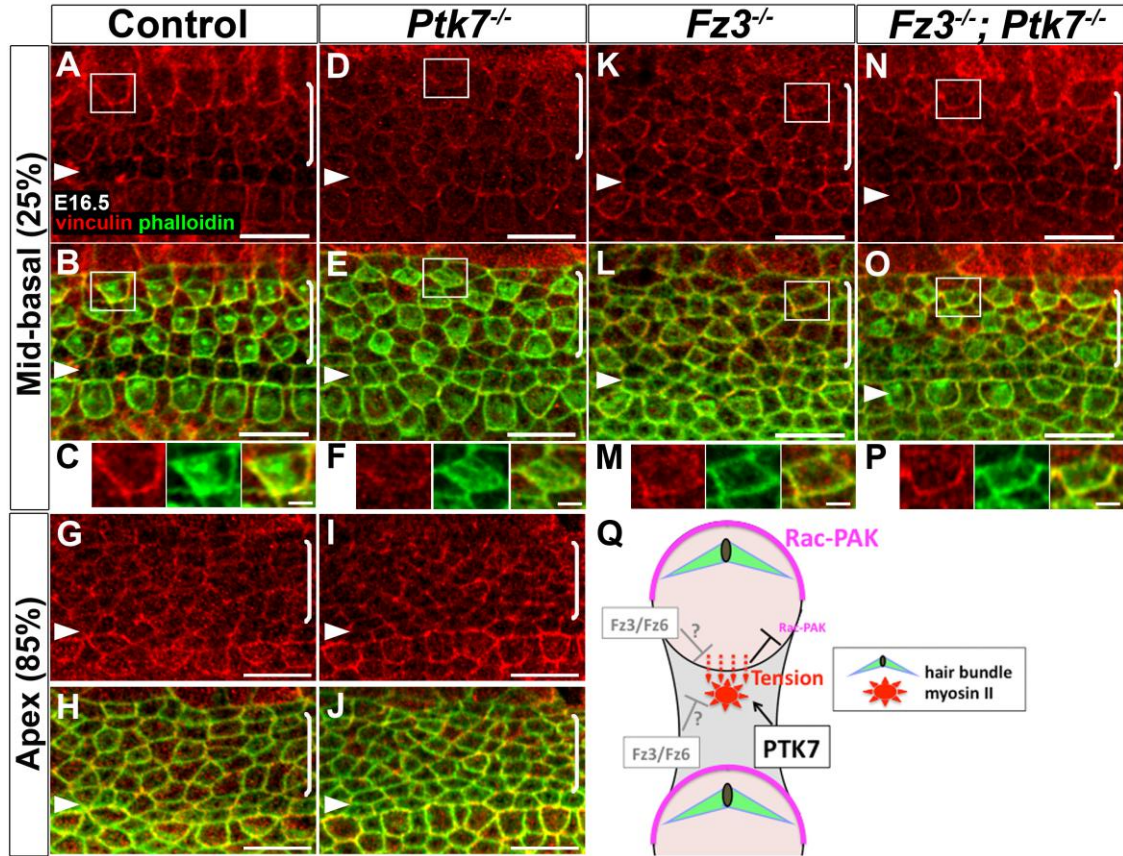


**Figure 13. Planar Asymmetry of Junctional Vinculin Is Abolished in *Ptk7*<sup>-/-</sup> OC and Restored in *Fz3*<sup>-/-</sup>; *Ptk7*<sup>-/-</sup> OC.**

(A–P) Confocal images of vinculin (red) and phalloidin (green) staining at E16.5.

(A–C) In the mid-basal region (25% cochlear length) of control OC, vinculin was asymmetrically localized along cell-cell junctions and enriched on the medial side of hair cell membranes. (D–F) In the mid-basal region of *Ptk7*<sup>-/-</sup> OC, junctional vinculin localization lost planar asymmetry and was greatly reduced compared to controls. (G–J) In the apex (85% cochlear length), junctional vinculin staining in the control (G, H) and *Ptk7*<sup>-/-</sup> (I, J) OC was similar, with no apparent planar asymmetry. (K–M) In the midbasal region of *Fz3*<sup>-/-</sup> OC, junctional vinculin staining was similar to controls but its planar asymmetry was less robust. (N–P) In the midbasal region of the *Fz3*<sup>-/-</sup>; *Ptk7*<sup>-/-</sup> OC, planar asymmetry of junctional vinculin was restored. (C, F, M, P) High magnification of the boxed hair cell above.

Lateral is up in all micrographs. Scale bars represent 2 μm in (C), (F), (M), and

(P) and 10 μm in other panels. (Q) A proposed model for regulation of hair cell

PCP by *Ptk7*. Acting in supporting cells (shaded gray), *Ptk7* mediates the

assembly of a contractile apical myosin II network to exert pulling forces on the

medial border of hair cells, leading to enhanced contractile tension as evidenced

by increased vinculin recruitment. In turn, polarized contractile tension promotes

asymmetric Rac-PAK activity on the lateral side of hair cell cortex (shown in

magenta) to orient the stereociliary bundle. *Fz3/Fz6* may act in hair cells and/or

supporting cells to counterbalance *Ptk7*-mediated contractile tension on hair

cells.

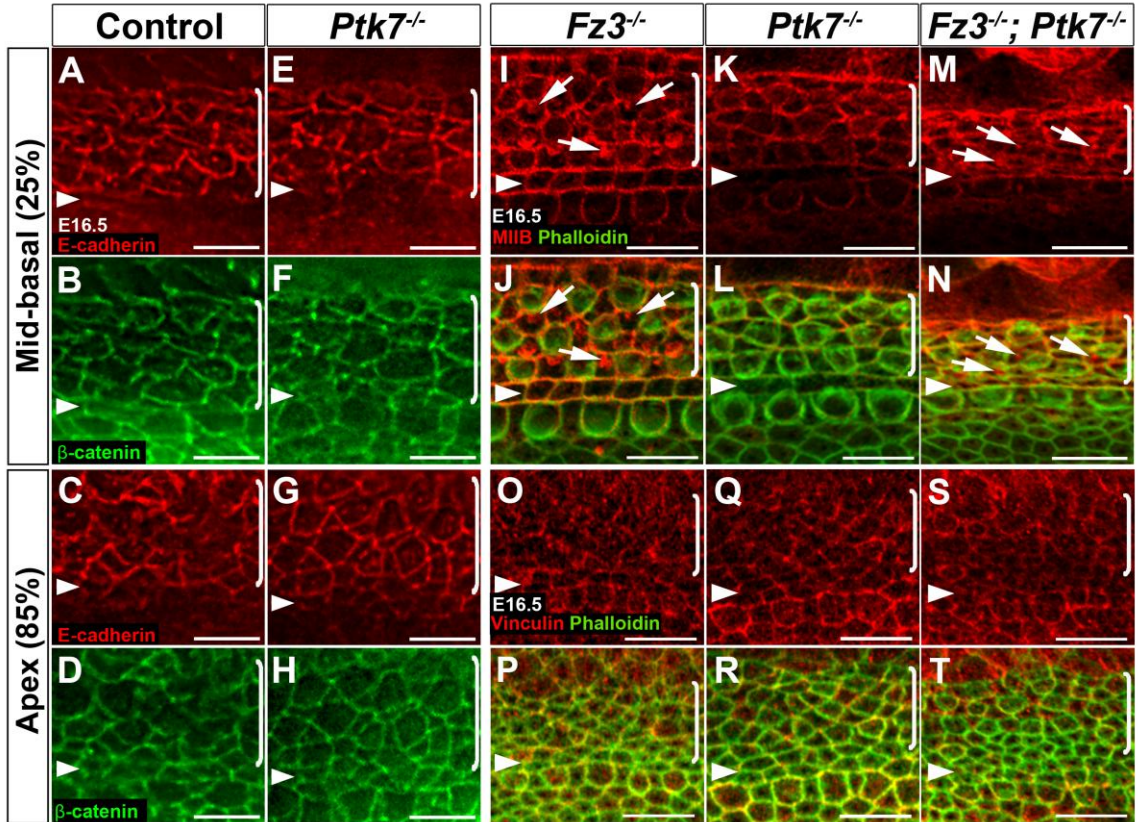


**Figure 14. E-cadherin and  $\beta$ -catenin localization in *Ptk7*<sup>-/-</sup> cochleae and myosin IIB and vinculin localization in *Fz3*<sup>-/-</sup>; *Ptk7*<sup>-/-</sup> cochleae.**

(A-H) E16.5 cochlear whole-mounts stained with E-cadherin (red) and  $\beta$ -catenin (green) antibodies. Compared to controls (A-D), distribution of these junctional proteins were normal in *Ptk7*<sup>-/-</sup> OC (E-H) embryos. (I-N) Confocal images of MIIB (red) and phalloidin (green) staining in the mid-basal region of OC at E16.5. (I, J) In *Fz3*<sup>-/-</sup> OC, MIIB is localized to cell-cell contacts, as well as in apical foci in supporting cells (arrows). (K, L) In *Ptk7*<sup>-/-</sup> OC, junctional localization of MIIB is reduced and apical MIIB foci in supporting cells are absent. (M, N) In *Fz3*<sup>-/-</sup>; *Ptk7*<sup>-/-</sup> OC, junctional staining of MIIB was increased compared to *Ptk7*<sup>-/-</sup> OC and assembly of MIIB foci in supporting cells was restored. (O-T) Confocal images of vinculin (red) and phalloidin (green) staining in the apex at E16.5. Similar staining of junctional vinculin were observed in *Fz3*<sup>-/-</sup> (O, P), *Ptk7*<sup>-/-</sup> (Q, R) and *Fz3*<sup>-/-</sup>; *Ptk7*<sup>-/-</sup> OC (S, T) with no apparent planar asymmetry. Percentages indicate the distance of the positions analyzed from the base relative to the length of the cochlea. Arrowheads indicate the row of pillar cells. Brackets indicate OHC rows. Lateral is up in all micrographs. Scale bars, A-H, 6  $\mu$ m; I-T, 10  $\mu$ m.

(Panels A-H were contributed by Sipe CW.)

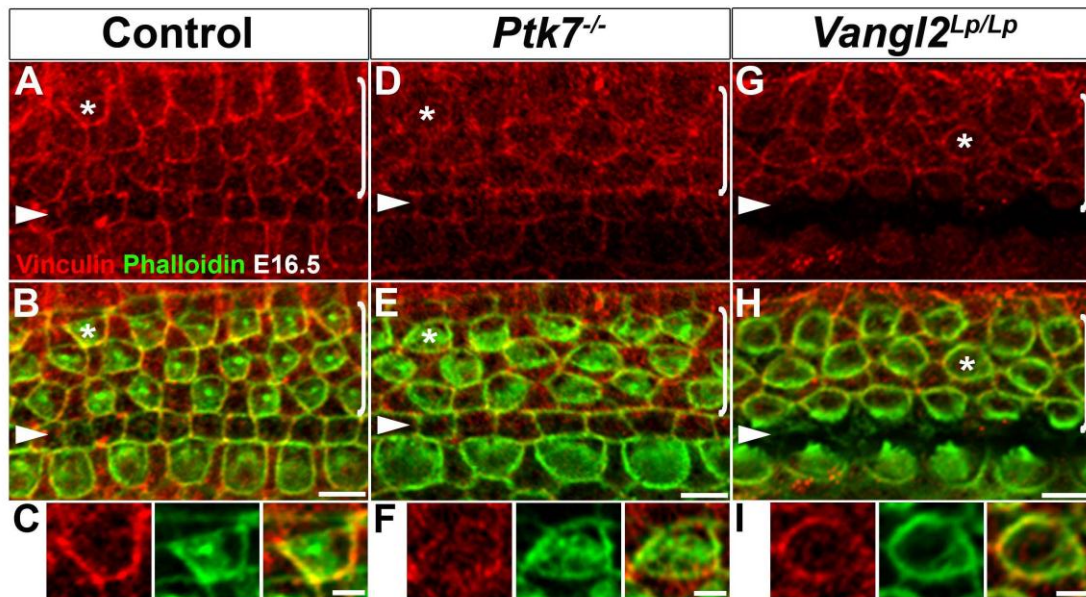


**Figure 15. Vinculin planar asymmetry is differentially regulated by *Ptk7* and the non-canonical Wnt/PCP pathway.** Whole mount E16.5 cochleae stained with vinculin (red) and phalloidin (green). (A-B) In control OC, vinculin is localized to cell contacts and is medially enriched in hair cells. (D-E) Junctional vinculin staining is reduced and planar asymmetry is lost in *Ptk7*<sup>-/-</sup> OC. (G-H) In *Vangl2*<sup>Lp/Lp</sup> OC, vinculin is distributed more evenly at cell-cell contacts, and in some cases, planar asymmetry of vinculin was misoriented (asterisk). (C, F, I) Higher magnification cells marked with asterisk in (A), (D) and (G), respectively. Arrowheads indicate the row of pillar cells. Brackets indicate OHC rows. Lateral is up in all micrographs. Scale bars; C, F, I, 2 $\mu$ m; others 5  $\mu$ m.

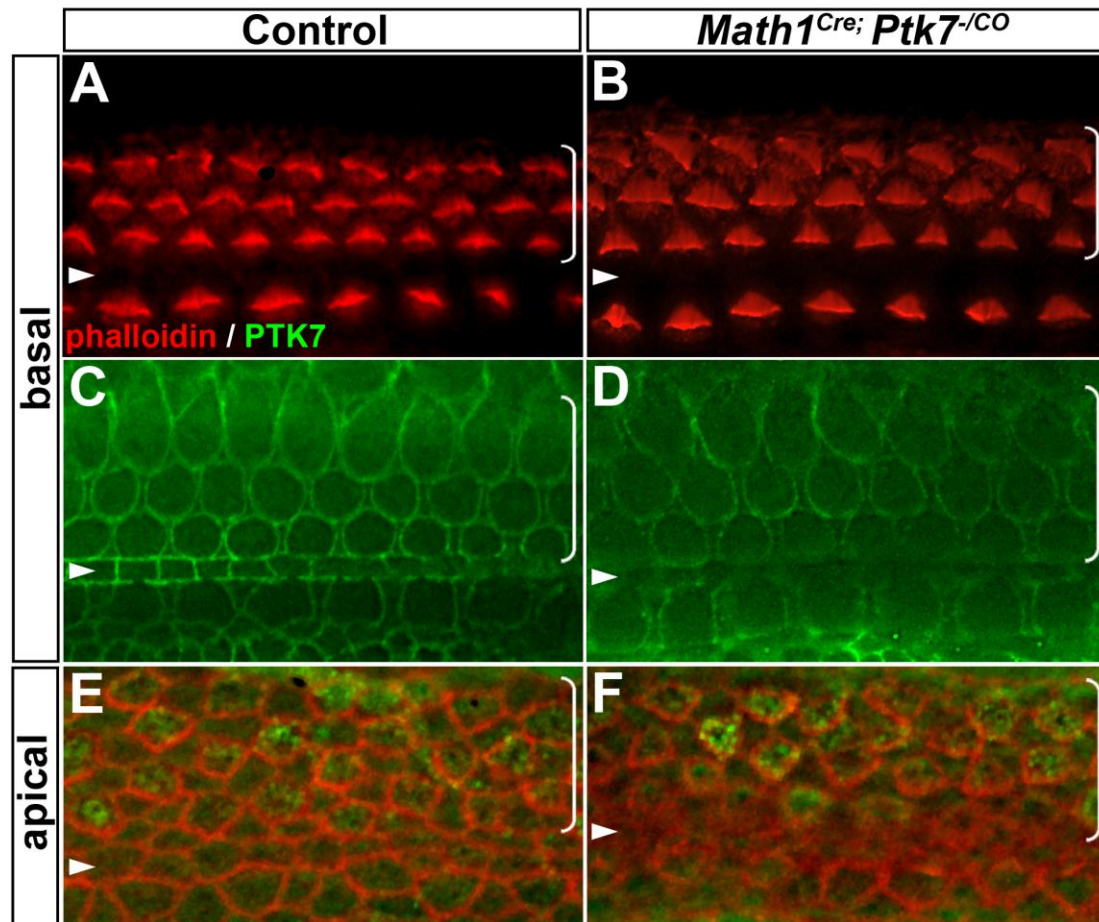


**Figure 16. Analysis of *Math1<sup>Cre</sup>; Ptk7<sup>CO</sup>* cochleae.** (A-B) E17.5 whole mount cochleae stained with phalloidin (red) to visualize the stereociliary bundle. In the basal region, no significant differences were observed in stereociliary bundle orientation in *Math1<sup>Cre</sup>; Ptk7<sup>CO</sup>* OC (B) compared to control (A). (C-E) Immunostaining of PTK7 (green). (C-D) In the basal region (15% of cochlear length) of control (C) and *Math1<sup>Cre</sup>; Ptk7<sup>CO</sup>* (D) OC, PTK7 is localized along hair cell and supporting cell contacts. (E-F) In the apex region of control OC (90% cochlear length), PTK7 staining is observed on the apical surfaces of outer hair cells and is not disrupted in *Math1<sup>Cre</sup>; Ptk7<sup>CO</sup>* (F) OC. Arrowheads indicate the row of pillar cells. Brackets indicate OHC rows. Lateral is up in all micrographs.

**CHAPTER 3: PTK7-Src signaling at epithelial cell contacts mediates spatial organization of actomyosin and planar cell polarity.**

This chapter is based on a manuscript that is currently under review.

### 3.1 Introduction

Actomyosin contractility in nonmuscle cells is a central regulator of cell shape change and tissue morphogenesis [164]. Actin filaments and the myosin II motor, which consists of two heavy chains, two essential light chains and two regulatory light chains (RLC), assemble into contractile subcellular structures and supracellular networks to drive diverse physiological processes, including cell division, cell migration and tissue morphogenesis [163]. During development, dynamic actomyosin networks have been shown to mediate the collective behavior of an interacting network of cells. For example, during *Drosophila* gastrulation and vertebrate neural tube closure, coordinated apical constriction, or contraction of the cell apex, results in bending and invagination of an epithelial cell sheet [178, 179]. During embryonic axis elongation in *Drosophila* and *Xenopus*, anisotropic contractile forces mediate directional cell intercalation and convergent extension [33, 162, 213]. However, mechanisms underlying precise spatial and temporal control of actomyosin assembly on a tissue scale remain poorly understood.

Emerging evidence indicates that planar cell polarity (PCP) signaling plays an important role in spatial regulation of actomyosin contractility during vertebrate tissue morphogenesis. First discovered in *Drosophila* where it regulates polarity within the plane of the wing epithelial cell sheet, an evolutionarily conserved core PCP pathway regulates morphogenesis of both epithelial and non-epithelial tissues in vertebrates, including convergent extension, neural tube closure and PCP in the auditory sensory epithelium [22]. The core PCP pathway signals

through the small GTPase RhoA and its downstream effector Rho-associated kinases (ROCK), which phosphorylates myosin RLC to stimulate actomyosin contractility.

In addition to the core PCP pathway, both invertebrates and vertebrates employ alternative mechanisms for spatial regulation of actomyosin contractility to drive planar polarized cell behavior. In *Drosophila*, germband extension is driven by anisotropic junctional contractility independently of the core PCP pathway and is likely mediated by cadherin-mediated mechanotransduction and junctional remodeling [33, 36, 162]. In the mouse, genetic evidence suggest that a *Protein tyrosine kinase 7 (Ptk7)*-mediated pathway acts in concert with the core PCP pathway to differentially regulate actomyosin contractility and orient PCP in the auditory sensory epithelium [214].

*Ptk7* was previously identified as a novel regulator of PCP in vertebrates [1]. *Ptk7* is required for many of the same morphogenetic processes regulated by the core PCP pathway [1, 149, 152, 155, 157]. *Ptk7* encodes a conserved receptor-tyrosine kinase (RTK)-like molecule, which is predicted to lack endogenous kinase activity because the invariant 'DFG' motif essential for correct positioning of ATP is replaced with 'ALG'. Interestingly, studies in various model organisms suggest that vertebrate *Ptk7* orthologs have evolved different functions and signaling mechanisms [149, 156, 157, 214]. Whereas *Xenopus* *Ptk7* mediates membrane recruitment of the core PCP protein Dishevelled via its cytoplasmic domain, *Ptk7* regulates PCP and Wnt signaling in zebrafish via its extracellular domain. In the mouse, *Ptk7* regulates PCP in the auditory sensory

epithelium through modulation of junctional contractility, but the underlying mechanism is unknown.

We have uncovered a possible connection between *Ptk7* and myosin II in Madin-Darby canine kidney (MDCK) epithelial cells. In MDCK cells, *Ptk7* knockdown (KD) gives rise to cell shape and actomyosin defects that are consistent with our published observations *in vivo* in *Ptk7*<sup>-/-</sup> OC. We found that PTK7 interacts with the tyrosine kinase Src and regulates active Src localization at cell-cell contacts. Interestingly, expression of dominant negative (DN) Src in MDCK cells resulted in similar actomyosin defects as *Ptk7*KD cells. Our biochemical data suggests that *Ptk7* stimulates Src signaling activity at cell-cell contacts. We further identify ROCK2 as a target of junctional PTK7-Src signaling. *Ptk7*KD cells reduced the level of active Src at cell-cell contacts, resulting in delocalization of ROCK2 from cell-cell contacts and decreased junctional contractility, accompanied by increased total ROCK activity and basal actomyosin defects. These findings provide evidence that *Ptk7* signals through Src to regulate actomyosin contractility.

Here, we used the mouse auditory sensory epithelium *in vivo* to shed light on the mechanisms by which *Ptk7* regulates actomyosin contractility during mammalian epithelial morphogenesis. We present evidence that planar polarized Src signaling is critical for PCP regulation in the auditory sensory epithelium and that PTK7-Src signaling regulates tyrosine phosphorylation of junctional ROCK2. In addition, we have identified other potential targets of *Ptk7*-Src signaling that are important for actomyosin regulation in the OC.

## 3.2 Results

### 3.2.1 PTK7 positively regulates Src signaling and ROCK2 phosphorylation in the mouse auditory sensory epithelium

Having identified Src as a likely signaling intermediary of *Ptk7* in MDCK cells, we investigated whether Src signaling is relevant for *Ptk7*-mediated epithelial PCP regulation *in vivo*. The mouse auditory sensory epithelium, or the organ of Corti (OC), located in the cochlea is a well-established model for PCP signaling. The V-shaped hair bundles atop auditory hair cells and their uniform orientation serve as a robust readout for PCP. To determine if *Ptk7* regulates active Src localization in the OC, we first examined pY416-Src localization at embryonic day (E) 16.5. Active Src was localized to intercellular junctions in control OC. Interestingly, pY416-Src staining was planar polarized along cell boundaries between outer hair cells (OHC) and supporting cells, with an average medial/lateral intensity ratio of 1.7 (Figure 17A-C, M). By contrast, overall staining and planar asymmetry of pY416-Src was significantly reduced in *Ptk7*<sup>-/-</sup> OC (Figure 17D-F, M). Overall levels of pY416-Src were decreased by ~40% in *Ptk7*<sup>-/-</sup> cochleae (Figure 17O). Taken together, these results indicate that PTK7 positively regulates junctional Src signaling in the OC.

To identify targets of PTK7-Src signaling important for myosin II regulation in the OC, we examined the localization and phosphorylation of ROCK2, a likely target of junctional Src signaling in MDCK cells. Rho kinase (ROCK) stimulates myosin II activity through direct phosphorylation of RLC and inhibition of the RLC phosphatase by phosphorylating the myosin phosphatase target subunit 1

(MYPT1). In control OC, ROCK2 was localized to intercellular junctions in a punctate pattern. Despite cellular disorganization, ROCK2 was still localized to intercellular junctions in *Ptk7*<sup>-/-</sup> OC (Figure 18). Remarkably, pY722-ROCK2 showed planar-polarized junctional localization in control OC, similar to that of pY416-Src (Figure 17G-I, N). This planar asymmetry was likewise disrupted in *Ptk7*<sup>-/-</sup> OC (Figure 17J-L, N). Thus, PTK7 mediates ROCK2 tyrosine phosphorylation at cell-cell contacts *in vivo*.

### **3.2.2 Src inhibition and hyperactivation both result in PCP defects in the OC**

Disrupted localization of active Src in *Ptk7*<sup>-/-</sup> cochleae suggests that Src signaling is required for PCP in the OC. In the mouse, Src family kinases (SFKs) Src, Yes and Fyn are ubiquitously expressed and function redundantly [215]. Therefore, to determine the role of Src signaling in the OC, we took a pharmacological approach and treated cochlear explants with the SFK inhibitor SU6656 [216]. Vehicle-treated explants had normal PCP: the axonemal kinocilium at the vertex of V-shaped hair bundles were positioned near the lateral pole of hair cells (Figure 19A, C). By contrast, many hair bundles in SU6656-treated explants were misoriented relative to the medial-lateral axis of the cochlea (Figure 19B, arrows; 19D). Immunoblotting of treated cochlear tissues confirmed that Src inhibitors effectively reduced pY416-Src levels (Figure 19E). Thus, we conclude that SFKs and/or structurally related kinases are required for PCP in the OC.

Planar polarized pY416-Src localization suggests that spatial regulation of Src signaling is important for PCP in the OC. To test this idea, we uniformly elevated levels of Src signaling in the cochlea using a conditional allele of C-terminal Src kinase [217]. *Csk* negatively regulates SFK activity by phosphorylating a conserved C-terminal tyrosine critical for auto-inhibition (Y527 in Src). *Csk* knockout mice exhibited hyperactivation of SFKs, resulting in neural tube defects and lethality around E10.5 [218]. In *Csk<sup>CKO</sup>* mutants, where *Csk* was deleted in the cochlea using a *Pax2Cre* driver [219], two classes of PCP defects were observed. *Csk<sup>CKO</sup>* cochleae were generally shorter and widened (Figure 19F, G). In the basal region of the cochlea, the hair bundle and the kinocilium were often misoriented relative to the medial-lateral axis of the cochlea (Figure 17I, K, arrows). In the apical (and occasionally basal) region of the cochlea, there was an extra row of outer hair cells (Figure 19L, M), likely due to defects in medial-lateral cell intercalation. Overall pY416-Src levels in *Csk<sup>CKO</sup>* cochleae were increased by ~2 folds (Figure 19N). These results suggest that the level of Src signaling is critical for PCP establishment.

To determine if altered Src signaling affects the core PCP pathway, we examined the asymmetric localization of the core PCP proteins Dvl2 and Fz3. To better match the developmental stage examined in different mutants, we inhibited Src signaling systemically *in vivo* using Bosutinib, a bioavailable dual Src/Abl inhibitor [220]. Membrane recruitment and asymmetric localization of Dvl2 in the OC was largely unchanged in both Bosutinib-treated and *Csk<sup>CKO</sup>* OC (Figure 20A-F). Previous observations suggest that Fz3 localization is sensitive to changes in

cortical cytoskeleton [79, 214]. In Bosutinib-treated and *Csk<sup>CKO</sup>* OC, Fz3 was still asymmetrically localized, albeit with reduced staining intensity, suggesting that altered Src signaling may affect the cortical cytoskeleton (Figure 20G-L).

Together, these results suggest that the core PCP pathway was still active when Src signaling is perturbed.

### **3.2.3 Src signaling mediates ROCK2 phosphorylation at intercellular junctions in the OC**

Our data so far suggest that Src is a signaling intermediary between PTK7 and actomyosin contractility. To further test this idea, we assayed the effects of Src inhibition and hyperactivation on the localization of myosin IIB, active Src and pY722-ROCK2 in the OC, all of which are regulated by PTK7. At E16.5, *Ptk7* regulates both junctional myosin IIB and a network of apical myosin IIB foci in supporting cells [214]. Similar to *Ptk7<sup>-/-</sup>* mutants, both Bosutinib treatment and *Csk* deletion disrupted the apical myosin IIB foci in supporting cells, while junctional myosin IIB staining was relatively unchanged, suggesting that normal levels of Src signaling is important for the assembly of the apical myosin network (Figure 21A-F). Of note, *Csk<sup>CKO</sup>* OC was disorganized and much wider along the medial-lateral axis, consistent with cell intercalation defects (Figure 21E, F).

Importantly, planar polarized pY416-Src localization to intercellular junctions was disrupted by both conditions. Whereas Src inhibition greatly reduced junctional pY416-Src staining, in *Csk<sup>CKO</sup>* OC pY416-Src became circumferentially localized around intercellular junctions (Figure 21G-L).

Strikingly, while altered Src signaling did not significantly impact ROCK2 localization to intercellular junctions (Figure 21M-R), pY722-ROCK2 localization closely correlated with pY416-Src staining. It was greatly reduced by Src inhibition and became circumferentially localized around intercellular junctions in *Csk<sup>CKO</sup>* OC (Figure 21S-X). Together, these results identify ROCK2 as a target of junctional Ptk7-Src signaling in the OC.

### **3.2.4 Identification of vinculin and cortactin as potential targets of PTK7-Src signaling in the organ of Corti (unpublished)**

Our analysis in MDCK cells and mouse organ of Corti suggests that PTK7-Src signaling regulates myosin II contractility and ROCK2 localization through both direct and indirect mechanisms. In addition to ROCK2, we hypothesize that there are additional targets of PTK7-Src signaling at intercellular junctions that participate in myosin II regulation. Dynamic actin assembly mediated by the WAVE2-Arp2/3 actin nucleator complex was shown to promote myosin II recruitment and is necessary for generating junctional tension [221]. A number of actin regulatory proteins serve as Src substrates including cortactin and vinculin. Cortactin is a multidomain actin-binding protein enriched at the cell cortex. Src phosphorylation of cortactin promotes Arp2/3 complex-mediated actin polymerization [222]. To test if cortactin is a relevant target of Src signaling in the OC, we analyzed cortactin localization. In E16.5 control OC, we observed that cortactin localizes to cell-cell contacts in a planar polarized fashion similar to

pY416-Src (Figure 22), suggesting a role for cortactin in Src-regulation of actomyosin contractility in the OC.

Previously, we found that vinculin, a tension sensitive actin binding molecule, is enriched along the medial borders between hair cells and supporting cells and its planar asymmetry is dependent on *Ptk7* (See Chapter 2 Figure 13) [214]. Vinculin binds to actin and can nucleate F-actin assembly directly or by interacting with Arp2/3 [223–225]. Interestingly, vinculin was one of the earliest identified tyrosine phosphorylation targets of Src [226]. Src tyrosine phosphorylation of residue 1065 in vinculin induces conformational changes which affect vinculin stability and recruitment at adhesion complexes and force generation, and is essential for Arp2/3 binding [225, 227, 228]. Using a phosphorylation-specific antibody directed against tyrosine 1065, we observed pY1065-vinculin staining at cell-cell junctions and it was enriched at medial borders of hair cells, similar to pY416-Src localization (Figure 23A-C). In *Ptk7* mutants, junctional pY1065-vinculin localization was significantly reduced and its planar asymmetry was lost (Figure 23D-F). These results suggest that *Ptk7* signals through Src to promote vinculin phosphorylation at cell-cell contacts.

### **3.2.5 Vinculin is required for hair cell PCP and regulates apical myosin IIB foci assembly in the OC (unpublished)**

Our observation that junctional planar asymmetry of both total and phosphorylated vinculin was disrupted in *Ptk7* mutants correlates with hair bundle misorientation. We next addressed the functional importance of vinculin in

hair cell PCP. Vinculin (*Vcl*) knockout mice are embryonic lethal due to severe heart and brain defects [229]. Thus, we inactivated vinculin in the cochlea using a *Foxg1<sup>Cre</sup>* driver line and a conditional allele of vinculin (*Vcl<sup>fl</sup>*) [186, 230]. In *Foxg1<sup>Cre</sup>; Vcl<sup>fl/-</sup>* mutant OC, stereociliary bundle misorientation was restricted in the third row of OHCs (Figure 24A-D). While three rows of outer hair cells are normally found in the apex of control OC, conditional vinculin mutant cochleae exhibited an extra row of outer hair cells in the apex (Figure 24E, F). These PCP defects are highly reminiscent of those found in *Ptk7<sup>-/-</sup>* mutants. These results demonstrate that vinculin planar asymmetry is required for hair cell PCP.

Vinculin is recruited to sites of increased tension in a myosin II-dependent manner, and it has become apparent that vinculin is important for force transmission at cell-cell contacts [170]. We posit that vinculin is likely involved in regulating actomyosin contractile tension in the OC. To determine the role of vinculin in actomyosin contractility, we analyzed myosin IIB localization in vinculin mutants. In control OC, myosin IIB is localized to cellular junctions and to apical foci in supporting cells (Figure 25A, B, arrows). In *Foxg1<sup>Cre</sup>; Vcl<sup>fl/-</sup>* mutant OC, junctional myosin IIB localization was modestly reduced and apical myosin IIB foci in supporting cells were either barely detectable or significantly smaller in size (Figure 25C-F, arrows). These results indicate that vinculin regulates the robust assembly of myosin IIB foci in the OC and may function to reinforce actomyosin contractility.

### 3.3 Discussion

How actomyosin contractility is coordinately regulated in groups of mechanically coupled cells to drive tissue morphogenesis is a fundamental question in developmental biology. In addition to the RhoA-ROCK signaling axis [231–234], our study now reveals a novel layer of actomyosin regulation at intercellular junctions. We present evidence that PTK7-Src signaling at cell-cell contacts spatially organizes the actomyosin cytoskeleton to regulate junctional contractility and PCP. Moreover, we identify ROCK2 as one of the targets of junctional PTK7-Src signaling and for the first time implicate ROCK2 tyrosine phosphorylation in the regulation of PCP in the OC.

It is worth noting that MDCK cells and the OC have interesting differences in the regulation of ROCK2 localization and phosphorylation. In MDCK cells, ROCK2 junctional localization depends on PTK7-Src signaling, however the steady state level of ROCK2 phosphorylation is normally very low. In the mouse, on the other hand, ROCK2 was still localized to cell-cell contacts in *Ptk7*<sup>-/-</sup> OC, suggesting that there are additional mechanisms that regulate junctional ROCK localization *in vivo*, as observed in other developing epithelia [235]. By contrast, phospho-Y722 ROCK2 was localized to intercellular junctions in wild-type OC but was severely disrupted in both *Ptk7*<sup>-/-</sup> and Src-inhibited OC. Together, these results suggest that PTK7-Src signaling regulates junctional contractility in part through ROCK2 phosphorylation.

How ROCK2 tyrosine phosphorylation regulates junctional contractility remains to be determined. ROCK2 phosphorylation at Y722 has been shown to be required for focal adhesion turnover and decrease its binding to and activation

by RhoA-GTP [236, 237]. ROCK2 phosphorylation at intercellular junctions may likewise promote the turnover of cadherin adhesions and render ROCK2 insensitive to junctional RhoA-GTP levels. In the mouse OC, pY722 ROCK2 is enriched along the medial boundaries of hair cells. We have previously proposed that junctional contractility is increased at these boundaries, based on the polarized recruitment of vinculin [214]. Thus, junctional ROCK2 tyrosine phosphorylation may be associated with increased contractile tension. Because we found evidence that junctional ROCK2 levels are sensitive to adhesive forces (data not shown), we further speculate that ROCK2 Y722 phosphorylation is part of a feedback regulatory loop that balances junctional ROCK2 levels with intercellular adhesion strength. Curiously, despite decreased junctional contractility, *Ptk7* loss led to increased total levels of RLC phosphorylation both *in vitro* and *in vivo*. This is likely connected to altered ROCK2 localization and activity, as an Y722F ROCK2 mutant showed increased kinase activity and when overexpressed also caused increased RLC phosphorylation [236, 237].

In addition to ROCK2, we propose that two actin regulatory proteins, cortactin and vinculin serve as additional effectors of PTK7-Src signaling. A recent study proposed that Arp2/3 mediated actin assembly is required for promoting and stabilizing junctional tension [221]. Both cortactin and vinculin bind to Arp2/3 and were localized asymmetrically on medial borders of hair cells similarly to active Src, where we believe tension is increased. We further showed that *Ptk7* promotes Src-dependent tyrosine phosphorylation of vinculin at cell-cell contacts in the OC. Vinculin is functionally important for hair cell PCP and is

supported by two pieces of evidence. First, *Ptk7* and the non-canonical Wnt PCP pathway act in concert to regulate planar asymmetry of vinculin. Second, analysis of loss of function vinculin mutants revealed hair cell PCP defects, and diminished assembly of apical MIIB foci in supporting cells. The weak PCP phenotypes observed in vinculin mutants suggests that it is one of many potential Src effectors in hair cell PCP. Vinculin is an important component of the force transmission complex at intercellular junctions and may be involved in myosin II recruitment in a positive feedback loop [169, 170]. We hypothesize that phosphorylation of cortactin and vinculin at cellular junctions by Src regulates junctional contractility through mechanisms that involve localized actin assembly. Further work will be directed towards establishing whether these actin regulators promote contractile tension in the OC through Arp2/3 based-actin assembly.

In the mouse OC, planar polarized junctional Src signaling requires PTK7 and is crucial for PCP regulation. At present, it is unclear whether PTK7 plays an instructive or permissive role in polarized Src signaling. Although PTK7 is expressed in both hair cells and supporting cells, it is conceivable that its activity and/or localization are regulated by post-translational mechanisms, such as proteolysis [154] and tyrosine phosphorylation. Indeed, reciprocal regulation between Src and RTKs have been widely observed [238]. In addition to PTK7, Src signaling in the OC is likely regulated by multiple pathways. In other systems, Src can be rapidly activated by mechanical force [239] and cadherin adhesion [240]. Because hair cells and supporting cells are mechanically coupled through cadherin-based cell-cell contacts and engage in “tug of war” interactions during

morphogenesis, we speculate that Src signaling is cooperatively regulated by PTK7 and cadherin-mediated mechanotransduction [198]. We show that altered Src signaling reduced asymmetric localization of Fz3 but not Dvl2, suggesting that Src signaling levels may be important for the robustness of the core PCP pathway, which acts in concert with *Ptk7* to regulate contractility. Conversely, the core PCP pathway may spatially coordinate the “tug of war” interactions between hair cells and supporting cells and participate in cadherin-mediated mechanotransduction, for example, through regulation of E-cadherin surface expression [116, 241].

How does junctional contractility affect stereociliary bundle orientation? It has been established that the positioning of the hair cell basal body and the associated kinocilium plays an instructive role in stereociliary bundle orientation. Our previous work suggests a model in which microtubule capture at the hair cell cortex anchors the basal body at the lateral pole of hair cells through a positive feedback loop involving Rac-PAK signaling [128, 131]. We propose that increased tension exerted on the medial boundary of hair cells locally inhibit cortical capture of microtubules, thereby favoring microtubule capture at the lateral pole to position the basal body.

## 3.4 Figures

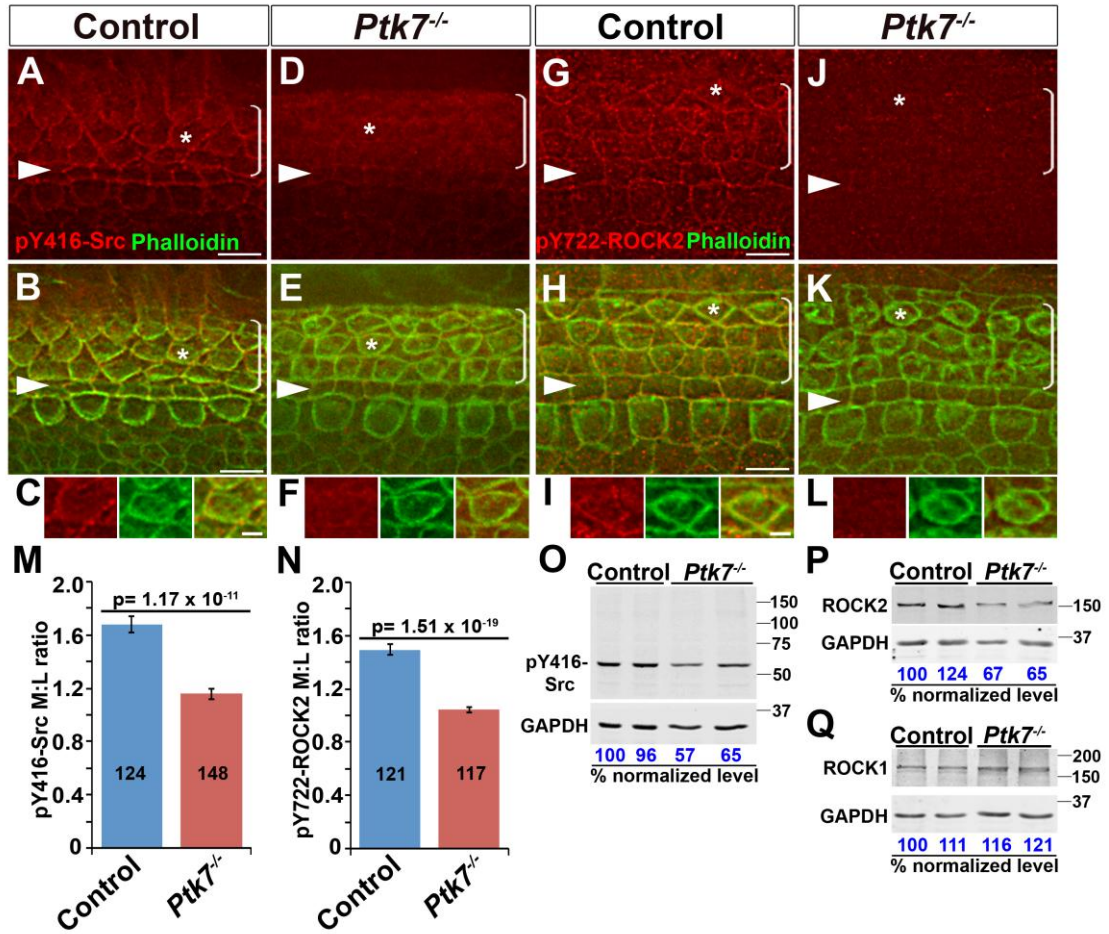


**Figure 17. PTK7 regulates planar polarized Src signaling and ROCK2 phosphorylation at intercellular junctions in the mouse OC.**

(A-F) E16.5 cochleae stained for pY416-Src (red) and phalloidin (green). (A-C) pY416-Src was enriched on the medial boundaries of hair cells in the control. (D-F) Junctional pY416-Src staining was significantly reduced in *Ptk7*<sup>-/-</sup> OC. (C, F) Higher magnifications of the hair cell indicated by asterisks in B and E, respectively. (G-L) E16.5 cochleae stained for pY722-ROCK2 (red) and phalloidin (green). (G-I) In control OC, pY722-ROCK2 staining showed similar planar asymmetry to that of pY416-Src. (J-L) Junctional pY722-ROCK2 staining was significantly reduced in *Ptk7*<sup>-/-</sup> OC. (I, L) Higher magnification of the hair cell indicated by asterisks in H and K, respectively. Images were taken from the mid-basal region of the cochlea (25% cochlear length). Arrowheads indicate the row of pillar cells. Brackets indicate OHC rows. Lateral is up in all micrographs. Scale bars, (C, F, I, L), 2  $\mu\text{m}$ , all other panels, 4  $\mu\text{m}$ . (M, N) Quantification of medial to lateral (M:L) staining intensity ratios of junctional pY416-Src (M) and pY722-ROCK2 (N). Planar asymmetry of both localizations was lost in *Ptk7*<sup>-/-</sup> OC. (O-Q) Total levels of pY416-Src (O), ROCK2 (P) and ROCK1 (Q) in E16.5 cochlear lysates. Lysates from two cochleae of the same genotype were pooled and loaded in each lane. Numbers indicate percentage of normalized levels.

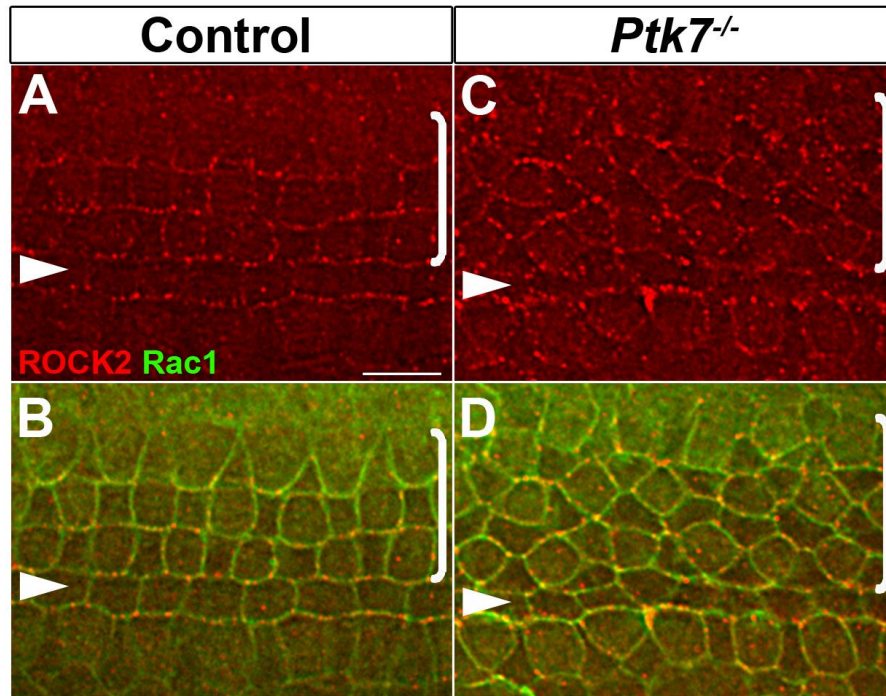


**Figure 18. ROCK2 is still localized to intercellular junctions in *Ptk7*<sup>-/-</sup> cochleae.**

(A-D) ROCK2 (red) and Rac1 (green) immunostaining in the mid-basal region of E16.5 OC (25% cochlear length). (A, B) In control OC, ROCK2 localizes to cell-cell contacts in a punctate pattern and shows diffused staining in the cytoplasm of hair cells and supporting cells. (C, D) ROCK2 localization at cell-cell contacts is largely unchanged in *Ptk7*<sup>-/-</sup> OC, although OHC rows are slightly disorganized. Arrowheads indicate the row of pillar cells. Brackets indicate OHC rows. Lateral is up in all micrographs. Scale bars, 4  $\mu\text{m}$ .

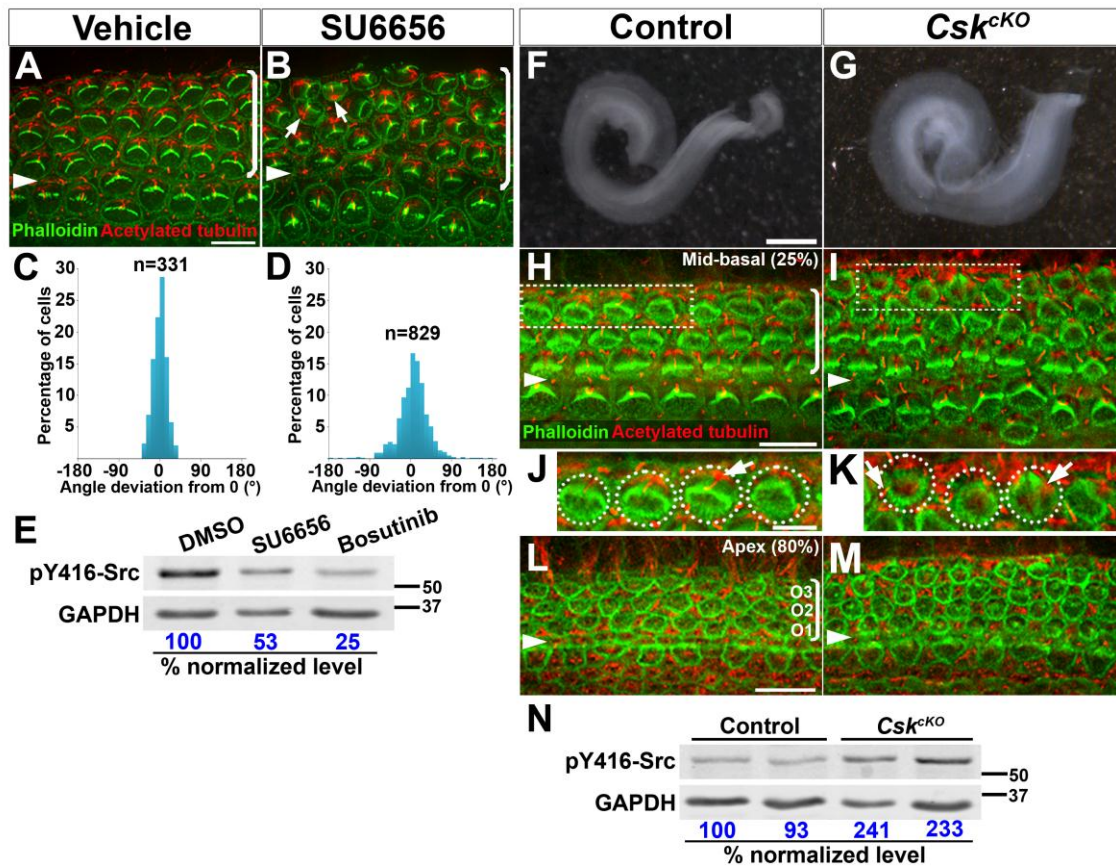


**Figure 19. Src inhibition and hyperactivation both result in PCP defects in the OC.**

(A, B, H-M) Phalloidin (green, labels the hair bundle) and acetylated-tubulin (red, labels the kinocilium) staining of Src-inhibited cochlear explants (A, B) and E18.5 *Csk<sup>CKO</sup>* OC (F-K). (A, B) Hair bundle orientation is disrupted in SU6656-treated cochlear explants (B, arrows). Hair bundle fragmentation is also observed (B, open arrow). (C, D) Quantification of kinocilium positions in vehicle (C) and SU6656-treated (D) explants. (E) SU6656- and Bosutinib-treatment reduced pY416-Src levels in cochlear explants. (F, G) Flat mounted cochleae from E18.5 control and *Csk<sup>CKO</sup>* embryos. (G) *Csk<sup>CKO</sup>* have shorter and widened cochlear ducts. (H-K) *Csk<sup>CKO</sup>* hair cells have defects in hair bundle orientation and kinocilium position (J, K). Images were taken from the mid-basal region of the cochlea (25% cochlear length). (J, K) Higher magnification of the boxed OHCs in H and I, respectively. Arrows indicate the kinocilium position. (L, M) *Csk<sup>CKO</sup>* mutants (M) have an extra row of OHCs in the apical region of the cochlea (80% cochlear length). (N) pY416-Src levels are increased by ~2 folds in *Csk<sup>CKO</sup>* cochlear tissues. Arrowheads indicate the row of pillar cells. Brackets indicate OHC rows. Lateral is up in all micrographs. Scale bars, (A, B), 6  $\mu\text{m}$ ; (J, K), 5  $\mu\text{m}$ ; all other panels, 10  $\mu\text{m}$ .

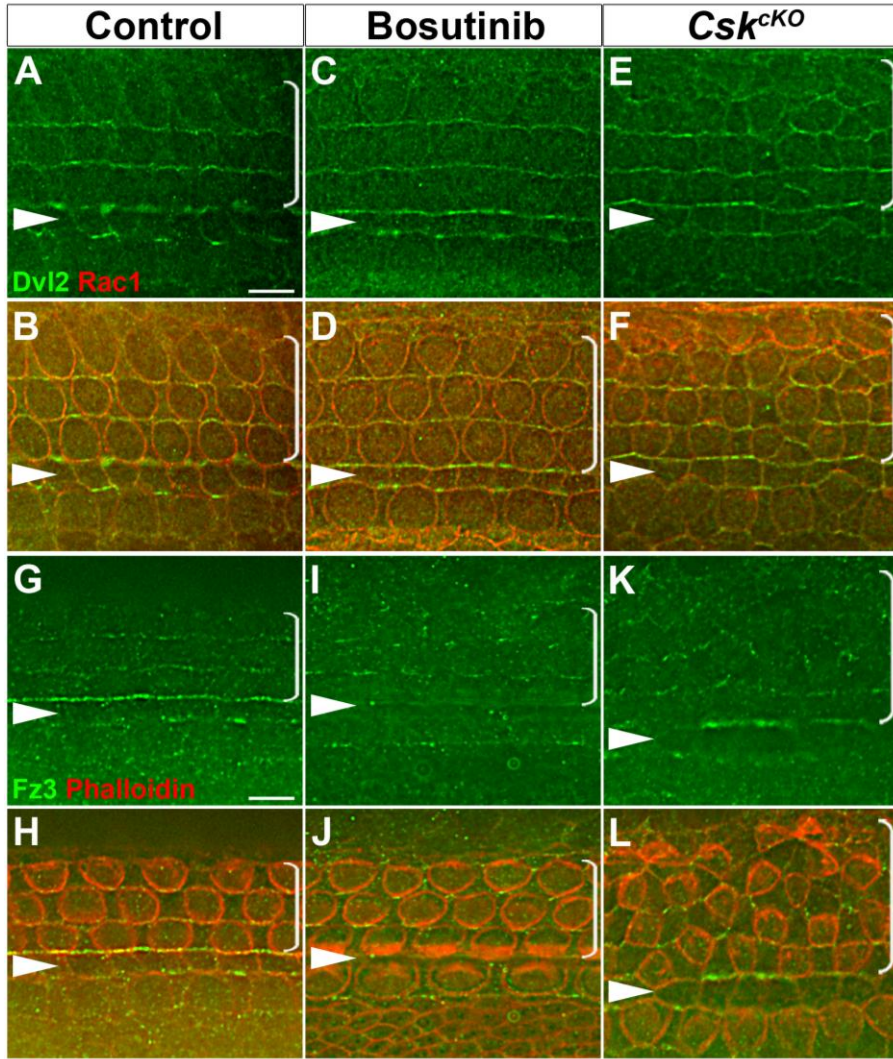


**Figure 20. Localization of core PCP proteins Dvl2 and Fz3 in Src-inhibited and *Csk*<sup>CKO</sup> cochleae.**

(A-F) Dvl2 (green) and Rac1 (red) immunostaining in E17.5 OC. (A, B) Dvl2 is asymmetrically localized along lateral borders of hair cells in control OC.

Asymmetric localization of Dvl2 was unchanged in Bosutinib-treated OC (C, D)

and slightly disorganized in *Csk*<sup>CKO</sup> OC (E, F). (G-L) Fz3 immunostaining (green)

and phalloidin staining (red) in E17.5 OC. (G, H) Fz3 is enriched along medial

boundaries of hair cells and supporting cells in control OC. Asymmetric

localization of Fz3 was reduced in both Bosutinib-treated (I, J) and *Csk*<sup>CKO</sup> OC (K,

L). Images were taken from the mid-basal region of the OC (25% cochlear

length). Arrowheads indicate the row of pillar cells. Brackets indicate OHC rows.

Lateral is up in all micrographs. Scale bars, 4  $\mu$ m.

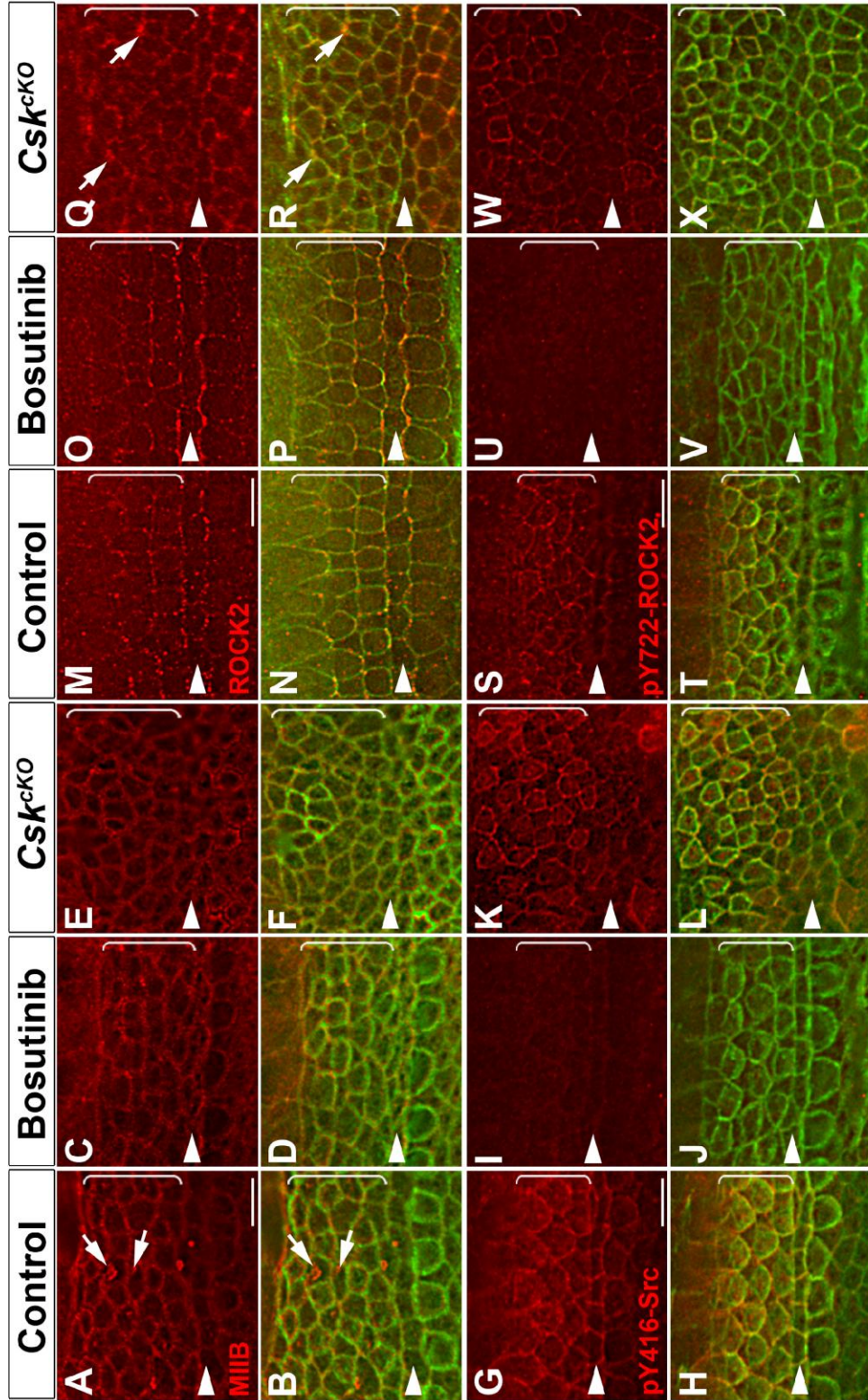


**Figure 21. Src inhibition and hyperactivation have opposing effects on pY416-Src and pY722-ROCK2 localization in the OC.**

(A-X) E16.5 cochleae stained for myosin IIB (A-F), pY416-Src (G-L), ROCK2 (M-R) and pY722-ROCK2 (S-X). Green, phalloidin staining. (A, B) In control OC, myosin IIB (red) is localized to intercellular junctions and to apical foci in supporting cells (arrows). (C-F) Apical myosin IIB foci are absent in Bosutinib-treated OC (C, D) and *Csk<sup>CKO</sup>* OC (E, F). Junctional myosin IIB localization is unchanged. (G-H) In control OC, pY416-Src (red) is enriched along medial boundaries between hair cells and neighboring supporting cells. pY416-Src staining was significantly reduced in Bosutinib-treated OC (I, J) and became circumferentially localized along cell-cell contacts in *Csk<sup>CKO</sup>* OC (K, L). (M-P) ROCK2 (red) was distributed along intercellular junctions in a punctate manner in control (M, N) and Bosutinib-treated OC (O, P). (Q, R) In *Csk<sup>CKO</sup>* OC, ROCK2 is still localized to intercellular junctions. Of note, multicellular rosettes were frequently observed, where ROCK2 was enriched at their vertices (arrows). (S, T) In control OC, pY722-ROCK2 (red) staining shows similar planar asymmetry to that of pY416-Src. pY722-ROCK2 staining was greatly reduced in Bosutinib-treated OC (U, V) and became circumferentially localized along cell-cell contacts in *Csk<sup>CKO</sup>* OC (W, X). Images were taken from the mid-basal region of the OC (25% cochlear length). Arrowheads indicate the row of pillar cells. Brackets indicate OHC rows. Lateral is up in all micrographs. Scale bars, 4  $\mu$ m.

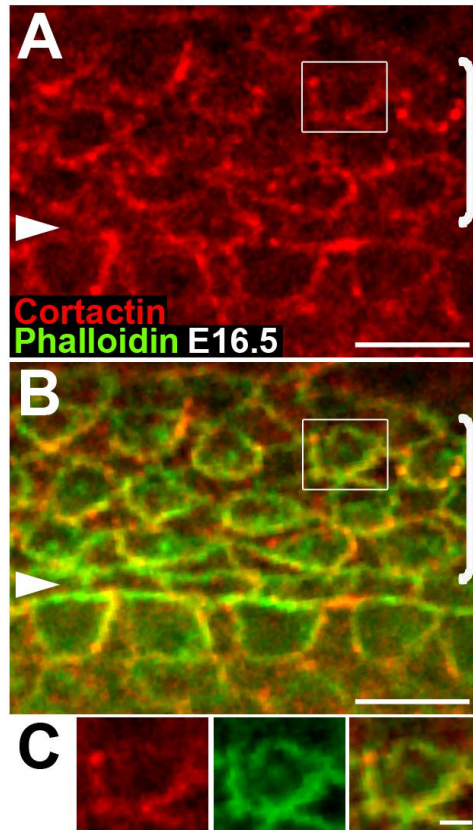


**Figure 22. Cortactin localization in the OC.**

E16.5 control OC stained for cortactin (red) and phalloidin (green). (A-B) In the mid-basal region of the cochlea (25% cochlear length), cortactin is localized to cell-contacts and enriched along medial borders between hair cells and supporting cells. (C) Higher magnification of the hair cell boxed in panels (A) and (B). Arrowheads indicate the row of pillar cells. Brackets indicate OHC rows. Lateral is up in all micrographs. Scale bars, A-B, 6 $\mu$ m; C, 2 $\mu$ m.

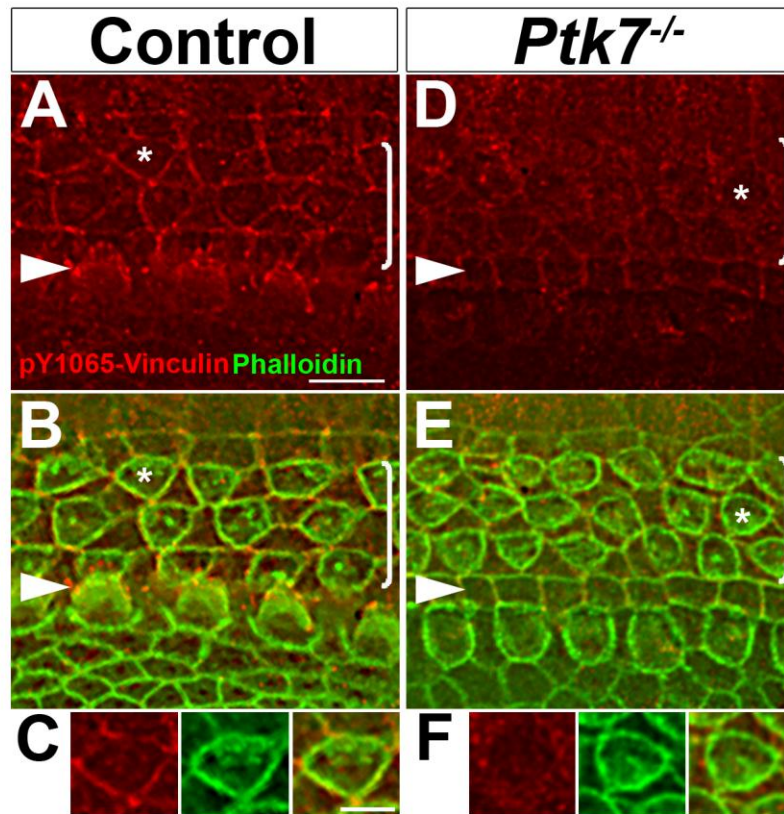


**Figure 23. *Ptk7* promotes phosphorylation of junctional vinculin in the OC.**

(A-F) E16.5 cochleae were stained for pY1065-Vinculin (red) and phalloidin (green). (A-C) In control OC, pY1065-Vinculin staining showed similar planar asymmetry to that of pY416-Src. (D-F) In *Ptk7*<sup>-/-</sup> OC, junctional pY1065-Vinculin staining was significantly reduced in *Ptk7*<sup>-/-</sup> OC. (C, F) Higher magnification of the hair cell indicated by asterisks in A and D, respectively. Images were taken from the mid-basal region of the cochlea (25% cochlear length). Arrowheads indicate the row of pillar cells. Brackets indicate OHC rows. Lateral is up in all micrographs. Scale bars, C, F, 2  $\mu$ m; others 4  $\mu$ m.

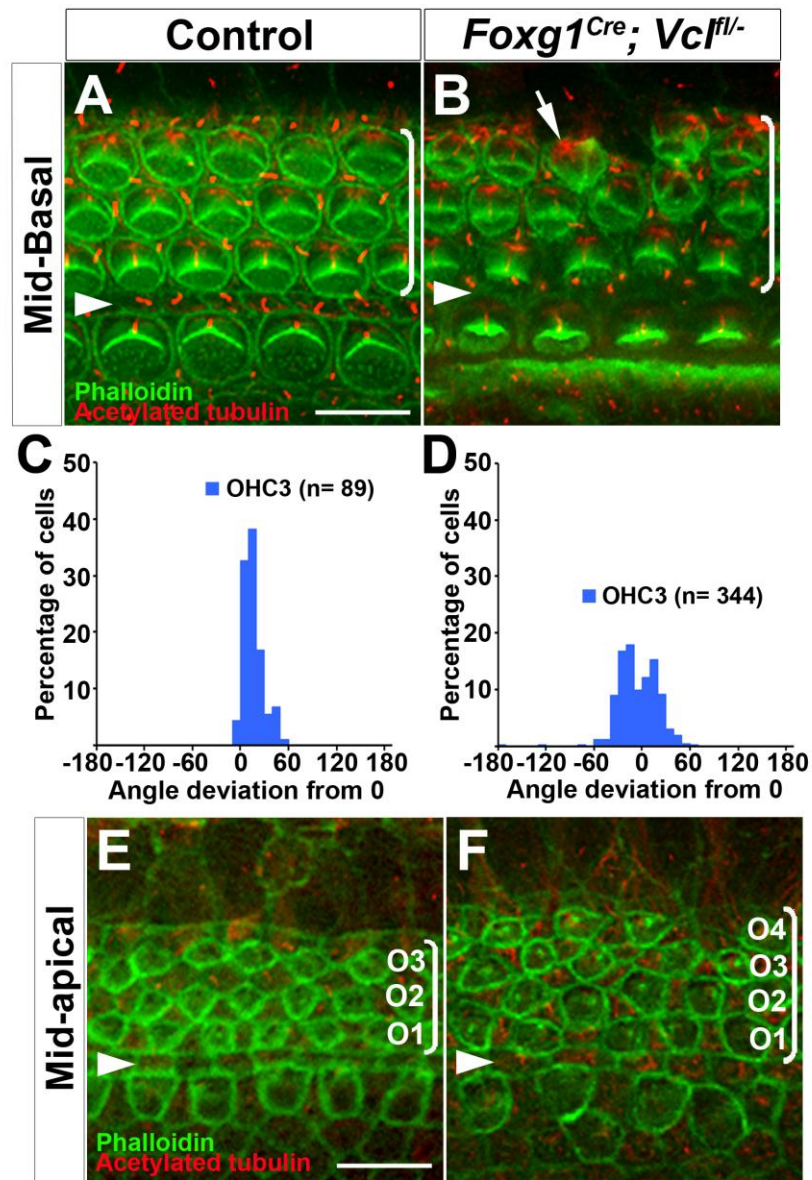


**Figure 24. Vinculin is required for hair cell PCP.**

E18.5 whole-mount cochleae stained with phalloidin (green) and acetylated-tubulin (red) to visualize the stereociliary bundle and kinocilium, respectively. (A) In the mid-basal region (25% cochlear length) of control OC, stereociliary bundles are uniformly oriented with their vertices pointing towards the lateral edge of the cochlea. (B) *Foxg1<sup>Cre</sup>; Vcl<sup>fl/-</sup>* OC exhibit stereociliary misorientation primarily in the third row of OHCs. Example of misoriented bundle is indicated by white arrow. (C, D) Quantification of OHC3 stereociliary bundle orientation in control (C) and *Foxg1<sup>Cre</sup>; Vcl<sup>fl/-</sup>* OC (D). (E) In the mid-apex (80% of cochlear length) of control OC, 3 rows of OHCs are present. (F) Supernumerary rows of OHCs are found in the mid-apex region of *Foxg1<sup>Cre</sup>; Vcl<sup>fl/-</sup>* OC. Arrowheads indicate the row of pillar cells. Brackets indicate OHC rows. Lateral is up in all micrographs. Scale bar, 5  $\mu\text{m}$ .

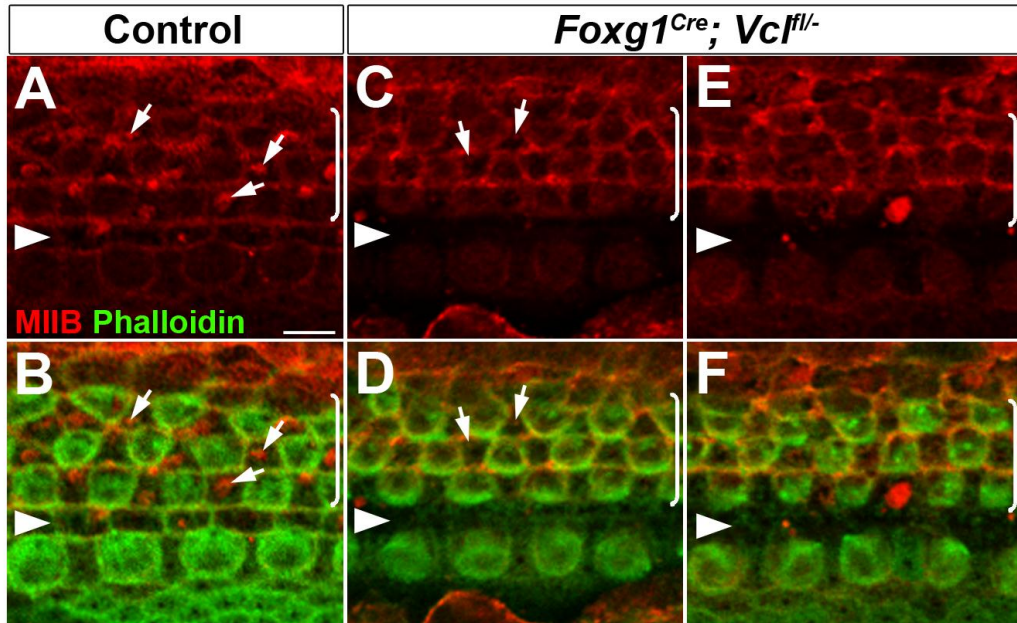


**Figure 25. Vinculin regulates the assembly of apical myosin II foci in supporting cells.**

E16.5 cochleae stained with myosin IIB (MIIB, red) and phalloidin (green). (A-B) In control OC, myosin IIB is localized to cell junctions of both hair cells and supporting cells, and found in apical foci (arrows) in supporting cells. (C-D) In *Foxg1<sup>Cre</sup>; Vcl<sup>fl/-</sup>* OC, apical MIIB foci (arrows) are significantly reduced and smaller in size while junctional localization of MIIB is normal. (E-F) In some cases, MIIB foci were absent from supporting cells in conditional vinculin mutant OC. (Note: the big blob of MIIB staining is an artifact). Arrowheads indicate the row of pillar cells. Brackets indicate OHC rows. Lateral is up in all micrographs. Scale bar, 5  $\mu$ m.

## **APPENDIX I: The Role of EphrinB ligands in Cochlear Morphogenesis**

### **I.1 Introduction**

The erythropoietin-producing hepatocellular (Eph) receptors belong to the largest family of receptor tyrosine kinases (RTKs) and interact with their cell-surface bound ligands, ephrins. Ephrins are grouped into two classes: the A-class are GPI-linked and the B-class are transmembrane ligands. The B-class ephrins consists of three members: ephrin B1, B2 and B3, and serve as ligands for ephrinB receptors (EphB). EphB/EphrinB signaling has been implicated in many developmental processes such as neural crest migration, axon guidance, angiogenesis and tissue patterning by regulating cellular processes such as cell adhesion versus repulsion, cell motility, migration and cell-cell communication [242–244].

Unlike most RTK signaling, Eph/Ephrin signaling is bidirectional, in that both the receptor and ligand can signal. Ephrin binding results in ‘forward’ signaling by inducing Eph receptor dimerization and subsequent activation of phosphotyrosine-mediated pathways. Conversely, ephrins can signal into the cells that express them upon receptor binding and this mode of signaling is termed ‘reverse signaling’. Eph receptor forward signaling mechanisms follow the classical RTK signaling activation cascade. Activation of an Eph kinase domain promotes receptor dimerization and tyrosine phosphorylation provides binding sites for adaptor molecules. Class B ephrins do not harbor intrinsic catalytic abilities but their C-terminal tails have several motifs that facilitate signaling.

Highly conserved between the C-terminal domains of all ephrinB ligands are five tyrosine residues that can be phosphorylated and a PDZ-binding domain (YKV) [245]. Phosphorylation of these tyrosine residues provides binding sites for SH2/3 containing adaptor protein, Grb4. A unifying theme in EphB/EphrinB signaling is that their downstream molecular targets converge on regulating the cytoskeleton [246]. The most well-known effectors of the EphB/EphrinB interaction are Src family kinases and Ras/Rho family GTPases. Phosphorylation of ephrinB C-terminal fragments by Src recruits adaptor proteins such as Grb4 to mediate rearrangement of the cytoskeleton [247–249].

The effects of ephrin signaling on cell behavior depend on the cell type; resulting in either increased adhesion (attraction) or decreased adhesion (repulsion) [250]. Density of receptor-ligand complexes may determine the outcome of their interactions. Initial interactions support adhesion, but it is known that Eph/ephrin clusters assemble into larger signaling complexes, switching to more repulsive activities [243]. The Eph-ephrin interaction is of high affinity and thus, it has been elusive how these complexes mediate repulsive activities. Repulsion can be mediated by terminating signals upon receptor-ligand binding and is achieved by two mechanisms, proteolytic cleavage of either the ephrins or Eph receptors and rapid trans-endocytosis of the ligand-receptor complexes (Himanen JP, 2007).

EphB/EphrinB signaling does not operate in isolation. In fact, Eph receptors and ephrins can function independently and crosstalk with other signaling pathways. Evidence linking EphB/EphrinB and Wnt signaling has been

shown to play an important role in various morphogenetic processes. In *Xenopus*, ephrinB1 intersects with the noncanonical Wnt/PCP pathway by interacting with Dishevelled and promoting RhoA activity to regulate cell sorting and directional cell migration [251, 252]. This interaction can be modulated by FGF and EphB receptors [253]. Moreover, downregulation of ephrinB1/2 signaling by ADAM13 protease activity promotes canonical Wnt activity and is required for early cranial neural crest induction [254]. Since canonical and non-canonical Wnt pathways are known to inhibit each other, cleavage of ephrinB signaling molecules may function to derepress canonical Wnt signaling.

Preliminary observations in our lab include a biochemical interaction between ephrinB1 and Frizzled3/Frizzled6 (Figure 26), two Frizzled receptors that function redundantly in hair cell PCP. Interestingly, Fz3 and Fz6 do not interact with the full-length EphrinB1 species but rather interacts preferentially with faster-migrating forms of EphrinB1. These observations suggest that Fz3/6 interact with post-translationally modified forms of ephrinB1 and may form a potential ligand-receptor pair for PCP signaling. In light of our data and other published studies, we became interested in exploring the role of B class ephrins in cochlear morphogenesis.

## **I.2 Results**

### **I.2.1 Expression of EphrinB1 and EphrinB2 in the developing OC**

The mRNAs for all three EphrinB genes are highly expressed in the inner ear during mouse development, peaking at E15 in the mouse and declines postnatally [255, 256]. However, the protein expression patterns of these ligands have not been thoroughly investigated during early cochlear development.

To examine the cellular/subcellular distribution of class B ephrins, we analyzed their localizations in E16.5 cochleae. Using an antibody that detects the ectodomain of ephrinB1, we were very intrigued by the expression pattern presented. EphrinB1 protein expression was observed at cell-cell contacts in the region medial to the OC known as the Greater Epithelial Ridge (GER) (Figure 27A, B). Furthermore, the epithelial cells of the GER immediately adjacent to the row of inner hair cells displayed the highest expression of ephrinB1 (Figure 27A, B). This “graded” pattern of protein localization corresponds well with the medial to lateral differentiation gradient of sensory hair cells.

Interestingly, at approximately 4 $\mu$ m below the plane of the previously described ephrinB1 localization, ephrinB1 staining was also detected in halo-like structures in hair cells (Figure 27C, D). The identity of these subcellular structures is elusive. To verify specificity of the ephrinB1 antibody used, we examined ephrinB1 localization in *Efnb1* mutant OC (Figure 27E-G). We found that while ephrinB1 localization at cell-cell contacts in the GER was lost, the halo-like subcellular structures in hair cells remained positive for ephrinB1 (Figure 27E-H). It is unclear if this localization is due to cross-reactivity of ephrinB1 antibody with other ephrinB molecules or due to non-specific binding.

In contrast, ephrinB2 was predominantly localized in punctae in the cytoplasm of supporting cells and weakly distributed in hair cells (Figure 28A, B). We did not observe EphrinB2 staining in halo-like subcellular structures in the hair cells. In *Efnb1*<sup>-Y</sup> OC, ephrinB2 localization was maintained and appeared to be slightly upregulated in *Efnb1* mutant OC (Figure 28C, D). Taken together, the observed protein localizations of ephrinB1 and ephrinB2 in the cochlea suggest that class B ephrins may play a role in cochlear morphogenesis.

### **1.2.2 EphrinB1 is not required for hair cell PCP**

The elevated expression of class B ephrins during early development correlates well with the timeline during which the OC undergoes terminal morphogenesis and establishes the asymmetric stereociliary bundle on each hair cell. To test if class B ephrins have a role in cochlear morphogenesis, we investigated the effects of ephrinB1 on hair cell PCP. Stereociliary bundles are evident as early as E17.5 and their orientation was used as a readout for PCP. *EphrinB1* (*Efnb1*) is X-linked and therefore, female heterozygotes are mosaics due to random X-inactivation. It is also known that in female *Efnb1*<sup>+/-</sup> embryos, mutant cells exhibit strong sorting effects from wild-type cells [250]. In control OC, hair cells uniformly orient the vertices of their stereociliary bundles towards the lateral edge of the cochlear duct. We found that *Efnb1*<sup>-Y</sup> male, and *Efnb1*<sup>+/-</sup> and *Efnb1*<sup>-/-</sup> female embryos exhibit relatively mild stereociliary bundle orientation defects in the cochlea; most stereociliary bundles were oriented towards the lateral edge of the OC with deviations less than 30° from normal and exhibited

normal V-shape bundle morphology (Figure 29A-C, data not shown). The weak bundle misorientation phenotype in *Efnb1* mutants may be indicative of functional redundancy between *Efnb* genes in hair cell PCP and supported by the persistence of ephrinB2 signaling in *Efnb1* mutant OC (Figure 28C-D).

Compound *ephrinB2* mutant mice are embryonic lethal due to severe defects in angiogenesis and auditory brainstem responses (i.e hearing) are defective in postnatal ephrinB2 heterozygous mutant mice [257, 258]. To overcome the lethality, we are attempting to generate *Efnb1*; *Efnb2* double mutants by conditionally inactivating *Efnb2* in the cochlea using a *Foxg1<sup>Cre</sup>* driver line in combination with *Efnb1* mutations. Thus far, examination of transheterozygote *Efnb1*; *Efnb2* cochleae did not reveal any significant differences in stereociliary bundle orientation compared to control cochleae (Figure 29D). These results indicate that ephrinB1 is not required for hair cell PCP and that class B ephrins may function redundantly in cochlear morphogenesis.

### **I.2.3 Genetic Interaction between *EphrinB1* and *Fz3/Fz6* in the OC**

In light of the observed *in vitro* interaction between Fz3/Fz6 and ephrinB1 (Figure 26), we went on to study the genetic interaction between *ephrinB1* and *Fz3/Fz6* genes in hair cell PCP. *Fz3* and *Fz6* function redundantly to regulate hair cell PCP [59]. In the inner ears of *Fz3*; *Fz6* double mutants, severe misorientation defects are observed in the row of inner hair cells (Figure 30B). In our preliminary analysis, we recovered one triple mutant embryo that did not

exhibit significant differences in IHC stereociliary bundle orientation compared to *Fz3/Fz6* double mutants (Figure 30B, C). On the other hand, reduced ephrinB1 dosage in *Fz3<sup>-/-</sup>; Fz6<sup>+/-</sup>* OC does not exacerbate stereociliary bundle misorientation (Figure 30E). Thus, there is no strong genetic interaction between *Efnb1* and *Fz3/6* in the cochlea and may be further masked by functional redundancy among ephrinB genes in hair cell PCP.

### **I.3 Discussion**

Our initial investigation indicates that class B ephrins are expressed in the OC during terminal morphogenesis when hair cells establish uniform stereociliary bundle orientation. This distinct organization is achieved in two ways: first, by local alignment of each hair cell's intrinsic cytoskeletal machinery to generate the asymmetric stereociliary hair bundle and secondly, by global coordination of cells in relation to its neighbors [259]. In both stages, a global guidance cue is required. These guidance cues could be generated from a localized source near the polarized epithelium [123]. Our analysis of ephrinB1 protein localization revealed that it is present in the region medial to the OC, suggesting that it may serve as a guidance cue for hair cell PCP. Furthermore, non-overlapping cellular localizations between ephrinB1 and ephrinB2 may reflect diversity in their functions and that they may contribute towards the stereociliary bundle orientation in different subsets of hair cells.

A study looking at *Wnt5a* proposes that there is an intrinsic difference between the medial and lateral sides of the cochlear epithelium and that this can

direct the orientation of the stereocilia [138]. The identity of the molecules contributing to such difference has not been successfully defined, mainly in part due to functional redundancy between genes in mammals. We speculate that the high concentration of EphrinB1 expression at the cells immediately adjacent to the inner hair cells could be contributing to the commonly postulated “morphogen gradient” for PCP. The weak hair bundle misorientation phenotype in loss of function EphrinB1 mutants indicates that it is not necessary for hair cell PCP but one cannot discount the possibility that it functions redundantly with other class B ephrins for hair cell PCP. Analysis of *Efnb1*; *Efnb2* double mutants and possibly *Efnb1*; *Efnb2*; *Efnb3* triple mutants will be necessary to determine if class B ephrins serve as instructive cues for hair cell PCP.

The detection of a biochemical interaction between Fz3/Fz6 and ephrinB1 yields the hypothesis that ephrinB1 may signal through Fz receptors. When overexpressed in cells, multiple forms of ephrinB1 can be detected with different apparent molecular weights (MW). These different forms of ephrinB1 could be due to post-translational modifications such as phosphorylation, glycosylation or protease-mediated cleavage. Class B ephrins have been found to be glycosylated in vivo [260]. Alternatively, class B ephrins can also be proteolytically cleaved by metalloproteinases and their membrane-tethered fragments subsequently cleaved by  $\gamma$ -secretases to release the intracellular domain for attenuating Eph-mediated signaling [261]. It remains to be determined whether or not this interaction is direct and warrants in-depth analysis to characterize this interaction further. The lack of a strong genetic interaction

between *Efnb1* and *Fz3/Fz6* in the cochlea may be explained by potential compensation by other ephrinB genes. Nevertheless, we are excited by the prospect that perhaps these two components form a ligand-receptor pair for PCP signaling.

Eph/Ephrin signaling normally mediates cell adhesion and class B ephrins are well-known repulsion cues for EphB-expressing neurons, during axon guidance. *Fz3<sup>-/-</sup>; Fz6<sup>-/-</sup>* mutants exhibit severe misorientation in the inner row of hair cells that is most often biased towards a complete reversal of the stereocilia hair [59]. In other PCP mutants, the stereocilia misorientation is distributed randomly. The uniform polarity disruption in *Fz3<sup>-/-</sup>; Fz6<sup>-/-</sup>* suggests that there must be strong repulsive cues that instruct inner hair cells to orient their stereocilia away from the signal. EphrinB signaling mediates repulsive cellular behaviors, such as growth cone repulsion during axon guidance and migration of cells into the presumptive eye field in the *Xenopus*. It would be interesting to test if Class B ephrins function as “repulsive” cues for stereocilia orientation in these hair cells. In light of our findings, we hypothesize that class B ephrins signal through Fz to regulate hair cell PCP by “repelling” stereocilia away from its source.

## I.4 Figures

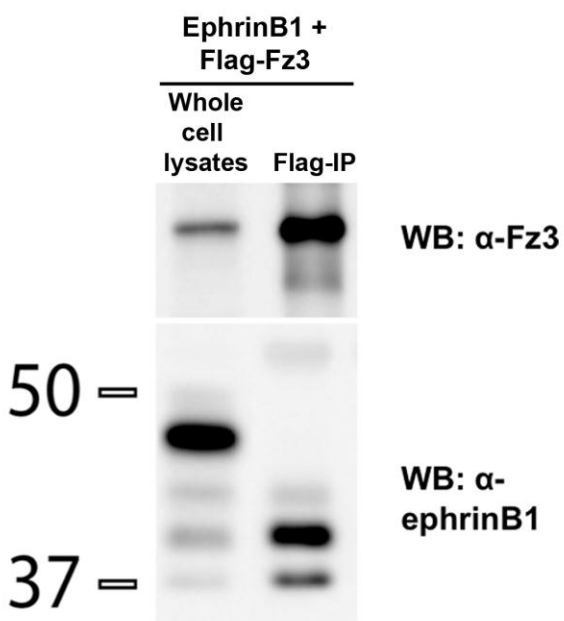


**Figure 26. EphrinB1 forms a complex with Fz3 *in vitro*.**

Lysates from HEK293T cells transfected with Flag-tagged Fz3 and ephrinB1 were subjected immunoprecipitation by Flag-beads and blotted for Fz3 or ephrinB1 antibodies (unpublished, Anna Andreeva).

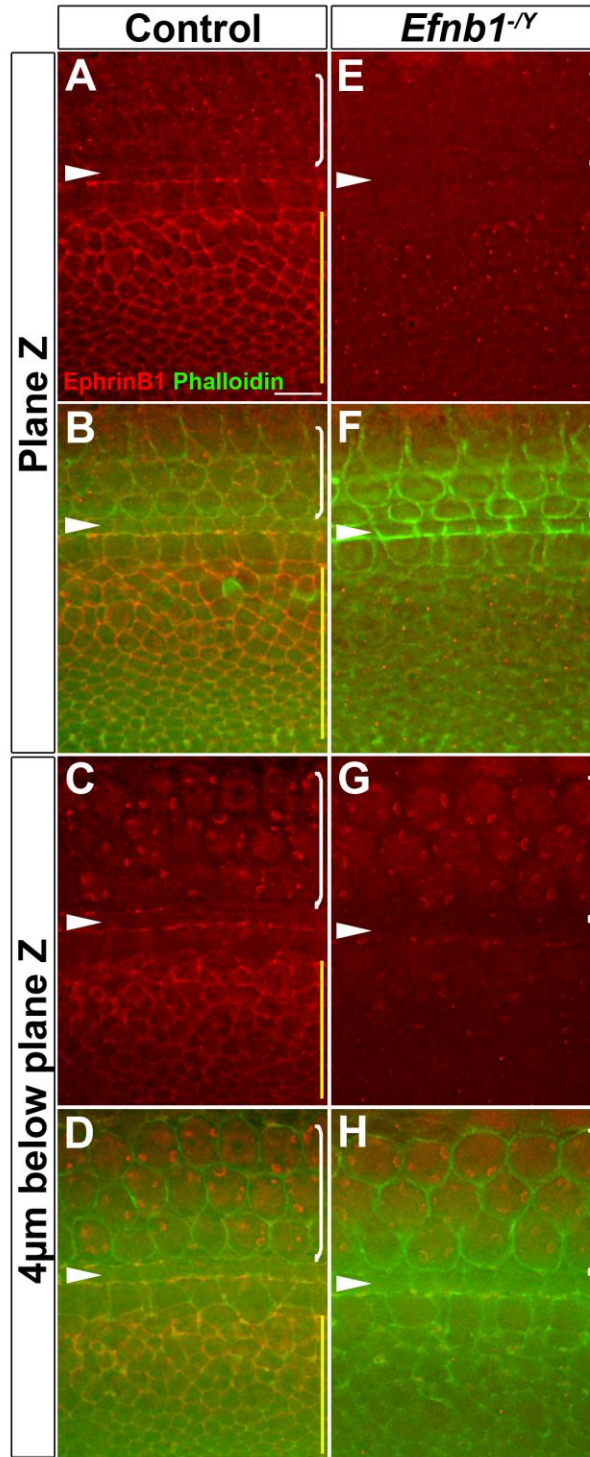


**Figure 27. EphrinB1 expression in the developing OC.**

E16.5 whole-mount cochleae were stained for EphrinB1 (red) and phalloidin (green). (A-B) In the mid-basal region of control OC, EphrinB1 localizes to cell-cell contacts in the region medial to the OC (called the Greater Epithelial Ridge (GER), region marked by yellow line). Notice the intense EphrinB1 expression in cells of the GER closest to the row of inner hair cells. (C-D) Approximately 4 $\mu$ m below the optical plane shown in (A), strong ephrinB1 staining was found in unidentified halo-like subcellular structures in hair cells. (E-F) In *Efnb1*<sup>-Y</sup> OC, ephrinB1 staining in the GER was significantly reduced. (G-H) Staining of the halo-structures in hair cells was still present, albeit with reduced intensity, in *Efnb1*<sup>-Y</sup> OC. Arrowheads indicate the row of pillar cells. Brackets indicate OHC rows. Lateral is up in all micrographs. Scale bar, 10 $\mu$ m.

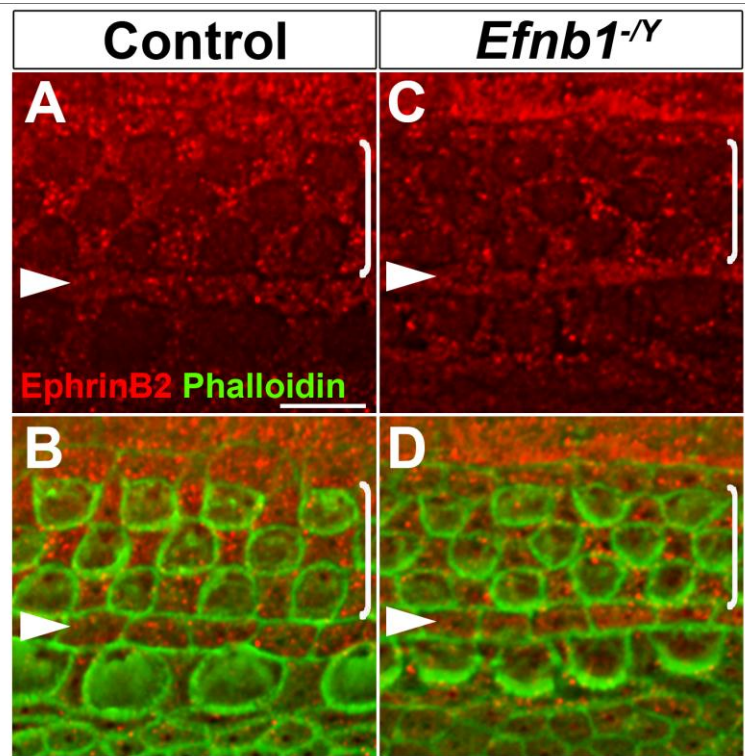


**Figure 28. EphrinB2 expression in the cochlea.**

E16.5 whole mount cochleae stained for EphrinB2 (red) and phalloidin (green).

(A-B) In the mid-basal region of control OC, ephrinB2 is strongly present in punctae in the apical cytoplasm of supporting cells and more diffusely distributed in hair cells. (C-D) EphrinB2 staining is maintained and slightly upregulated in *Efnb1*<sup>-/-</sup> mutant OC. Brackets indicate OHC rows. Lateral is up in all micrographs. Scale bar, 10 $\mu$ m.

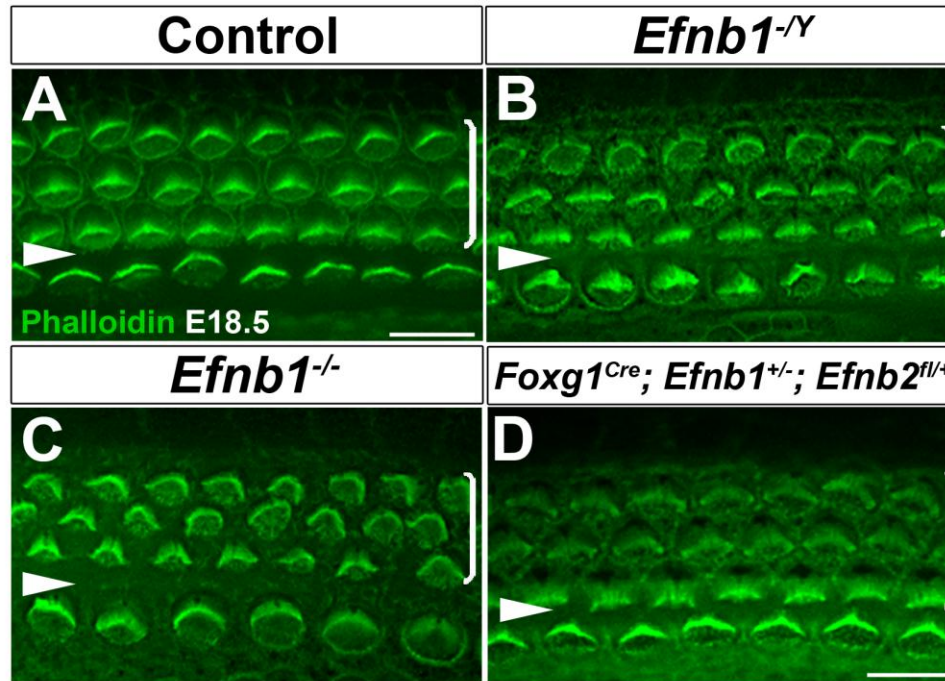


**Figure 29. EphrinB1 is not required for hair cell PCP.**

E18.5 cochleae were stained with phalloidin (green) to visualize the stereocilia bundle. Genotypes are indicated above the panels. (A) In the basal region (15% cochlear length) of control OC, stereociliary bundles uniformly orient towards the lateral edge of hair cells. (B-C) Mild misorientation of stereociliary bundles (deviations of  $<30^\circ$  from expected position) were observed in *Efnb1*<sup>-/-</sup> and *Efnb1*<sup>-/-</sup> OC. (D) Stereociliary bundle orientation was largely normal in double heterozygote *Foxg1*<sup>Cre</sup>; *Efnb1*<sup>+/-</sup>; *Efnb2*<sup>fl/+</sup> OC. White arrowheads indicate the row of pillar cells. Brackets indicate OHC rows. Lateral is up in all micrographs. Scale bar, 10µm.

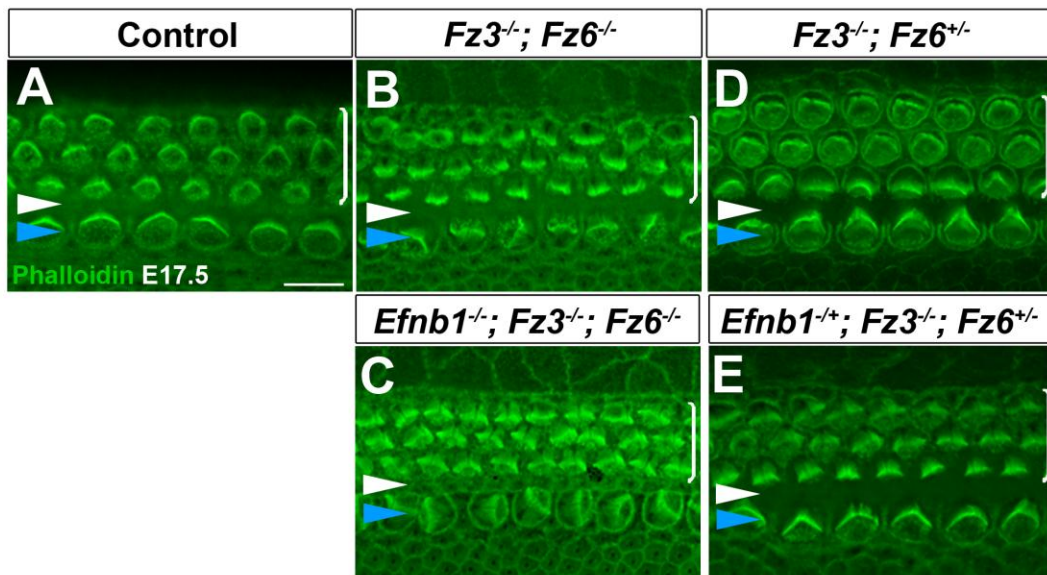


**Figure 30. Genetic interaction between *EphrinB1* and *Fz3/Fz6*.** Basal region (15% cochlear length) of E17.5 cochleae stained with phalloidin (green) to visualize the stereocilia bundle. Genotypes are indicated above the panels. (A) In control OC, stereociliary bundles are uniformly oriented with their vertices pointed towards the lateral edge of the OC. (B-C) In contrast, both *Fz3*<sup>-/-</sup>; *Fz6*<sup>-/-</sup> (B) and *Efnb1*<sup>-/-</sup>; *Fz3*<sup>-/-</sup>; *Fz6*<sup>-/-</sup> (C) OC exhibit severe stereociliary bundle misorientation in the inner hair cell (IHC) row. (D-E) Reducing EphrinB1 gene dosage in *Fz3*<sup>-/-</sup>; *Fz6*<sup>+/-</sup> OC (E) does not exacerbate its stereociliary bundle orientation phenotype. White arrowheads indicate the row of pillar cells, blue arrowheads indicate row of inner hair cells. Brackets indicate OHC rows. Lateral is up in all micrographs. Scale bar, 10µm

## APPENDIX II: Dynamics of the myosin II network in the developing OC

### II.1 Introduction

Actomyosin contractility generates the forces responsible for major cell shape changes and rearrangements in tissue morphogenesis [262, 263]. These forces are also provides a source of mechanical cues that regulate diverse cellular behaviors, such as cell growth, cell polarity establishment and locomotion. Distinct outcomes of contractility are determined by spatial and temporal regulation of actomyosin networks. At the tissue level, coupling of actomyosin networks at intercellular and cell-matrix adhesive contacts facilitate force transmission to produce global and coherent tissue changes in mechanics and shape. Our work provides evidence in support of an alternate pathway mediated by *Ptk7* that acts in parallel with the noncanonical Wnt/ PCP pathway to regulate actomyosin contractility and align hair cell PCP in the OC [214]. We showed that *Ptk7* regulates the assembly of a contractile apical myosin II network in supporting cells in the OC. However, the underlying mechanism(s) by which actomyosin contractility regulates hair cell PCP is unknown.

Dynamic actomyosin foci have been observed in a number of cell types that exhibit contractile behaviors. During *Drosophila* germband extension (GBE), cell intercalation is driven by planar polarized contractile forces mediated by a medial apical actomyosin meshwork [162]. The apical myosin II foci that we observed in supporting cells may function analogously to the myosin II network in the *Drosophila* germband. Interestingly, vinculin, a tension sensitive molecule

recruited to adhesion sites in a myosin II dependent-manner, is enriched along medial borders of hair cells in the OC suggesting that hair cells are under tension. Furthermore, stereociliary bundle orientation defects correlated with disrupted vinculin planar asymmetry in *Ptk7*<sup>-/-</sup> and *Vangl2*<sup>Lp/Lp</sup> OC. Taken together, we hypothesize that the apical myosin II network in supporting cells exerts anisotropic contractile forces at boundaries between hair cells and supporting cells to orient hair cell PCP.

Our assessment of the myosin II network in the OC has been based solely on steady state distribution myosin II in fixed tissues, which offer limited insights to the dynamics and role of actomyosin contractility during hair cell PCP. Therefore, we used time-lapse live imaging to investigate and characterize behaviors of the myosin II network in the developing OC.

## **II.2 Results**

### **II.2.1 Live imaging set up**

To gain mechanistic insights into how actomyosin contractility regulates hair cell PCP, we developed a live-imaging protocol to visualize the myosin II network in the cochlea. We established cochlear explants from knock-in mouse embryos that endogenously express GFP-tagged myosin IIB (MIIB-GFP) [264]. These cochlear explants were originally dissected from E15.5 embryos and allowed to recover *in vitro* for 12 hours before imaging. Using a heated stage and the Deltavision deconvolution inverted microscope, we imaged regions of

cochlear explants that were comparable to the mid-basal region of E16.5 cochlea, where we observed prominent immunostaining of apical myosin IIB foci in supporting cells. Under these conditions, we were able to detect live MIIB-GFP signals at cell-cell contacts in the OC that resemble Myosin IIB immunostaining patterns in fixed tissues (Figure 31). MIIB-GFP in apical foci in supporting cells were present but more nebulous in these tissues presumably due to low levels of endogenous expression. We therefore focused our analysis on the dynamics of the junctional myosin IIB network. Overall, we have established a protocol that allows consistent staging and imaging of the myosin IIB-GFP network during establishment of PCP in cochlear explants.

## **II.2.2 Myosin II is recruited to medial borders of hair cells**

To investigate the functions of the myosin II network during PCP, we monitored the distribution and temporal evolution of junctional MIIB-GFP in E16.5 control OC. Our initial time-lapse movies were made at one-frame intervals every two minutes for approximately two hours (Figure 32A-D, Movie 1). These movies revealed dynamic changes in junctional MIIB-GFP signal intensity over time. Interestingly, we observed progressive accumulation of MIIB-GFP signals along the medial borders of hair cells (Figure 32A-D, Movie 1). Using MIIB-GFP intensity as a measure of tension, we quantified fluorescence intensity changes over time at selected regions of interest in the OC. At medial borders of hair cells, we found that MIIB-GFP intensity increased in a pulsatile manner over time (Figure 32E, F). On the other hand, MIIB-GFP intensity at lateral borders of hair

cells was weaker relative to medial borders of hair cells and a steady level of MIIB-GFP intensity was maintained over time (Figure 32G). These results suggest that contractile tension is higher on medial borders and supports our hypothesis that anisotropic contractile forces are exerted at selected hair cell-supporting cell contacts.

### **II.2.3 Dynamics of the myosin II network is disrupted in *Ptk7*<sup>-/-</sup> OC**

In *Ptk7*<sup>-/-</sup> OC, planar asymmetry of junctional vinculin was lost, suggesting that *Ptk7* promotes anisotropic contractile tension in the OC. To determine the requirement for *Ptk7* in anisotropic contractile tension in the OC, we imaged *Ptk7*<sup>-/-</sup> cochlear explants that were transgenic for myosin IIB-GFP (Figure 33A-D, Movie 2). Quantification of MIIB-GFP intensity at medial borders of *Ptk7*<sup>-/-</sup> hair cells revealed subtle and less apparent pulsatile increases in MIIB-GFP intensity through time (Figure 33E-G). In several hair cells, intensity of MIIB-GFP at both medial and lateral borders were equivalent (Figure 33F, H). At the lateral borders of hair cells, MIIB-GFP intensity remained steady over time (Figure 33H, Movie 2). Interestingly, we also observed that MIIB-GFP signals often accumulated at multicellular junctions in the OC. These observations suggest that *Ptk7* promotes contractile tension at medial borders of hair cells by regulating myosin II dynamics in the OC.

## **II.3 Discussion**

Live imaging of cochlear explants from MIIB-GFP transgenic mouse embryos reveals dynamic actomyosin activity at cellular contacts in the OC. Although myosin II foci in supporting cells were more challenging to image, preliminary analysis of the junctional myosin II network has been informative. In lower model organisms, myosin II is recruited to sites of increased tension in a positive feedback manner [180]. Using MIIB-GFP intensity as an indicator of tension, we discovered that myosin II is preferentially recruited to medial borders of hair cells. This observation provides the first direct evidence for anisotropic tension at contacts between hair cell and supporting cells during PCP signaling and complements well with our observations in fixed tissues. Attaining more quantitative description of the forces at these cellular contacts will greatly supplement our model for polarized tension in the OC.

Recent studies incorporating quantitative live imaging methods with biophysical and computational approaches reveal two conserved features in actomyosin dynamics: actomyosin flow patterns and pulsed contractility [162, 164, 262, 265]. These features explain the self-organizing properties of the actomyosin network. Myosin II redistribution induced by flow enhances a gradient of contractility and localized actin assembly to spatially orient cell deformation. Pulsation of the actomyosin network regulates the frequency and speed of the cellular deformation in question. Our time-lapse movies suggest that these dynamic properties are conserved in the OC. Evaluation of junctional MIIB-GFP intensity over time in control OC indicates that the junctional myosin II network pulses. Pulsatile actomyosin networks have also been postulated to function as

ratchets which allow feedback mechanisms to stabilize contractile forces and effectively generate contractility [266]. In *Ptk7*<sup>-/-</sup> OC, dynamic fluctuations and pulsation of the junctional myosin II network were diminished along with weakened accumulation of myosin II at medial borders of hair cells. We therefore propose that *Ptk7* regulates myosin II dynamics in a feedback loop to promote anisotropic contractile tension in the OC.

In our current working model, we posit that actomyosin tension spatially regulates basal body position through Rac-PAK signaling and hence defines the orientation of the stereociliary bundle in the OC. Therefore, to determine if polarized contractile tension regulated by myosin II dynamics is functionally important for hair cell PCP, future work will be directed towards correlating myosin II network dynamics with basal body behaviors by imaging cochlear explants that are doubly transgenic MIIB-GFP and centrin2-GFP [267].

## II.4 Figures

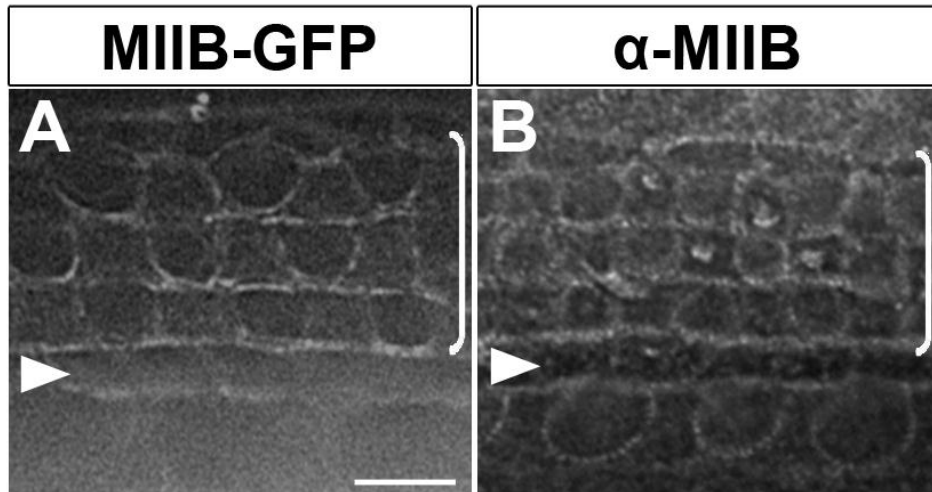


**Figure 31. Comparison of Myosin IIB-GFP expression in live cochlear explants with Myosin IIB immunostaining in fixed cochlear tissues.**

(A) MIIB-GFP localization of E15.5 (+12 hours in vitro) control cochlear explants. MIIB-GFP signals are observed on cell-cell junctions. (B) Immunostaining of myosin IIB in E16.5 control OC. Myosin IIB is localized to cell-cell junctions and in foci in supporting cells. Images were taken from mid-basal regions of the cochlea. White arrowheads indicate the row of pillar cells. Brackets indicate OHC rows. Lateral is up in all micrographs. Scale bar, 6 $\mu$ m.

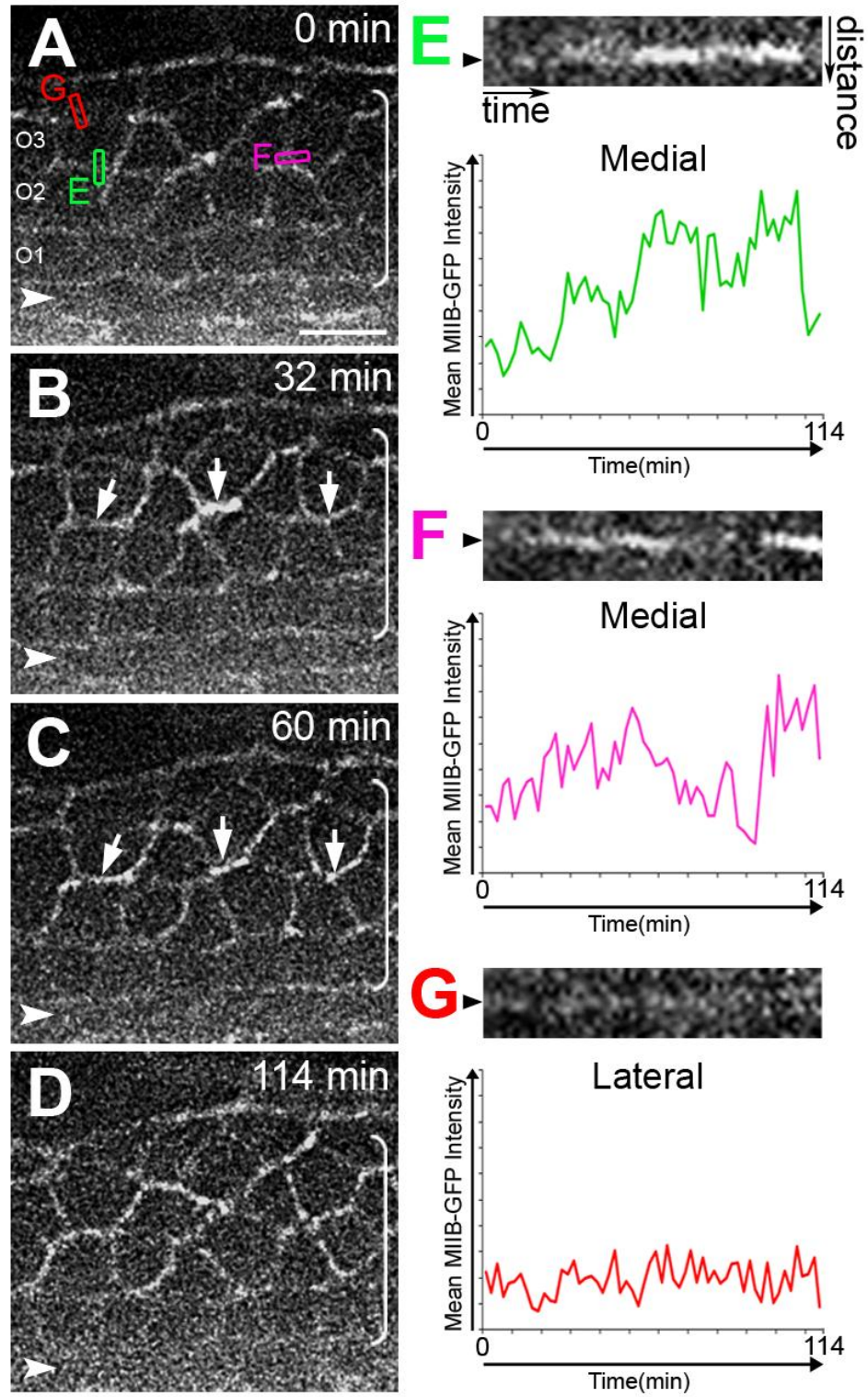


**Figure 32. Myosin II is recruited to medial borders of hair cells in control**

**OC.** (A-D) Four different timeframes extracted from a time-lapse movie imaging MIIB-GFP in E15.5 (+12 hours in vitro) wild-type cochlear explants. Images of the MIIB network were taken every 2 minutes for a total of 114 minutes. Arrows indicate position of cell junctions. (E-G) Kymographs and fluorescence intensity plots of regions of interest indicated in (A). (E-F) At medial borders of hair cells, MIIB-GFP intensity increases in a pulsatile manner over time. (G) MIIB-GFP intensity remains steady through time at lateral contacts of hair cells. Black arrowheads indicate position of cell junction. White arrowheads indicate the row of pillar cells. Brackets indicate OHC rows. Lateral is up in all micrographs. Scale bar, 4 $\mu$ m.

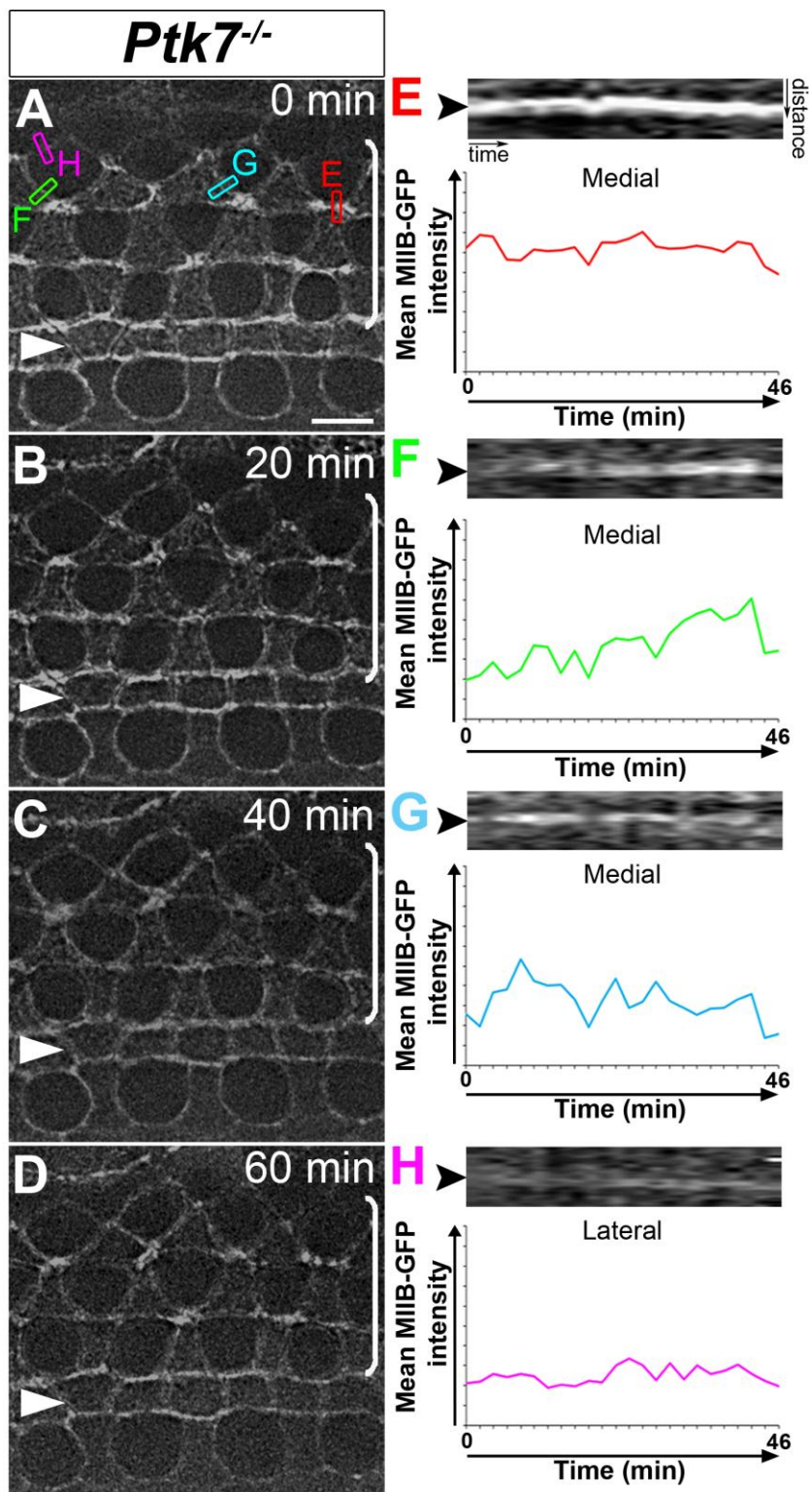


**Figure 33. Dynamics of the myosin II network is disrupted in *Ptk7*<sup>-/-</sup> OC.**

(A-D) Four different time-points extracted from a movie imaging the myosin IIB network in E16.5 (+12 hours *in vitro*) *Ptk7*<sup>-/-</sup> cochlear explants. Images were taken every minute for a total of 1 hour. (E-H) Kymographs and quantifications of junctional MIIB-GFP intensity at selected regions of interest, indicated in (A). (E-G) At medial borders of *Ptk7*<sup>-/-</sup> hair cells, MIIB-GFP intensity fluctuates less and does not show robust accumulation over time. (H) At lateral borders of hair cells, MIIB-GFP intensity is low and remains steady through time. White arrowheads indicate the row of pillar cells. Brackets indicate OHC rows. Lateral is up in all micrographs. Scale bar, 4 $\mu$ m.

## APPENDIX III: Crosstalk between *Ptk7*-mediated pathway and hair cell intrinsic polarity pathways

### III.1 Introduction

Accumulating evidence suggests a two-tiered hierarchy for hair cell PCP regulation; tissue-level PCP signaling provides extrinsic or tissue polarity cues that are interpreted by hair cell-intrinsic pathways that regulate planar polarization of individual hair cells. In the OC, active p21-activated kinase (PAK), a downstream effector of the Rac GTPases, localizes asymmetrically at the hair cell cortex and likely serves as cell intrinsic polarity cues [79, 128]. Localized cortical Rac-PAK activity is important for hair bundle orientation and is spatially coordinated by the noncanonical Wnt/PCP pathway. Data from our lab has led to the elucidation of a novel hair cell intrinsic polarity pathway whereby microtubule-capture at the hair cell cortex establishes a constrained cortical domain of Rac-PAK signaling to form a positive feedback loop that reinforces microtubule cortical attachments for proper positioning of the basal body at the lateral pole of the hair cell [79, 128, 131]. However, how tissue polarity cues impinge on the cell-intrinsic polarity machinery is incompletely understood.

Evidence in previous chapters suggests that PTK7-*Src* signaling regulates actomyosin contractility to orient hair cell PCP. We propose that *Ptk7*-mediated contractile tension exerted on medial borders of hair cells spatially restricts microtubule cortical capture to the lateral edge of hair cells through mechanotransduction mechanisms that ultimately orient Rac-PAK signaling.

Evidence from *in vitro* studies suggests that tension and myosin II can inhibit Rac activity [209, 210]. The observation that vinculin and pPAK localizes to complementary domains on the hair cell cortex also lends support to this idea. To identify the molecular components of the proposed mechanotransduction pathway, we took a candidate approach based on published literature. We hypothesize that mechanical forces control the activity and/or localization of regulators of Rac GTPases and microtubule cortical capture to orient PCP in the OC.

Here I describe the rationale and preliminary analysis of several candidate molecules, which include Par-3,  $\beta$ -Pix, FilGAP, srGAP2/3 and Gpsm2.

## **III.2 Results**

### **III.2.1 *Ptk7* regulates cortical localization of Par-3 in the OC**

Rationale: The *Ptk7*-myosin II pathway that we have established in the OC bears similarities with the myosin II/Par-3-based signaling mechanism that operates during germband extension (GBE) in the *Drosophila* [36]. They both function independently of the core PCP signaling pathway and implicate planar polarized myosin II contractility. In the germband epithelium, myosin II and F-actin are concentrated at anterior-posterior (A-P) borders while Bazooka/Par-3 is enriched at the reciprocal dorsal-ventral (D-V) interfaces [32, 36].

Complementary localizations of cortical Par-3 and myosin II are required for proper cell intercalation and Par-3 localization is regulated by Rho-kinase [268].

Furthermore, Par-3 is also involved in spatial regulation of Rac activity in other systems by associating with Rac guanine exchange factors (GEF) Tiam1 and Tiam2 [269, 270].

In addition, Par-3 belongs to a conserved Par-3/Par-6/aPKC complex that regulates cell polarity in various organisms by generating cortical landmarks that establish asymmetric distribution of effector proteins [271]. During asymmetric cell division in *Drosophila* neuroblasts, Par-3 promotes cortical localization of Pins (vertebrate homolog LGN/Gpsm2) [272]. Pins forms a cortical protein complex with the G-protein subunit  $\alpha$  ( $G\alpha$ ) and nuclear mitotic apparatus (NuMA), which binds to and anchors dynein to the cell cortex. Dynein at the cell cortex exerts pulling forces on astral microtubules to orient the spindle. A recent study reported that conditional deletion of mammalian Pins in the inner ear results in stereocilia bundle orientation and hair bundle polarity defects [273]. It is likely that microtubules emanating from the kinocilium are preferentially captured at the cortex where LGN is localized. Therefore, Par-3 may directly regulate Rac activity through Tiam1 and indirectly through microtubule cortical capture.

Experiment: To determine whether Par-3 is involved in *Ptk7*-myosin II pathway, we analyzed Par-3 localization in the developing OC. At E16.5, Par-3 is localized at the lateral cortex of hair cells in control OC (Figure 34A, B), similar to pPAK cortical localization [79] and LGN/Gpsm2 localization (see below) [132]. In *Ptk7* mutant cochleae, asymmetric Par-3 localization was mislocalized and sometimes ectopically distributed around the hair cell cortex (Figure 34C, D). This result suggests that *Ptk7* regulates Par-3 asymmetry and is consistent with

a role of Par-3 in promoting cortical capture of microtubules and Rac activation at the lateral pole of hair cells.

### **III.2.2 GEFs and GAPs for Rac**

Rationale: In other systems, mechanical tension can result in the deactivation of Rac signaling [274–276]. Rac GTPases function as molecular switches that cycle between a GTP-bound (active) state and a GDP-bound (inactive) state. Two classes of proteins, Guanine Nucleotide Exchange Factors (GEFs) and GTPase activating proteins (GAPs) are known to promote and inhibit Rac activity respectively. In addition, a number of these proteins are associated with cell-adhesions and cytoskeletal regulators, making them well positioned as candidates that translate mechanical signals into biochemical signaling.

Indeed, several studies have shown that the localization and activity of these proteins at these sites can be modulated by physical cues such as actomyosin-based tension and stretching. For instance, a Rac-specific GEF  $\beta$ -Pix interacts with myosin II and its recruitment to cell substrate adhesions is negatively regulated by myosin II contractility [277]. On the other hand, in response to tension, a Rac GAP FilGAP dissociates from an actin crosslinking protein filamin A and is redistributed to the plasma membrane where it is necessary for suppressing Rac activity [212, 278]. In addition, the family of Slit-Robo GAPs (srGAPs) consisting of 3 members, srGAP1, -2 and -3, exhibits Rac specific GAP activity [279, 280]. These proteins share a highly conserved molecular structure that includes an F-BAR domain, a RhoGAP domain and a

SH3 domain. F-BAR domain containing proteins are known for their ability to sense and induce membrane curvature [281, 282]. Dimerization of F-BAR domains creates a crescent-shaped surface that interacts with negatively charged membrane lipids. In the mouse, srGAPs are involved in various aspects of neuronal morphogenesis and migration [283]. It has been proposed that srGAP2 negatively regulates neuronal migration and promotes neurite outgrowth primarily through its F-BAR domain and by locally attenuating Rac activity.

Experiment: To identify relevant regulatory proteins that may play a role in modulating Rac activity during hair cell PCP signaling, we examined the localizations of the following GEFs:  $\beta$ -Pix, and GAPs: FilGAP, srGAP2 and srGAP3 in E16.5 control and *Ptk7*<sup>-/-</sup> OC. Among these proteins, we were unable to detect specific staining of  $\beta$ -Pix and srGAP3 in the OC (data not shown). Analysis of FilGAP localization in control OC revealed that it was localized to centrioles and diffusely distributed in a punctate manner in the cytoplasm of hair cells and supporting cells (Figure 35A, B). This localization pattern was not significantly altered in *Ptk7*<sup>-/-</sup> OC (Figure 35C, D). We observed that srGAP2 was localized along cell-cell junctions and occasionally appeared enriched along the medial borders of outer hair cells (Figure 36A-C). However, absence of *Ptk7* in the OC did not affect the localization of srGAP2 at cell-cell junctions (Figure 36D-F). These results suggest that FilGAP and srGAP2 are unlikely to participate in *Ptk7*-mediated mechanotransduction pathway during hair cell PCP.

### III.2.3 Gpsm2 localization is misoriented *Ptk7*<sup>-/-</sup> OC.

Rationale: We hypothesize that the mechanisms that regulate microtubule cortical capture at the hair cell cortex may be analogous to those involved in spindle orientation during asymmetric cell division. In *Drosophila* neuroblasts, Par-3 functions to promote cortical localization of Pins (mammalian homolog Gpsm2) and facilitate the recruitment of dynein, which pulls on astral microtubules to orient the spindle.

Experiment: We therefore tested if *Ptk7* regulates microtubule cortical attachments through Gpsm2 by examining Gpsm2 localization in the OC. In control OC, Gpsm2 is localized at two domains: around the basal body and is asymmetrically enriched at the lateral hair cell cortex in a similar manner to Par-3 and pPAK (Figure 37A, B, data not shown). In contrast, Gpsm2 asymmetry was misoriented in *Ptk7*<sup>-/-</sup> OC (Figure 37C, D). This result suggests that *Ptk7* regulates Gpsm2 asymmetry and implicate Gpsm2 as another potential cortical regulator that links upstream *Ptk7*-mediated mechanical signals to the microtubule effector machinery.

### III.3 Discussion

Our preliminary results support Par-3 as a candidate effector that transduces signals mediated by *Ptk7*-Myosin II pathway to the microtubule based cell intrinsic pathway in the OC. In the OC, Par-3 is asymmetrically localized at the hair cell cortex, opposite to where we propose tension and myosin II

contractility is high, reflecting similarities with the Par-3/myosin II pathway in *Drosophila*. In *Ptk7* mutants, planar asymmetry of Par-3 was misoriented. The C-terminal domain of Par-3 is required for its membrane association and can be phosphorylated by ROCK and Src [268, 284]. ROCK phosphorylation of the C-terminal domain of Par-3 disrupts Par-3 membrane localization. Thus, *Ptk7* may regulate cortical Par-3 localization through Src or by regulating actomyosin contractility.

Par-3 and Gpsm2 plays a conserved role during asymmetric cell division [272, 285]. They serve as cortical landmarks to modulate interactions between microtubules and the cell cortex to orient the spindle. In the OC, Par-3 and Gpsm2 were both localized at the lateral cortex, supporting its potential role in establishing microtubule-cortex interactions. We found that *Ptk7* regulates asymmetry of both Par-3 and Gpsm2, further implicating them as candidate cortical proteins that link tissue level polarity cues to the microtubule effector machinery. Recently, Gpsm2 was identified as a causative gene for congenital human deafness DFNB82 and Chudley-McCullough syndrome, both of which result in profound sensorineural hearing loss [286, 287]. Based on their localizations in the OC, we hypothesize that Par-3 may integrate upstream mechanical signals mediated by *Ptk7* to spatially regulate cortical Rac-PAK activity by recruiting a cortical complex that includes Gpsm2, hence promoting microtubule-cortical interactions and anchoring the basal body at the lateral pole of hair cells.

Our attempts to identify candidate Rac GAPs and GEFs revealed that FilGAP and srGAP2 are not essential components of our proposed *Ptk7*-mediated mechanotransduction pathway. It is possible that other members of the srGAP family play a more dominant role during hair cell PCP signaling. Based on inner ear gene expression data analysis, srGAP3 is the highest expressed member among srGAPs in hair cells (retrieved from SHIELD: Shared Harvard Inner-Ear Laboratory Database, <https://shield.hms.harvard.edu/>). Nevertheless, continued efforts will be made towards testing Rac-specific GAP and GEF proteins that transduce *Ptk7*-mediated mechanical signals in the OC. It will also be important to establish force-responsiveness of the identified candidates by assessing their localizations in response to blebbistatin and ROCK inhibitors.

### III.4 Figures

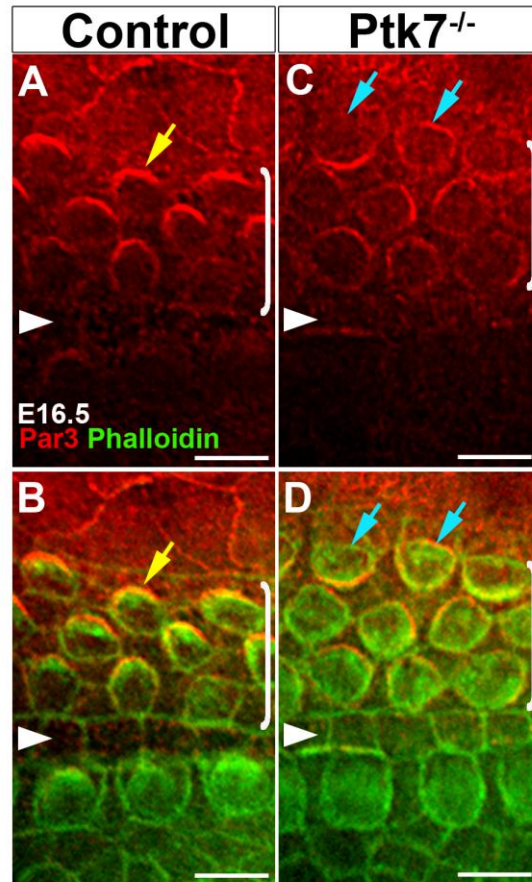


**Figure 34. Asymmetric localization of Par-3 is regulated by *Ptk7*.**

E16.5 cochleae stained with Par3 (red) and phalloidin (green). (A-B) In the mid-basal region of control OC, Par3 strongly localizes at the lateral cortex of hair cells (yellow arrow). (C-D) In *Ptk7*<sup>-/-</sup> OC, asymmetry of Par3 is mislocalized or distributed more evenly on the hair cell cortex (blue arrows). White arrowheads indicate the row of pillar cells. Brackets indicate OHC rows. Lateral is up in all micrographs. Scale bar, 4 $\mu$ m.

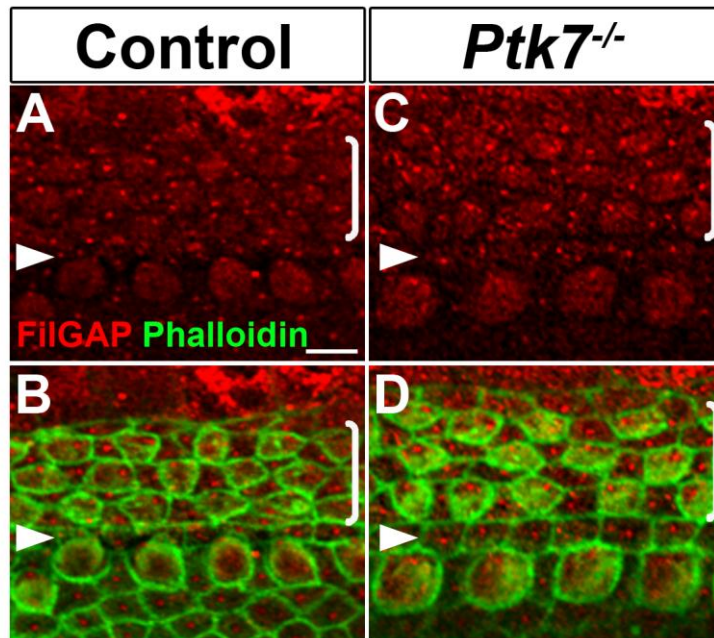


**Figure 35. FilGAP localization in the OC.**

E16.5 whole mount cochleae stained with FilGAP (red) and phalloidin (green).

(A, B) In control OC, FilGAP strongly localized to the centrioles and was diffusely distributed in the cytoplasm of hair cells and supporting cells. (C, D) No significant differences in FilGAP localization were observed in *Ptk7*<sup>-/-</sup> OC. White arrowheads indicate the row of pillar cells. Brackets indicate OHC rows. Lateral is up in all micrographs. Scale bar, 4 $\mu$ m

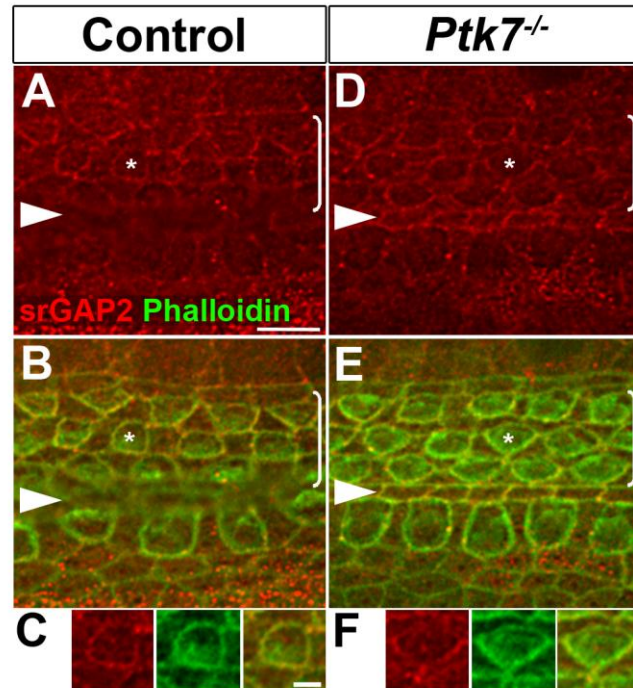


**Figure 36. srGAP2 localization in the OC.**

E16.5 whole-mount cochleae stained with srGAP2 (red) and phalloidin (green). (A, B) In control OC, srGAP2 localized to cell-cell contacts and was occasionally enriched on the medial borders of hair cells (asterisk). (D, E) No changes in srGAP2 localization were noted between control and *Ptk7* mutant OC. (C, F) Higher magnification of the hair cell indicated by asterisks in A and D, respectively. Images were taken from the mid-basal region of the cochlea (25% cochlear length). White arrowheads indicate the row of pillar cells. Brackets indicate OHC rows. Lateral is up in all micrographs. Scale bar, (C, F), 2 $\mu$ m; others, 6 $\mu$ m.

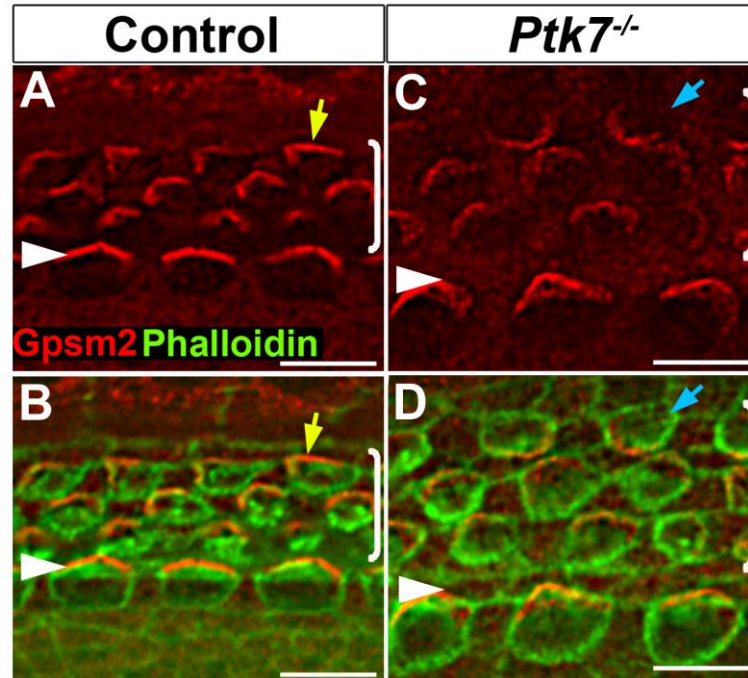


**Figure 37. Gpsm2 asymmetric localization is regulated by *Ptk7*.**

E16.5 cochleae stained with Gpsm2 (red) and phalloidin (green). (A-B) In the mid-basal region of control OC, Gpsm2 localizes at the lateral cortex of hair cells (yellow arrow). (C-D) In *Ptk7*<sup>-/-</sup> OC, asymmetry of Gpsm2 is mislocalized (blue arrow). White arrowheads indicate the row of pillar cells. Brackets indicate OHC rows. Lateral is up in all micrographs. Scale bar, 4 $\mu$ m.

## CHAPTER 4: Summary and Future Work

## 4.1 Summary

The vast array of morphogenetic and physiological processes that depend on the establishment of planar cell polarity (PCP) emphasizes its importance in human health and disease. While extensive studies have identified the genetic factors that regulate PCP, the underlying cellular and molecular mechanisms remain poorly understood in mammalian epithelia. Much of the framework for understanding PCP specification has been centered on the evolutionarily conserved non-canonical Wnt/core PCP pathway, initially discovered in *Drosophila*. The existence of multiple genes encoding vertebrate core PCP protein homologs presents a challenge in determining their specific functions in vertebrate PCP-regulated processes. Furthermore, we have begun to appreciate that PCP specification can be context specific and that vertebrates have adapted additional mechanisms to polarize diverse cellular outcomes. Prior to this work, *Ptk7* was identified as a novel regulator of PCP in vertebrates [1]. The major goal of this work was to address the cellular and molecular mechanisms by which *Ptk7* regulates mammalian epithelial PCP using the auditory sensory epithelium.

By employing a combination of mouse genetics, *ex vivo* organotypic explants and multiple imaging techniques, we have taken great stride towards achieving significant advances in our understanding of hair cell PCP regulation. The work presented in this dissertation has led us to propose a conceptually new model for hair cell PCP regulation that centers on actomyosin-based contractile tension. We demonstrate that an alternate *Ptk7*-mediated pathway functions in parallel with the noncanonical Wnt/PCP pathway to regulate actomyosin

contractility and orient hair cell PCP. For the first time, our genetic mosaic analysis of *Ptk7* illustrates that supporting cells, the immediate neighbors of sensory hair cells, play an active role in hair cell PCP. Specifically, *Ptk7* promotes the assembly of a contractile apical myosin II network in supporting cells. Our data suggests that the apical myosin II network functions to exert polarized contractile forces at contacts between supporting cells and hair cells. Furthermore, we uncovered a mechanism for *Ptk7*-mediated actomyosin regulation in hair cell PCP. Our data suggests that PTK7 promotes localized Src activity at cell-cell contacts to regulate actomyosin contractility and that ROCK2 is a target of junctional PTK7-Src signaling in the OC.

How does actomyosin contractile tension orient hair cell PCP? In the OC, tissue level PCP signaling provides extrinsic or tissue polarity cues that are interpreted by hair cell intrinsic effector machinery. Previously published work from our lab suggests a model for a microtubule-mediated cell intrinsic polarity machinery. In this model, interactions between microtubules and the hair cell cortex establishes a restricted domain of Rac-PAK signaling, setting up a positive feedback loop to anchor the basal body at the lateral edge of the cell [128, 131]. Taken together, we propose the following working model where *Ptk7*-mediated polarized contractile forces are exerted on medial borders of hair cells to antagonize microtubule-cortical interactions, thereby favoring microtubule capture at the lateral pole to position the basal body (Figure 38).

Several elements in our proposed model for hair cell PCP regulation warrant further investigation and validation. One of the important elements to be

addressed is the mechanism by which polarized contractile tension signals are transduced to the microtubule-based cell intrinsic machinery. Having defined the PTK-Src signaling pathway as a critical regulator of actomyosin contractility, efforts will be made towards dissecting downstream mechanisms that modulate polarized contractile tension in the OC. These studies will continue to provide additional insights on how PCP is regulated at the tissue level and how these mechanisms are interlocked with cell-intrinsic effector modules. Understanding how epithelial tissues respond to mechanical signals will also have broad implications for epithelial tissue morphogenesis and physiology.

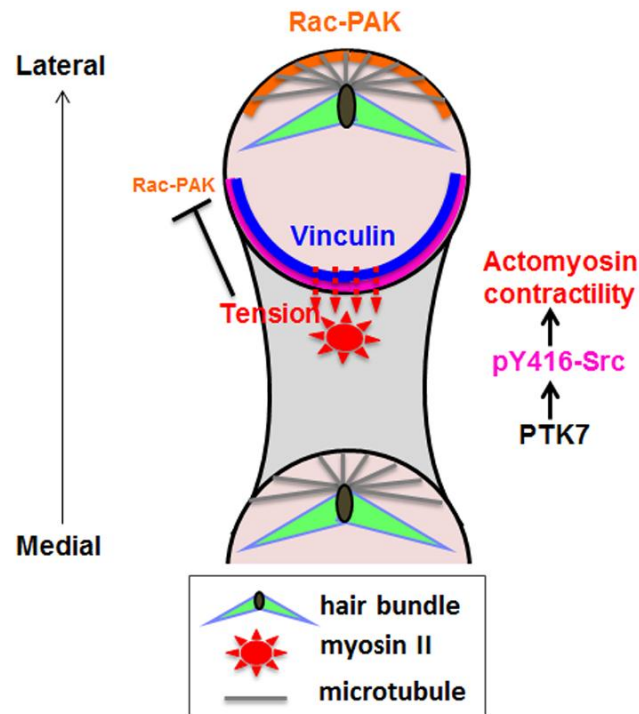


**Figure 38. Model proposed for hair cell PCP regulation by *Ptk7*.**

*Ptk7* regulates the assembly of an apical myosin II network in supporting cells, through planar polarized Src signaling (magenta) at cell-cell contacts. The apical myosin II network in supporting cells function to exert polarized contractile tension on medial borders of hair cells, evidenced by increased vinculin recruitment (blue). Anisotropic contractile tension spatially regulates cortical Rac-PAK activity (orange) and promotes microtubule capture at the lateral side of the hair cell to position the basal body and hence, aligns the stereociliary bundle.

## 4.2 Future Directions

### 4.2.1 Does polarized tension regulate basal body positioning in the OC?

In Chapter 2, we found that in *Vangl2*<sup>L<sup>D</sup>/L<sup>D</sup></sup> and *Ptk7*<sup>-/-</sup> mutant cochlea, disruptions of vinculin planar asymmetry correlated with stereociliary bundle misorientation. Together with evidence from preliminary time-lapse imaging of the myosin II network in OC and the analysis of vinculin loss of function mutants, we demonstrate that polarized contractile tension is required for hair cell PCP. Our working model proposes that polarized myosin II based contractile tension provides tissue level polarity cues that are interpreted by the microtubule based cell-intrinsic pathway to position the basal body at the lateral pole of hair cells. As a first step to validating this model, we could establish a role for polarized contractile tension in basal body positioning in the OC. We can test this by studying and correlating myosin II dynamics with basal body movements during PCP signaling by live imaging cochlear explants that are doubly transgenic for myosin IIB-GFP and Centrin2-GFP (marking centrioles) [267]. Preliminary live imaging of myosin II-GFP transgenic cochlear explants indicate that myosin II is increased on medial borders in a pulsatile manner. If our model is correct, pulsatile increases in myosin II signals will be accompanied with biased tugging of the centrioles towards the lateral side of hair cells. Comparisons of centriole movements in these cochlear explants in the absence or presence of ROCK inhibitor Y27632 or in the genetic background of *Ptk7* null mutations contractile tension is disrupted or weakened, will define a role for polarized contractile tension in basal body positioning. Randomized Brownian-like movement of the

basal body under conditions that disrupt tension in the OC will support the hypothesis that polarized contractile tension functions as a tissue polarity cue to orient hair cell PCP.

#### **4.2.2 Does polarized contractile tension mediated by PTK7-Src signaling pathway spatially regulate cortical Rac-PAK activity?**

Work from our lab has previously shown that Rac-PAK signaling functions as a cell-intrinsic polarity cue in hair cells and that the noncanonical Wnt/PCP pathway regulates an asymmetric cortical domain of Rac-PAK activity in the OC [79, 128]. Our model posits that *Ptk7*-mediated contractile tension exerted on medial borders of hair cells restricts microtubule-cortical capture to the lateral edge of hair cells by regulating Rac-PAK signaling. The observed complementary localizations of vinculin, a tension sensitive molecule, and Rac-PAK on the hair cell cortex are consistent with this idea. Therefore, to determine if Rac-PAK signaling provides the link between PTK7-Src signaling, actomyosin contractility and stereociliary bundle orientation, a comprehensive examination of cortical Rac-PAK localization using an antibody for Rac1-GTP in OC of *Ptk7*<sup>-/-</sup>, Src-inhibited, Csk and Vinculin conditional mutants will be necessary.

How does Ptk7-Src signaling regulate Rac-PAK localization? Par-3 is a scaffolding protein that recruits members of the Par-3/Par-6/aPKC complex essential for cell polarity in diverse cellular contexts. In the OC, we found that Par-3 is normally localized asymmetrically on the lateral cortex of hair cells similar to cortical active PAK localization and that *Ptk7* regulates asymmetric Par-

3 localization. Therefore, we propose that Par-3 is an effector of *Ptk7*-Src signaling that transduces tissue mechanical signals into differential biochemical activities of Rac to orient hair cell PCP. Several papers suggest that Par3 can regulate the activity of Rac by associating with Rac guanine exchange factors (GEF) Tiam1 and Tiam2 [269]. Interestingly, Tiam1 localizes on microtubules in hair cells and is proposed to be delivered to the lateral hair cell cortex to mediate Rac-PAK signaling [131]. Furthermore, Rac activity can be negatively regulated by tension through modulating Rac GAPs and GEFs [209, 210]. The requirement for Par-3 in cortical Rac-PAK signaling will have to be further addressed by analyzing Par-3 mouse mutants.

#### **4.2.3 How does PTK7-Src signaling regulate actomyosin contractility?**

In chapter 3, our analysis in MDCK cells and mouse OC suggests that PTK7-Src signaling regulates actomyosin contractility through both direct and indirect mechanisms. Time-lapse imaging of myosin II network in cochlear explants in the presence of Src inhibitors will be necessary to determine if PTK7-Src signaling regulates myosin II dynamics. Our preliminary examination of the live myosin II network in MIIB-GFP transgenic cochlear explants reveals recruitment of myosin II in a pulsatile manner along medial contacts of hair cells. In contrast, in *Ptk7* mutants, myosin II dynamics was disrupted and recruitment of myosin II to the medial borders was significantly reduced. Similar defects in myosin II dynamics between *Ptk7* mutant explants and Src-inhibited explants will suggest that PTK7-Src signaling locally modulate junctional myosin II dynamics.

A recent study proposed that Arp2/3-mediated actin assembly is required for promoting myosin II recruitment and stabilizing junctional tension [221]. Vinculin and cortactin, are actin-binding proteins that interact with Arp2/3 and are well-established substrates of Src tyrosine phosphorylation [227, 288]. In the OC, we show that both cortactin and vinculin were localized asymmetrically on medial borders of hair cells similarly to active Src, where contractile tension is increased. Preliminary analysis of actin distribution in hair cells indicates that actin is enriched on the medial border of hair cells. Moreover, *Ptk7* regulates Src-dependent tyrosine phosphorylation of vinculin at cell-cell contacts. We therefore hypothesize that *Ptk7*-Src signaling regulates actomyosin contractility by promoting Arp2/3-dependent actin polymerization activity. Changes in Arp2/3 localization in the *Ptk7*<sup>-/-</sup> and Src-loss of function or gain of function mutants will support this hypothesis. *Arp2/3* knockout mice are embryonic lethal. Therefore, application of pharmacological inhibitors of Arp2/3 such as CK-636 or CK548 on MIIB-GFP transgenic cochlear explants and documenting their effects on myosin II dynamics and localization, and stereociliary bundle orientation will be informative in the role of Arp2/3-dependent actin polymerization in actomyosin regulation and hair cell PCP.

#### **4.2.4 Does proteolytic cleavage of PTK7 regulate planar polarized Src signaling in the OC?**

In Chapter 3, we show that planar polarized junctional Src signaling is dependent on PTK7 and is required for the assembly of myosin II foci in

supporting cells. In the OC, *Ptk7* is ubiquitously expressed in hair cells and supporting cells, and stands in contrast to the asymmetric localization of active Src at cell-cell contacts. This raises the question of how *Ptk7* mediates planar polarized Src signaling in the OC.

We hypothesize that PTK7 localization and activity are modulated by post-translational mechanisms such as phosphorylation and proteolytic cleavage. It has been shown that in colon cancer cell lines, PTK7 is sequentially cleaved by MT1-MMP and  $\gamma$ -secretase [152–154, 289]. In the developing OC, *Ptk7* exhibits a dynamic expression pattern [1]. In addition to localizing at the adherens junctions, PTK7 is transiently localized on the apical surfaces of outer hair cells. Over the course of hair cell PCP establishment, PTK7 becomes predominantly localized at the adherens junctions. The functional relevance of this dynamic localization of PTK7 in hair cell PCP has not been explored. Interestingly, *in vitro* expression of a *Ptk7* construct lacking its cytoplasmic domain is predominantly localized to the apical surface of MDCK cells. Interaction between Src and PTK7 requires the cytoplasmic domain of PTK7, which harbors the kinase domain. Thus, proteolytic cleavage of PTK7 cytoplasmic domain provide a potential mechanism for regulating planar polarized Src signaling in the OC. Analyzing the effects of MMP and  $\gamma$ -secretase inhibitors on active Src localization and hair cell PCP will shed light on the role of proteolytic processing in PTK7-Src junctional signaling in the OC. Ultimately, studies of knock-in mice that express a non-cleavable form of PTK7 will be necessary to further elucidate the in-vivo relevance of PTK7 cleavage on hair cell PCP.

#### 4.2.5 How does the noncanonical Wnt/PCP pathway regulate actomyosin contractility in the OC?

In Chapter 2, we found that both *Ptk7* and the noncanonical Wnt/PCP pathway differentially regulate actomyosin contractility in the OC. Whether or not they have separate contributions to actomyosin contractility are not clear. Based on myosin IIB immunostaining, junctional myosin II localization was reduced and myosin IIB foci were absent in supporting cells in *Ptk7*<sup>-/-</sup> OC. In *Vangl2*<sup>Lp/Lp</sup> mutants, junctional myosin IIB localization was reduced but apical myosin II foci assembled in supporting cells and appeared smaller in size. Furthermore, disrupting *Ptk7* and *Vangl2* function causes distinct effects on planar asymmetry of junctional vinculin. *Ptk7* mutant OC displayed a loss of vinculin planar asymmetry while in *Vangl2*<sup>Lp/Lp</sup> OC, vinculin planar asymmetry was misoriented. Based on these observations, *Ptk7*-mediated assembly of myosin II foci in supporting cells is necessary for generating contractile tension, but additional mechanisms facilitated by noncanonical Wnt/PCP signaling may function to polarize contractile tension. A comparison of the live myosin II network in *Vangl2*<sup>Lp/Lp</sup> and *Ptk7*<sup>-/-</sup> cochlear explants will reveal if *Ptk7* and noncanonical Wnt/PCP pathway regulates distinct aspects of myosin II dynamics. Our preliminary live imaging of the myosin II network in the cochlea reveals that myosin II is preferentially recruited to medial borders of hair cells. Recruitment of myosin II to randomized locations along the hair cell cortex in *Vangl2*<sup>Lp/Lp</sup> OC will support the hypothesis that the noncanonical Wnt/PCP pathway polarizes

contractile tension at cell-cell contacts. The core PCP pathway may spatially coordinate the “tug of war” interactions between hair cells and supporting cells and participate in cadherin-mediated mechanotransduction, for example, through regulation of E-cadherin surface expression [241].

Our genetic data also indicates that *Fz3/Fz6* and *Ptk7* act in opposing fashions to orient hair cell PCP. We propose that *Fz3/Fz6* modulates actomyosin contractility in hair cells and/or supporting cells by counterbalancing pulling forces on hair cells. *Fz3/Fz6* may regulate myosin II activity directly through RLC phosphorylation and/or modulate Src activity at cell-cell contacts. It would be informative to examine the localization of active Src in *Fz3; Fz6* double mutant OC. Changes in planar asymmetry of active Src would support the latter. How might *Fz3* inhibit Src? Src are well known effectors of Eph/EphrinB and G-protein signaling [247]. While the *in vivo* relevance of the *Fz3* and EphrinB1 biochemical interaction awaits further investigation, *Fz3* may modulate Src activity through Eph/EphrinB signaling. Conversely, Src has been established as direct effectors of G-protein signaling [290, 291]. A recent study showed Fz receptors were recently found to interact Gai, Gaq, and Gas proteins [292].

## CHAPTER 5: Materials and Methods

## 5.1 Mice and Genotyping

All mice were maintained in compliance with NIH guidelines and the Animal Care and Use Committee at the University of Virginia. Mice were either obtained from the Jackson Laboratory, the referenced sources or produced in-house and maintained on a mixed genetic background.

For genotyping, mouse genomic DNA was extracted from embryo tail snips. These tissues were incubated with 100 $\mu$ l 50 mM NaOH at 95 °C for 30 minutes and neutralized with 30 $\mu$ l of 1M Tris-HCl (pH 7.5). PCR was performed using primers listed in Table 1 or in genotyping protocols for *Fz3*, *Fz6*, *Jnk1* and *Jnk2* mice available on the Jackson laboratory website (<http://jaxmice.jax.org/query>). *Myh10DN* genotyping was performed as previously described [195].

## 5.2 Generation of a floxed *Ptk7* allele

A gene-trapping strategy similar to that described by Skarnes et al. [293] was used to target loxP sites into the *Ptk7* locus. Briefly, a targeting vector containing the 'secretory gene trap' cassette [294] flanked by FRT sites and *Ptk7* genomic sequences flanked by loxP sites was electroporated into E14 ES cells (details of vector construction are available upon request). Homologous recombination events were detected by long-range PCR using the AccuPrime TAQ DNA polymerase system (Invitrogen). Two independent gene-trapped clones were injected into blastocysts and mutant mice were established by

chimera breeding. The floxed allele was generated by germline expression of the Flp recombinase to remove the gene-trap cassette and subsequently bred to homozygosity. *Ptk7*<sup>CO/CO</sup> animals are viable and fertile, indicating the floxed allele is fully functional.

### 5.3 *Ptk7* genotyping in mosaic analysis

PTK7 immunostaining was used to determine the *Ptk7* genotype of individual hair cells and supporting cells in mosaic OC. To ensure that cells were genotyped correctly, care was taken to confirm the presence or absence of PTK7 immunostaining by scanning through the entire Z-stack, about 4  $\mu\text{m}$  in thickness on average.

### 5.4 Immunohistochemistry

For cochlea whole mounts, temporal bones were collected at the indicated developmental timepoints and fixed in 4% paraformaldehyde (PFA) at 4°C overnight or at room temperature for 1 hour. Alternatively, cochleae were fixed in 10% trichloroacetic acid (TCA) for 1 hour at 4°C (see **Table 1.2**). Dissected cochleae were incubated in PBS + 5% heat-inactivated goat serum + 0.1% Triton + 0.02% NaN<sub>3</sub> (blocking solution) for 1 hour at room temperature, followed by overnight incubation with primary antibodies listed in Table 2 at 4°C. After three washes in PBS + 0.1% Triton, samples were incubated with secondary antibodies for 1 hour at room temperature. Cochleae were flat-mounted on glass

slides in Mowiol with 5% *N*-propyl gallate.

## 5.5 Cell culture and Western Blotting

For overexpression studies of PTK7 and Fz3, HEK293T cell lines were maintained in 10% FBS, 1% penicillin/streptomycin and high glucose DMEM (Gibco) at 37°C, 5% CO<sub>2</sub>. Full-length EphrinB1, Fz3 and PTK7 constructs were transfected into cells using Fugene6 (Roche).

For Western blotting, tissue samples were lysed in 1% TritonX-100 lysis buffer (0.14M NaCl, 20mM HEPES pH7.4, 25mM NaF, 5mM 1mM Na<sub>3</sub>VO<sub>4</sub>, 5mM Na<sub>4</sub>P<sub>2</sub>O<sub>7</sub>, 4mM EDTA) with 1X Protease inhibitor cocktail (Roche), and diluted with 4X SDS sample buffer. Samples were boiled at 95°C for 5 minutes and run in 8% or 15% acrylamide gels. Transfer was carried out on nitrocellulose membranes at 300mA. Membranes were blocked in 5% milk/PBST for 1 hour at room temperature and then incubated with primary antibodies diluted in 3% BSA/PBST/NaN<sub>3</sub> overnight at 4°C. Primary antibodies were: rabbit anti-PTK7 [1] (1:3000), rabbit anti-phospho RLC (1:500, Rockland), rabbit anti-Myosin IIB (1:1000, Sigma), rabbit anti-Myosin IIA (1:500, Covance), rabbit anti-Myosin IIC (1:2500, Covance), rabbit anti-Fz3 (1:1000, Sigma), rabbit anti-c-Jun (1:1000, Cell Signaling), rabbit anti-phospho-cJun (1:1000, Cell Signaling), goat anti-ROCK1 (1:500, Santa Cruz), rabbit anti-ROCK2 (1:500, Cell Signaling), rabbit anti-pY416 Src (1:500, Cell Signaling #2101) goat anti-EphrinB1 (1:200, R&D Systems). Horseradish peroxidase (HRP) conjugated-rabbit (1:10,000), goat (1:10,000) or mouse (1:10,000) secondary antibodies were diluted in 5%

milk/PBST and washed 3 times in PBST for 10 minutes each. Membranes were developed with Millipore Immobilon Western HRP chemiluminescence HRP substrate (mixed 1:1).

For quantification of MIIA, MIIB, MIIC, pRLC, pY416-Src, ROCK1 and ROCK2 Western blots, membranes were incubated with fluorescent-labeled secondary antibody at 1:15,000 dilution with 2% fish gelatin/PBST for 1 hour at room temperature, washed 3 times in PBST, and scanned using the Odyssey Infrared Imaging System (LI-COR, Inc., Lincoln, NE, USA). The relative levels of MIIA, MIIB, MIIC, pRLC pY416-Src, ROCK1 and ROCK2 were normalized to their respective GAPDH loading controls and expressed as a percentage of the normalized control level in lane 1.

## **5.6 Organotypic cochlear explant cultures**

Cochlear explants from E15.5 embryos were established on Matrigel-coated chamber slides and treated with either vehicle (DMF, dimethylformamide or DMSO, dimethyl sulfoxide) or drug (listed below) after four hours *in vitro*. Culture media contains DMEM/F12 (1:1) supplemented with N2 (1:100; Invitrogen) and penicillin or ampicillin and explants were maintained in 5% CO<sub>2</sub> at 37°C.

For inhibition of myosin II activity, 10 µM blebbistatin (Enzo LifeSciences) was used. After 24 hours of drug treatment, media were replaced with drug-free media. Explants were maintained for another three days *in vitro* and then processed for immunostaining (see 5.4).

For Src inhibition, explants were treated with either vehicle (DMSO) or 5  $\mu$ M SU6656 (Millipore). After 48 hours of drug treatment, media were replaced with drug-free media. Explants were maintained for another three days *in vitro* and then processed for immunostaining. For *in vivo* Src inhibition, a single dose of Bosutinib (LC laboratories) was administered intraperitoneally to wild-type dams on E16.5 or 17.5 at 30 mg/kg, and embryos were harvested four hours later and processed for immunostaining. Embryos from vehicle-injected dams were used as controls.

## **5.7 Image acquisition**

Z-stacks of images were acquired on a Deltavision deconvolution microscope using a 60x objective (NA 1.4) at 0.2 $\mu$ m intervals and processed with Softworx software (Applied Precision) and Adobe Photoshop CS2 (Adobe Systems). Alternatively, confocal images were collected on a Zeiss LSM700 Confocal Laser Scanning Microscope (Carl Zeiss) using a 63x objective (NA 1.4) at 0.4 $\mu$ m intervals. Optical slices along the Z-axis were generated using the Zen 2009 LE software (Carl Zeiss). The cochlear positions analyzed in the micrographs are indicated as the distance from the base relative to the length of the cochlea in percentages.

## **5.8 Analysis of stereociliary bundle orientation/kinocilium position**

Stereociliary bundles in E18.5 OC were visualized by phalloidin and

acetylated tubulin staining which mark the stereocilia and the kinocilium, respectively. Measurements of stereociliary bundle orientation were taken from hair cells in the basal region of the cochlea (at least 4 cochleae per genotype) using ImageJ software (<http://rsb.info.nih.gov/ij>). Bundle orientation was determined by the angle formed by the intersection of a line drawn through the axis of symmetry of the stereociliary bundle and one parallel to the medial-lateral axis of the OC (assigned as 0°). Clockwise deviations from 0° were assigned positive values and counterclockwise negative values.

### **5.9 Quantification of pY416-Src and pY722-ROCK2 localization**

Fluorescence intensity measurements of pY416-Src and pY722-ROCK2 immunostaining were taken from single z-plane images using line-scan analysis in ImageJ. The position of the cell junction along the line was determined by the peak of F-actin staining. For planar asymmetry measurements in the OC, junctional intensity at the medial and lateral boundaries was first normalized relative to a spot six pixels away in the cytoplasm, and then plotted as medial to lateral (M:L) intensity ratios. Average M:L ratio and standard error of the mean (S.E.M.). A student's two-tailed t-test was performed to determine statistical significance ( $\alpha=0.05$ ).

### 5.10 Live imaging of MIIB-GFP

Cochlear explants from E15.5 or E16.5 Myosin IIB-GFP (MIIB-GFP) knock-in mouse embryos were established on No.1 glass coverslips coated with matrigel. After recovery in vitro for 12 hours, explants were imaged on an inverted Deltavision deconvolution microscope. Coverslips were oriented such that the apical surfaces were facing down, mounted and secured in position by silicon grease balls to the bottom face of a 35mm No. 1.0 coverglass-bottom culture dish (MatTek). During live imaging, explants were maintained in 10mM HEPES buffered Phenol-red free DMEM on a heated stage at 37°C. For every time point, Z-stacks of images (step size of 0.3 $\mu$ m) of equivalent mid-basal region of the cochlea were obtained. Softworx was used to view time-lapse movies and to extract equivalent single Z-plane sections across time to align. Single optical sections were concatenated in ImageJ and aligned using StackReg plugin to account for tissue drift. Measurements of MIIB GFP intensity were taken using region of interest (ROI) tool and kymographs were created with a kymograph plug in in ImageJ.

**Table 1. Primers used for PCR genotyping**

<b>Strain</b>	<b>Sequence (5'-3')</b>
Cre	AGAACCTGAAGATGTTGCGCG
	GGCTATACGTAACAGGGTGT
Ptk7 <sup>CO</sup> / Ptk7 <sup>+</sup>	AGAGAGAGTTCATTTGTGATA
	AGCTATTCATACTCCGTTCC
	TGGTACTAGTATGTGCTCAG

**Table 2. Primary antibodies used for immunostaining**

<b>Antigen</b>	<b>Host Species</b>	<b>Dilution</b>	<b>Source / Catalog #</b>
Acetylated Tubulin	Mouse mAb	1:500	Sigma T6793
$\beta$ -catenin	Mouse	1:500	Cell Signaling
Cortactin	Mouse mAb	1:300	Gift from Thomas Parsons
Dvl2 <sup>1</sup>	Rabbit	1:100	Cell Signaling 3224
E-cadherin	Rat	1:200	Sigma U3254
Ecto-ephrinB1	Goat	1:100	R&D systems AF473
Ecto-ephrinB2	Goat	1:25	R&D systems AF496
Ecto-PTK7	Rabbit	1:500	[1]
FilGAP	Rabbit	1:100	Gift from Yasutaka Ohta
Fz3	Rabbit	1:200	Gift from Jeremy Nathans (JH5013)
Gpsm2	Rabbit	1:500	Gift from Qingwen Wan
Myosin IIA	Rabbit	1:300	Covance PRB- 440P
Myosin IIB	Rabbit	1:500	Sigma M7939

Myosin IIC	Rabbit	1:100	Covance PRB-444P
Par-3	Rabbit	1:100	Millipore 07-330
Phospho Y1065-Vinculin	Rabbit	1:200	Invitrogen 44-1078G
Phospho JNK	Rabbit	1:250	Cell Signaling
Phospho Y416-Src	Rabbit	1:500	Cell Signaling #2101
Phospho Y722-ROCK2	Rabbit	1:100	Gift from Zee-Fen Chang
Phospho MLC	Rabbit	1:400	Rockland 100-401-416
Rac1 <sup>1</sup>	Mouse mAb	1:200	Millipore 05-389
ROCK2 <sup>1</sup>	Rabbit	1:100	Cell Signaling 9029
srGAP2	Rabbit	1:100	Gift from Wei-Lin Jin
Vinculin	Mouse mAb	1:600	Sigma V9131

<sup>1</sup>Antibodies used with 10% trichloroacetic acid (TCA) fixation protocol

## CHAPTER 6: Bibliography

1. Lu, X., Borchers, A. G. M., Jolicoeur, C., Rayburn, H., Baker, J. C., and Tessier-lavigne, M. (2004). PTK7 / CCK-4 is a novel regulator of planar cell polarity in vertebrates. *Nature* 430, 93–98.
2. Curtin, J. A., Quint, E., Tsipouri, V., Arkell, R. M., Cattanach, B., Copp, A. J., Henderson, D. J., Spurr, N., Stanier, P., Fisher, E. M., et al. (2003). Mutation of *Celsr1* disrupts planar polarity of inner ear hair cells and causes severe neural tube defects in the mouse. *Curr. Biol.* 13, 1129–1133.
3. Devenport, D., and Fuchs, E. (2008). Planar polarization in embryonic epidermis orchestrates global asymmetric morphogenesis of hair follicles. *Nat. Cell Biol.* 10, 1257–1268.
4. Wang, Y., and Nathans, J. (2007). Tissue/planar cell polarity in vertebrates: new insights and new questions. *Development* 134, 647–658.
5. Muñoz-Soriano, V., Belacortu, Y., and Paricio, N. (2012). Planar cell polarity signaling in collective cell movements during morphogenesis and disease. *Curr. Genomics* 13, 609–22.
6. Simons, M., and Mlodzik, M. (2008). Planar cell polarity signaling: from fly development to human disease. *Annu. Rev. Genet.* 42, 517–540.
7. Bayly, R., and Axelrod, J. D. (2011). Pointing in the right direction: new developments in the field of planar cell polarity. *Nat. Rev. Genet.* 12, 385–91.
8. Wallingford, J. B. (2012). Planar cell polarity and the developmental control of cell behavior in vertebrate embryos. *Annu. Rev. Cell Dev. Biol.* 28, 627–53.
9. Jones, C., and Chen, P. (2007). Planar cell polarity signaling in vertebrates. *BioEssays news Rev. Mol. Cell. Dev. Biol.* 29, 120–132.
10. McNeill, H. (2010). Planar cell polarity: keeping hairs straight is not so simple. *Cold Spring Harb. Perspect. Biol.* 2, a003376.
11. Gubb, D., and Garcia-Bellido, A. (1982). A genetic analysis of the determination of cuticular polarity during development in *Drosophila melanogaster*. *J Embryol Exp Morphol* 68, 37–57.
12. Shimada, Y., Yonemura, S., Ohkura, H., Strutt, D., and Uemura, T. (2006). Polarized transport of Frizzled along the planar microtubule arrays in *Drosophila* wing epithelium. *Dev. Cell* 10, 209–222.

13. Lin, C., and Katanaev, V. L. (2013). Kermit interacts with *gao*, *vang*, and motor proteins in *Drosophila* planar cell polarity. *PLoS One* 8, e76885.
14. Adler, P. N., Taylor, J., and Charlton, J. (2000). The domineering non-autonomy of *frizzled* and *van Gogh* clones in the *Drosophila* wing is a consequence of a disruption in local signaling. *Mech. Dev.* 96, 197–207.
15. Vinson, C. R., and Adler, P. N. Directional non-cell autonomy and the transmission of polarity information by the *frizzled* gene of *Drosophila*. *Nature* 329, 549–51.
16. Taylor, J., Abramova, N., Charlton, J., and Adler, P. N. (1998). *Van Gogh*: a new *Drosophila* tissue polarity gene. *Genetics* 150, 199–210.
17. Lawrence, P. A., Casal, J., and Struhl, G. (2002). Towards a model of the organisation of planar polarity and pattern in the *Drosophila* abdomen. *Development* 129, 2749–2760.
18. Casal, J., Lawrence, P. A., and Struhl, G. (2006). Two separate molecular systems, *Dachsous*/*Fat* and *Starry night*/*Frizzled*, act independently to confer planar cell polarity. *Development* 133, 4561–4572.
19. Klein, T. J., and Mlodzik, M. (2005). Planar cell polarization: an emerging model points in the right direction. *Annu. Rev. Cell Dev. Biol.* 21, 155–176.
20. Wu, J., Roman, A.-C., Carvajal-Gonzalez, J. M., and Mlodzik, M. (2013). *Wg* and *Wnt4* provide long-range directional input to planar cell polarity orientation in *Drosophila*. *Nat. Cell Biol.* 15, 1045–55.
21. Thomas, C., and Strutt, D. (2012). The roles of the cadherins *Fat* and *Dachsous* in planar polarity specification in *Drosophila*. *Dev. Dyn. an Off. Publ. Am. Assoc. Anat.* 241, 27–39.
22. Goodrich, L. V., and Strutt, D. (2011). Principles of planar polarity in animal development. *Development* 138, 1877–92.
23. Strutt, D., and Warrington, S. J. (2008). Planar polarity genes in the *Drosophila* wing regulate the localisation of the FH3-domain protein *Multiple Wing Hairs* to control the site of hair production. *Dev. Cambridge Engl.* 135, 3103–3111.
24. Matis, M., and Axelrod, J. D. (2013). Regulation of PCP by the *Fat* signaling pathway. *Genes Dev.* 27, 2207–20.

25. Strutt, H., and Strutt, D. (2002). Nonautonomous planar polarity patterning in *Drosophila*: dishevelled-independent functions of frizzled. *Dev. Cell* 3, 851–863.
26. Zeidler, M. P., Perrimon, N., and Strutt, D. I. (2000). Multiple roles for four-jointed in planar polarity and limb patterning. *Dev. Biol.* 228, 181–196.
27. Adler, P. N., Charlton, J., and Liu, J. (1998). Mutations in the cadherin superfamily member gene *dachsous* cause a tissue polarity phenotype by altering frizzled signaling. *Development* 125, 959–68.
28. Ma, D., Yang, C., McNeill, H., Simon, M. A., and Axelrod, J. D. (2003). Fidelity in planar cell polarity signalling. *Nature* 421, 543–7.
29. Strutt, H., Mundy, J., Hofstra, K., and Strutt, D. (2004). Cleavage and secretion is not required for Four-jointed function in *Drosophila* patterning. *Development* 131, 881–90.
30. Simon, M. A. (2004). Planar cell polarity in the *Drosophila* eye is directed by graded Four-jointed and *Dachsous* expression. *Development* 131, 6175–6184.
31. Matakatsu, H., and Blair, S. S. (2004). Interactions between Fat and *Dachsous* and the regulation of planar cell polarity in the *Drosophila* wing. *Development* 131, 3785–3794.
32. Bertet, C., Sulak, L., and Lecuit, T. (2004). Myosin-dependent junction remodelling controls planar cell intercalation and axis elongation. *Nature* 429, 667–671.
33. Blankenship, J. T., Backovic, S. T., Sanny, J. S. P., Weitz, O., and Zallen, J. A. (2006). Multicellular rosette formation links planar cell polarity to tissue morphogenesis. *Dev. Cell* 11, 459–470.
34. Vichas, A., and Zallen, J. A. (2011). Translating cell polarity into tissue elongation. *Semin. Cell Dev. Biol.* 22, 858–864.
35. Zallen, J. A. (2007). Planar polarity and tissue morphogenesis. *Cell* 129, 1051–63.
36. Zallen, J. A., and Wieschaus, E. (2004). Patterned gene expression directs bipolar planar polarity in *Drosophila*. *Dev. Cell* 6, 343–355.
37. Gutzeit, H. O. (1990). The microfilament pattern in the somatic follicle cells of mid-vitellogenic ovarian follicles of *Drosophila*. *Eur. J. Cell Biol.* 53, 349–356.

38. Frydman, H. M., and Spradling, A. C. (2001). The receptor-like tyrosine phosphatase *lar* is required for epithelial planar polarity and for axis determination within *Drosophila* ovarian follicles. *Development* 128, 3209–3220.
39. Conder, R., Yu, H., Zahedi, B., and Harden, N. (2007). The serine/threonine kinase dPak is required for polarized assembly of F-actin bundles and apical-basal polarity in the *Drosophila* follicular epithelium. *Dev. Biol.* 305, 470–482.
40. Gutzeit, H. O., Eberhardt, W., and Gratwohl, E. (1991). Laminin and basement membrane-associated microfilaments in wild-type and mutant *Drosophila* ovarian follicles. *J. Cell Sci.* 100 ( Pt 4, 781–788.
41. Bateman, J., Reddy, R. S., Saito, H., and Van Vactor, D. (2001). The receptor tyrosine phosphatase *Dlar* and integrins organize actin filaments in the *Drosophila* follicular epithelium. *Curr. Biol.* 11, 1317–1327.
42. Viktorinová, I., König, T., Schlichting, K., and Dahmann, C. (2009). The cadherin *Fat2* is required for planar cell polarity in the *Drosophila* ovary. *Development* 136, 4123–4132.
43. Hirokawa, N., Tanaka, Y., and Okada, Y. (2009). Left-right determination: involvement of molecular motor KIF3, cilia, and nodal flow. *Cold Spring Harb. Perspect. Biol.* 1, a000802.
44. Hashimoto, M., Shinohara, K., Wang, J., Ikeuchi, S., Yoshida, S., Meno, C., Nonaka, S., Takada, S., Hatta, K., Wynshaw-Boris, A., et al. (2010). Planar polarization of node cells determines the rotational axis of node cilia. *Nat. Cell Biol.* 12, 170–176.
45. Antic, D., Stubbs, J. L., Suyama, K., Kintner, C., Scott, M. P., and Axelrod, J. D. (2010). Planar cell polarity enables posterior localization of nodal cilia and left-right axis determination during mouse and *Xenopus* embryogenesis. *PLoS One* 5, e8999.
46. Song, H., Hu, J., Chen, W., Elliott, G., Andre, P., Gao, B., and Yang, Y. (2010). Planar cell polarity breaks bilateral symmetry by controlling ciliary positioning. *Nature* 466, 378–82.
47. Zhang, Y., and Levin, M. (2009). Left-right asymmetry in the chick embryo requires core planar cell polarity protein *Vangl2*. *Genesis* 47, 719–728.
48. Ravni, A., Qu, Y., Goffinet, A. M., and Tissir, F. (2009). Planar cell polarity cadherin *Celsr1* regulates skin hair patterning in the mouse. *J. Invest. Dermatol.* 129, 2507–9.

49. Guo, N., Hawkins, C., and Nathans, J. (2004). Frizzled6 controls hair patterning in mice. *Proc. Natl. Acad. Sci. U. S. A.* *101*, 9277–9281.
50. May-Simera, H., and Kelley, M. W. (2012). Planar cell polarity in the inner ear. *Curr. Top. Dev. Biol.* *101*, 111–40.
51. Jessen, J. R., Topczewski, J., Bingham, S., Sepich, D. S., Marlow, F., Chandrasekhar, A., and Solnica-Krezel, L. (2002). Zebrafish trilobite identifies new roles for Strabismus in gastrulation and neuronal movements. *Nat. Cell Biol.* *4*, 610–615.
52. Marlow, F., Topczewski, J., Sepich, D., and Solnica-Krezel, L. (2002). Zebrafish Rho kinase 2 acts downstream of Wnt11 to mediate cell polarity and effective convergence and extension movements. *Curr. Biol.* *12*, 876–884.
53. Myers, D. C., Sepich, D. S., and Solnica-Krezel, L. (2002). Convergence and extension in vertebrate gastrulae: cell movements according to or in search of identity? *Trends Genet.* *18*, 447–455.
54. Keller, R., Davidson, L., Edlund, A., Elul, T., Ezin, M., Shook, D., and Skoglund, P. (2000). Mechanisms of convergence and extension by cell intercalation. *Philos. Trans. R. Soc. Lond. B. Biol. Sci.* *355*, 897–922.
55. Fraser, S. E., Harland, R. M., and Wallingford, J. B. (2002). Convergent Extension The Molecular Control of Polarized Cell Movement during Embryonic Development. *Dev. Cell* *2*, 695–706.
56. Gray, R. S., Roszko, I., and Solnica-Krezel, L. (2011). Planar cell polarity: coordinating morphogenetic cell behaviors with embryonic polarity. *Dev. Cell* *21*, 120–33.
57. Roszko, I., Sawada, A., and Solnica-Krezel, L. (2009). Regulation of convergence and extension movements during vertebrate gastrulation by the Wnt/PCP pathway. *Semin. Cell Dev. Biol.* *20*, 986–997.
58. Kibar, Z., Vogan, K. J., Groulx, N., Justice, M. J., Underhill, D. A., and Gros, P. (2001). Ltap, a mammalian homolog of Drosophila Strabismus/Van Gogh, is altered in the mouse neural tube mutant Loop-tail. *Nat. Genet.* *28*, 251–255.
59. Wang, Y., Guo, N., and Nathans, J. (2006). The role of Frizzled3 and Frizzled6 in neural tube closure and in the planar polarity of inner-ear sensory hair cells. *J. Neurosci.* *26*, 2147–2156.

60. Wang, J., Hamblet, N. S., Mark, S., Dickinson, M. E., Brinkman, B. C., Segil, N., Fraser, S. E., Chen, P., Wallingford, J. B., and Wynshaw-Boris, A. (2006). Dishevelled genes mediate a conserved mammalian PCP pathway to regulate convergent extension during neurulation. *Development* 133, 1767–78.
61. Wang, J., Mark, S., Zhang, X., Qian, D., Yoo, S.-J., Radde-Gallwitz, K., Zhang, Y., Lin, X., Collazo, A., Wynshaw-Boris, A., et al. (2005). Regulation of polarized extension and planar cell polarity in the cochlea by the vertebrate PCP pathway. *Nat. Genet.* 37, 980–5.
62. Henderson, D. J., Conway, S. J., Greene, N. D., Gerrelli, D., Murdoch, J. N., Anderson, R. H., and Copp, A. J. (2001). Cardiovascular defects associated with abnormalities in midline development in the Loop-tail mouse mutant. *Circ. Res.* 89, 6–12.
63. Fischer, E., Legue, E., Doyen, A., Nato, F., Nicolas, J.-F., Torres, V., Yaniv, M., and Pontoglio, M. (2006). Defective planar cell polarity in polycystic kidney disease. *Nat. Genet.* 38, 21–3.
64. Tissir, F., and Goffinet, A. M. (2013). Shaping the nervous system: role of the core planar cell polarity genes. *Nat. Rev. Neurosci.* 14, 525–35.
65. Tissir, F., and Goffinet, A. M. (2010). Planar cell polarity signaling in neural development. *Curr. Opin. Neurobiol.* 20, 572–577.
66. Wada, H., Tanaka, H., Nakayama, S., Iwasaki, M., and Okamoto, H. (2006). Frizzled3a and Celsr2 function in the neuroepithelium to regulate migration of facial motor neurons in the developing zebrafish hindbrain. *Development* 133, 4749–4759.
67. Glasco, D. M., Murdoch, J. N., Chandrasekhar, A., Cadete Vilhais-Neto, G., Yang, Y., Song, M.-R., Stewart, M., Sittaramane, V., Bryant, W., Paudyal, A., et al. (2012). The mouse Wnt/PCP protein Vangl2 is necessary for migration of facial branchiomotor neurons, and functions independently of Dishevelled. *Dev. Biol.* 369, 211–222.
68. Qu, Y., Glasco, D. M., Zhou, L., Sawant, A., Ravni, A., Fritsch, B., Damrau, C., Murdoch, J. N., Evans, S., Pfaff, S. L., et al. (2010). Atypical cadherins Celsr1-3 differentially regulate migration of facial branchiomotor neurons in mice. *J. Neurosci.* 30, 9392–9401.
69. Lyuksyutova, A. I., Lu, C.-C., Milanesio, N., King, L. A., Guo, N., Wang, Y., Nathans, J., Tessier-Lavigne, M., and Zou, Y. (2003). Anterior-posterior guidance of commissural axons by Wnt-frizzled signaling. *Science* 302, 1984–1988.

70. Wang, Y., Thekdi, N., Smallwood, P. M., Macke, J. P., and Nathans, J. (2002). Frizzled-3 is required for the development of major fiber tracts in the rostral CNS. *J. Neurosci.* *22*, 8563–8573.
71. Shima, Y., Kengaku, M., Hirano, T., Takeichi, M., and Uemura, T. (2004). Regulation of dendritic maintenance and growth by a mammalian 7-pass transmembrane cadherin. *Dev. Cell* *7*, 205–216.
72. Kimura, H., Usui, T., Tsubouchi, A., and Uemura, T. (2006). Potential dual molecular interaction of the *Drosophila* 7-pass transmembrane cadherin Flamingo in dendritic morphogenesis. *J. Cell Sci.* *119*, 1118–1129.
73. Rosso, S. B., Sussman, D., Wynshaw-Boris, A., and Salinas, P. C. (2005). Wnt signaling through Dishevelled, Rac and JNK regulates dendritic development. *Nat. Neurosci.* *8*, 34–42.
74. Collier, S., Lee, H., Burgess, R., and Adler, P. (2005). The WD40 repeat protein fritz links cytoskeletal planar polarity to frizzled subcellular localization in the *Drosophila* epidermis. *Genetics* *169*, 2035–2045.
75. Collier, S., and Gubb, D. (1997). *Drosophila* tissue polarity requires the cell-autonomous activity of the fuzzy gene, which encodes a novel transmembrane protein. *Development* *124*, 4029–4037.
76. Park, W. J., Liu, J., Sharp, E. J., and Adler, P. N. (1996). The *Drosophila* tissue polarity gene inturned acts cell autonomously and encodes a novel protein. *Development* *122*, 961–969.
77. Park, T. J., Haigo, S. L., and Wallingford, J. B. (2006). Ciliogenesis defects in embryos lacking inturned or fuzzy function are associated with failure of planar cell polarity and Hedgehog signaling. *Nat. Genet.* *38*, 303–311.
78. Habas, R., Dawid, I. B., and He, X. (2003). Coactivation of Rac and Rho by Wnt/Frizzled signaling is required for vertebrate gastrulation. *Genes Dev.* *17*, 295–309.
79. Grimsley-Myers, C. M., Sipe, C. W., Géléoc, G. S. G., and Lu, X. (2009). The small GTPase Rac1 regulates auditory hair cell morphogenesis. *J. Neurosci.* *29*, 15859–15869.
80. Grimsley-Myers, C. M., Sipe, C. W., Wu, D. K., and Lu, X. (2012). Redundant functions of Rac GTPases in inner ear morphogenesis. *Dev. Biol.* *362*, 172–86.

81. Boutros, M., Paricio, N., Strutt, D. I., and Mlodzik, M. (1998). Dishevelled activates JNK and discriminates between JNK pathways in planar polarity and wingless signaling. *Cell* *94*, 109–118.
82. Yamanaka, H., Moriguchi, T., Masuyama, N., Kusakabe, M., Hanafusa, H., Takada, R., Takada, S., and Nishida, E. (2002). JNK functions in the non-canonical Wnt pathway to regulate convergent extension movements in vertebrates. *EMBO Rep.* *3*, 69–75.
83. Vivancos, V., Chen, P., Spassky, N., Qian, D., Dabdoub, A., Kelley, M., Studer, M., and Guthrie, S. (2009). Wnt activity guides facial branchiomotor neuron migration, and involves the PCP pathway and JNK and ROCK kinases. *Neural Dev.* *4*, 7.
84. Aigouy, B., Farhadifar, R., Staple, D. B., Sagner, A., Röper, J.-C., Jülicher, F., and Eaton, S. (2010). Cell flow reorients the axis of planar polarity in the wing epithelium of *Drosophila*. *Cell* *142*, 773–786.
85. Harumoto, T., Ito, M., Shimada, Y., Kobayashi, T. J., Ueda, H. R., Lu, B., and Uemura, T. (2010). Atypical cadherins Dach2 and Fat control dynamics of noncentrosomal microtubules in planar cell polarity. *Dev. Cell* *19*, 389–401.
86. Mao, Y., Rauskolb, C., Cho, E., Hu, W.-L., Hayter, H., Minihan, G., Katz, F. N., and Irvine, K. D. (2006). Dach2: an unconventional myosin that functions downstream of Fat to regulate growth, affinity and gene expression in *Drosophila*. *Dev. Cambridge Engl.* *133*, 2539–2551.
87. Oishi, I., Suzuki, H., Onishi, N., Takada, R., Kani, S., Ohkawara, B., Koshida, I., Suzuki, K., Yamada, G., Schwabe, G. C., et al. (2003). The receptor tyrosine kinase Ror2 is involved in non-canonical Wnt5a/JNK signalling pathway. *Genes Cells* *8*, 645–54.
88. Gao, B., Song, H., Bishop, K., Elliot, G., Garrett, L., English, M. A., Andre, P., Robinson, J., Sood, R., Minami, Y., et al. (2011). Wnt signaling gradients establish planar cell polarity by inducing Vangl2 phosphorylation through Ror2. *Dev. Cell* *20*, 163–176.
89. Yamamoto, S., Nishimura, O., Miki, K., Nishita, M., Minami, Y., Yonemura, S., Tarui, H., and Sasaki, H. (2008). Cthrc1 selectively activates the planar cell polarity pathway of Wnt signaling by stabilizing the Wnt-receptor complex. *Dev. Cell* *15*, 23–36.
90. Andre, P., Wang, Q., Wang, N., Gao, B., Schilit, A., Halford, M. M., Stacker, S. A., Zhang, X., and Yang, Y. (2012). The Wnt coreceptor Ryk

- regulates Wnt/planar cell polarity by modulating the degradation of the core planar cell polarity component Vangl2. *J. Biol. Chem.* *287*, 44518–25.
91. Montcouquiol, M., Sans, N., Huss, D., Kach, J., Dickman, J. D., Forge, A., Rachel, R. A., Copeland, N. G., Jenkins, N. A., Bogani, D., et al. (2006). Asymmetric localization of Vangl2 and Fz3 indicate novel mechanisms for planar cell polarity in mammals. *J. Neurosci.* *26*, 5265–5275.
  92. Wansleeben, C., Feitsma, H., Montcouquiol, M., Kroon, C., Cuppen, E., and Meijlink, F. (2010). Planar cell polarity defects and defective Vangl2 trafficking in mutants for the COPII gene *Sec24b*. *Dev. Cambridge Engl.* *137*, 1067–1073.
  93. Merte, J., Jensen, D., Wright, K., Sarsfield, S., Wang, Y., Schekman, R., and Ginty, D. D. (2010). *Sec24b* selectively sorts Vangl2 to regulate planar cell polarity during neural tube closure. *Nat. Cell Biol.* *12*, 41–6; sup pp 1–8.
  94. Narimatsu, M., Bose, R., Pye, M., Zhang, L., Miller, B., Ching, P., Sakuma, R., Luga, V., Roncari, L., Attisano, L., et al. (2009). Regulation of Planar Cell Polarity by Smurf Ubiquitin Ligases. *Cell* *137*, 295–307.
  95. Heller, S., Chen, J., and Streit, A. (2013). Induction of the inner ear: Stepwise specification of otic fate from multipotent progenitors. *Hear. Res.* *297*, 3–12.
  96. Driver, E. C., and Kelley, M. W. (2009). Specification of cell fate in the mammalian cochlea. *Birth Defects Res. C. Embryo Today* *87*, 212–21.
  97. Fritzsche, B., Jahan, I., Pan, N., Kersigo, J., Duncan, J., and Kopecky, B. (2011). Dissecting the molecular basis of organ of Corti development: Where are we now? *Hear. Res.* *276*, 16–26.
  98. Phippard, D., Lu, L., Lee, D., Saunders, J. C., and Crenshaw, E. B. I. (1999). Targeted Mutagenesis of the POU-Domain Gene *Brn4/Pou3f4* Causes Developmental Defects in the Inner Ear. *J. Neurosci.* *19*, 5980–5989.
  99. Kiernan, A. E., Ahituv, N., Fuchs, H., Balling, R., Avraham, K. B., Steel, K. P., and Hrabé De Angelis, M. (2001). The Notch ligand *Jagged1* is required for inner ear sensory development. *Proc. Natl. Acad. Sci. U. S. A.* *98*, 3873–3878.
  100. Hayashi, T., Kokubo, H., Hartman, B. H., Ray, C. A., Reh, T. A., and Bermingham-McDonogh, O. (2008). *Hesr1* and *Hesr2* may act as early

- effectors of Notch signaling in the developing cochlea. *Dev. Biol.* 316, 87–99.
101. Doetzlhofer, A., Basch, M. L., Ohyama, T., Gessler, M., Groves, A. K., and Segil, N. (2009). Hey2 regulation by FGF provides a Notch-independent mechanism for maintaining pillar cell fate in the organ of Corti. *Dev. Cell* 16, 58–69.
  102. Driver, E. C., Pryor, S. P., Hill, P., Turner, J., Rüther, U., Biesecker, L. G., Griffith, A. J., and Kelley, M. W. (2008). Hedgehog signaling regulates sensory cell formation and auditory function in mice and humans. *J. Neurosci.* 28, 7350–8.
  103. Ohyama, T., Basch, M. L., Mishina, Y., Lyons, K. M., Segil, N., and Groves, A. K. (2010). BMP signaling is necessary for patterning the sensory and nonsensory regions of the developing mammalian cochlea. *J. Neurosci.* 30, 15044–15051.
  104. Kiernan, A. E., Pelling, A. L., Leung, K. K. H., Tang, A. S. P., Bell, D. M., Tease, C., Lovell-Badge, R., Steel, K. P., and Cheah, K. S. E. (2005). Sox2 is required for sensory organ development in the mammalian inner ear. *Nature* 434, 1031–1035.
  105. Dabdoub, A., Puligilla, C., Jones, J. M., Fritsch, B., Cheah, K. S. E., Pevny, L. H., and Kelley, M. W. (2008). Sox2 signaling in prosensory domain specification and subsequent hair cell differentiation in the developing cochlea. *Proc. Natl. Acad. Sci. U. S. A.* 105, 18396–18401.
  106. Chen, P., and Segil, N. (1999). p27(Kip1) links cell proliferation to morphogenesis in the developing organ of Corti. *Development* 126, 1581–90.
  107. Woods, C., Montcouquiol, M., and Kelley, M. W. (2004). Math1 regulates development of the sensory epithelium in the mammalian cochlea. *Nat. Neurosci.* 7, 1310–1318.
  108. Kawamoto, K., Ishimoto, S.-I., Minoda, R., Brough, D. E., and Raphael, Y. (2003). Math1 gene transfer generates new cochlear hair cells in mature guinea pigs in vivo. *J. Neurosci.* 23, 4395–4400.
  109. Gubbels, S. P., Woessner, D. W., Mitchell, J. C., Ricci, A. J., and Brigande, J. V. (2008). Functional auditory hair cells produced in the mammalian cochlea by in utero gene transfer. *Nature* 455, 537–541.

110. Kiernan, A. E., Cordes, R., Kopan, R., Gossler, A., and Gridley, T. (2005). The Notch ligands DLL1 and JAG2 act synergistically to regulate hair cell development in the mammalian inner ear. *Development* 132, 4353–4362.
111. Brooker, R., Hozumi, K., and Lewis, J. (2006). Notch ligands with contrasting functions: Jagged1 and Delta1 in the mouse inner ear. *Development* 133, 1277–1286.
112. Morsli, H., Choo, D., Ryan, A., Johnson, R., and Wu, D. K. (1998). Development of the mouse inner ear and origin of its sensory organs. *J. Neurosci.* 18, 3327–3335.
113. McKenzie, E., Krupin, A., and Kelley, M. W. (2004). Cellular growth and rearrangement during the development of the mammalian organ of Corti. *Dev. Dyn. an Off. Publ. Am. Assoc. Anat.* 229, 802–812.
114. Yamamoto, N., Okano, T., Ma, X., Adelstein, R. S., and Kelley, M. W. (2009). Myosin II regulates extension, growth and patterning in the mammalian cochlear duct. *Development* 136, 1977–86.
115. Montcouquiol, M., Rachel, R. A., Lanford, P. J., Copeland, N. G., Jenkins, N. A., and Kelley, M. W. (2003). Identification of Vangl2 and Scrb1 as planar polarity genes in mammals. *Nature* 423, 173–7.
116. Chacon-Heszele, M. F., Ren, D., Reynolds, A. B., Chi, F., and Chen, P. (2012). Regulation of cochlear convergent extension by the vertebrate planar cell polarity pathway is dependent on p120-catenin. *Dev. Cambridge Engl.* 139, 968–978.
117. Lindqvist, M., Horn, Z., Bryja, V., Schulte, G., Papachristou, P., Ajima, R., Dyberg, C., Arenas, E., Yamaguchi, T. P., Lagercrantz, H., et al. (2010). Vang-like protein 2 and Rac1 interact to regulate adherens junctions. *J. Cell Sci.* 123, 472–83.
118. Conti, M. A., and Adelstein, R. S. (2008). Nonmuscle myosin II moves in new directions. *J. Cell Sci.* 121, 11–18.
119. Dabdoub, A., and Kelley, M. W. (2005). Planar cell polarity and a potential role for a Wnt morphogen gradient in stereociliary bundle orientation in the mammalian inner ear. *J. Neurobiol.* 64, 446–57.
120. Sobkowicz, H. M., Slapnick, S. M., and August, B. K. (1995). The kinocilium of auditory hair cells and evidence for its morphogenetic role during the regeneration of stereocilia and cuticular plates. *J. Neurocytol.* 24, 633–653.

121. Schwander, M., Kachar, B., and Müller, U. (2010). Review series: The cell biology of hearing. *J. Cell Biol.* 190, 9–20.
122. Tilney, L. G., Tilney, M. S., and DeRosier, D. J. (1992). Actin filaments, stereocilia, and hair cells: how cells count and measure. *Annu. Rev. Cell Biol.* 8, 257–74.
123. Dabdoub, A. (2003). Wnt signaling mediates reorientation of outer hair cell stereociliary bundles in the mammalian cochlea. *Development* 130, 2375–2384.
124. Etournay, R., Lepelletier, L., Boutet de Monvel, J., Michel, V., Cayet, N., Leibovici, M., Weil, D., Foucher, I., Hardelin, J.-P., and Petit, C. (2010). Cochlear outer hair cells undergo an apical circumference remodeling constrained by the hair bundle shape. *Development* 137, 1373–1383.
125. Burns, J. C., Burns, J., Christophel, J. J., Collado, M. S., Magnus, C., Carfrae, M., and Corwin, J. T. (2008). Reinforcement of cell junctions correlates with the absence of hair cell regeneration in mammals and its occurrence in birds. *J. Comp. Neurol.* 511, 396–414.
126. Collado, M. S., Thiede, B. R., Baker, W., Askew, C., Igbani, L. M., and Corwin, J. T. (2011). The postnatal accumulation of junctional E-cadherin is inversely correlated with the capacity for supporting cells to convert directly into sensory hair cells in mammalian balance organs. *J. Neurosci.* 31, 11855–66.
127. Copley, C. O., Duncan, J. S., Liu, C., Cheng, H., and Deans, M. R. (2013). Postnatal refinement of auditory hair cell planar polarity deficits occurs in the absence of vangl2. *J. Neurosci.* 33, 14001–16.
128. Sipe, C. W., and Lu, X. (2011). Kif3a regulates planar polarization of auditory hair cells through both ciliary and non-ciliary mechanisms. *Dev. Cambridge Engl.* 138, 3441–3449.
129. Jones, C., Roper, V. C., Foucher, I., Qian, D., Banizs, B., Petit, C., Yoder, B. K., and Chen, P. (2008). Ciliary proteins link basal body polarization to planar cell polarity regulation. *Nat. Genet.* 40, 69–77.
130. Ross, A. J., May-Simera, H., Eichers, E. R., Kai, M., Hill, J., Jagger, D. J., Leitch, C. C., Chapple, J. P., Munro, P. M., Fisher, S., et al. (2005). Disruption of Bardet-Biedl syndrome ciliary proteins perturbs planar cell polarity in vertebrates. *Nat. Genet.* 37, 1135–1140.

131. Sipe, C. W., Liu, L., Lee, J., Grimsley-Myers, C., and Lu, X. (2013). Lis1 mediates planar polarity of auditory hair cells through regulation of microtubule organization. *Development* 140, 1785–95.
132. Tarchini, B., Jolicoeur, C., and Cayouette, M. (2013). A Molecular Blueprint at the Apical Surface Establishes Planar Asymmetry in Cochlear Hair Cells. *Dev. Cell* 27, 88–102.
133. Eaton, S. (1997). Planar polarization of *Drosophila* and vertebrate epithelia. *Curr. Opin. Cell Biol.* 9, 860–866.
134. Etheridge, S. L., Ray, S., Li, S., Hamblet, N. S., Lijam, N., Tsang, M., Greer, J., Kardos, N., Wang, J., Sussman, D. J., et al. (2008). Murine dishevelled 3 functions in redundant pathways with dishevelled 1 and 2 in normal cardiac outflow tract, cochlea, and neural tube development. *PLoS Genet.* 4, e1000259.
135. Giese, A. P., Ezan, J., Wang, L., Lasvaux, L., Lembo, F., Mazzocco, C., Richard, E., Reboul, J., Borg, J.-P., Kelley, M. W., et al. (2012). *Gipc1* has a dual role in *Vangl2* trafficking and hair bundle integrity in the inner ear. *Development* 139, 3775–85.
136. Deans, M. R., Antic, D., Suyama, K., Scott, M. P., Axelrod, J. D., and Goodrich, L. V (2007). Asymmetric distribution of prickle-like 2 reveals an early underlying polarization of vestibular sensory epithelia in the inner ear. *J. Neurosci.* 27, 3139–3147.
137. Daudet, N., Ripoll, C., Molès, J.-P., and Rebillard, G. (2002). Expression of members of Wnt and Frizzled gene families in the postnatal rat cochlea. *Mol. Brain Res.* 105, 98–107.
138. Qian, D., Jones, C., Rzadzinska, A., Mark, S., Zhang, X., Steel, K. P., Dai, X., and Chen, P. (2007). *Wnt5a* functions in planar cell polarity regulation in mice. *Dev. Biol.* 306, 121–33.
139. Kiyose, S., Nagura, K., Tao, H., Igarashi, H., Yamada, H., Goto, M., Maeda, M., Kurabe, N., Suzuki, M., Tsuboi, M., et al. (2012). Detection of kinase amplifications in gastric cancer archives using fluorescence in situ hybridization. *Pathol. Int.* 62, 477–84.
140. Shin, W.-S., Kwon, J., Lee, H. W., Kang, M. C., Na, H.-W., Lee, S.-T., and Park, J. H. (2013). Oncogenic role of protein tyrosine kinase 7 in esophageal squamous cell carcinoma. *Cancer Sci.* 104, 1120–6.

141. Park, S. K., Lee, H. S., and Lee, S. T. (1996). Characterization of the human full-length PTK7 cDNA encoding a receptor protein tyrosine kinase-like molecule closely related to chick KLG. *J. Biochem.* *119*, 235–9.
142. Katoh, M., and Katoh, M. (2007). Comparative integromics on non-canonical WNT or planar cell polarity signaling molecules: Transcriptional mechanism of PTK7 in colorectal cancer and that of SEMA6A in undifferentiated ES cells. *Int. J. Mol. Med.* *20*, 405–409.
143. Jung, J.-W., Shin, W.-S., Song, J., and Lee, S.-T. (2004). Cloning and characterization of the full-length mouse Ptk7 cDNA encoding a defective receptor protein tyrosine kinase. *Gene* *328*, 75–84.
144. Jung, J.-W., Ji, A.-R., Lee, J., Kim, U.-J., and Lee, S.-T. (2002). Organization of the human PTK7 gene encoding a receptor protein tyrosine kinase-like molecule and alternative splicing of its mRNA. *Biochim. Biophys. Acta - Gene Struct. Expr.* *1579*, 153–163.
145. Savory, J. G. A., Mansfield, M., Rijli, F. M., and Lohnes, D. (2011). Cdx mediates neural tube closure through transcriptional regulation of the planar cell polarity gene Ptk7. *Development* *138*, 1361–70.
146. Ng, D., Mowrey, P., Ragoussis, J., Mirza, G., Coll, E., Di Fazio, M. P., Turner, C., and Levin, S. W. (2001). Molecularly defined interstitial tandem duplication 6p case with mild manifestations. *Am. J. Med. Genet.* *103*, 320–5.
147. Ataseven, B., Angerer, R., Kates, R., Gunesch, A., Knyazev, P., Högel, B., Becker, C., Eiermann, W., and Harbeck, N. (2013). PTK7 Expression in Triple-negative Breast Cancer. *Anticancer Res.* *33*, 3759–63.
148. Boudeau, J., Miranda-Saavedra, D., Barton, G. J., and Alessi, D. R. (2006). Emerging roles of pseudokinases. *Trends Cell Biol.* *16*, 443–52.
149. Shnitsar, I., and Borchers, A. (2008). PTK7 recruits dsh to regulate neural crest migration. *Development* *135*, 4015–24.
150. Peradziryi, H., Kaplan, N. A., Podleschny, M., Liu, X., Wehner, P., Borchers, A., and Tolwinski, N. S. (2011). PTK7/Otk interacts with Wnts and inhibits canonical Wnt signalling. *Eur. Mol. Biol. Organ. J.* *30*, 3729–3740.
151. Kobus, F. J., and Fleming, K. G. (2005). The GxxxG-containing transmembrane domain of the CCK4 oncogene does not encode preferential self-interactions. *Biochemistry* *44*, 1464–70.

152. Paudyal, A., Damrau, C., Patterson, V. L., Ermakov, A., Formstone, C., Lallane, Z., Wells, S., Lu, X., Norris, D. P., Dean, C. H., et al. (2010). The novel mouse mutant, *chuzhoi*, has disruption of Ptk7 protein and exhibits defects in neural tube, heart and lung development and abnormal planar cell polarity in the ear. *BMC Dev. Biol.* 10, 87.
153. Golubkov, V. S., and Strongin, A. Y. (2012). Insights into ectodomain shedding and processing of protein-tyrosine pseudokinase 7 (PTK7). *J. Biol. Chem.* 287, 42009–18.
154. Golubkov, V. S., Chekanov, A. V., Cieplak, P., Aleshin, A. E., Chernov, A. V., Zhu, W., Radichev, I. A., Zhang, D., Dong, P. D., and Strongin, A. Y. (2010). The Wnt/planar cell polarity protein-tyrosine kinase-7 (PTK7) is a highly efficient proteolytic target of membrane type-1 matrix metalloproteinase: implications in cancer and embryogenesis. *J. Biol. Chem.* 285, 35740–9.
155. Yen, W. W., Williams, M., Periasamy, A., Conaway, M., Burdsal, C., Keller, R., Lu, X., and Sutherland, A. (2009). PTK7 is essential for polarized cell motility and convergent extension during mouse gastrulation. *Development* 136, 2039–48.
156. Hayes, M., Naito, M., Daulat, A., Angers, S., and Ciruna, B. (2013). Ptk7 promotes non-canonical Wnt/PCP-mediated morphogenesis and inhibits Wnt/ $\beta$ -catenin-dependent cell fate decisions during vertebrate development. *Development* 140, 1807–18.
157. Wehner, P., Shnitsar, I., Urlaub, H., and Borchers, A. (2011). RACK1 is a novel interaction partner of PTK7 that is required for neural tube closure. *Development* 138, 1321–7.
158. Wagner, G., Peradziryi, H., Wehner, P., and Borchers, A. (2010). PlexinA1 interacts with PTK7 and is required for neural crest migration. *Biochem. Biophys. Res. Commun.* 402, 402–407.
159. Puppo, F., Thomé, V., Lhoumeau, A.-C., Cibois, M., Gangar, A., Lembo, F., Belotti, E., Marchetto, S., Lécine, P., Prébet, T., et al. (2011). Protein tyrosine kinase 7 has a conserved role in Wnt/ $\beta$ -catenin canonical signalling. *EMBO Rep.* 12, 43–9.
160. Winberg, M. L., Tamagnone, L., Bai, J., Comoglio, P. M., Montell, D., and Goodman, C. S. (2001). The transmembrane protein Off-track associates with Plexins and functions downstream of Semaphorin signaling during axon guidance. *Neuron* 32, 53–62.

161. Cafferty, P., Yu, L., and Rao, Y. (2004). The receptor tyrosine kinase Off-track is required for layer-specific neuronal connectivity in *Drosophila*. *Development* *131*, 5287–95.
162. Rauzi, M., Lenne, P.-F., and Lecuit, T. (2010). Planar polarized actomyosin contractile flows control epithelial junction remodelling. *Nature* *468*, 1110–4.
163. Vicente-Manzanares, M., Ma, X., Adelstein, R. S., and Horwitz, A. R. (2009). Non-muscle myosin II takes centre stage in cell adhesion and migration. *Nat. Rev. Mol. Cell Biol.* *10*, 778–90.
164. Lecuit, T., Lenne, P.-F., and Munro, E. (2011). Force generation, transmission, and integration during cell and tissue morphogenesis. *Annu. Rev. Cell Dev. Biol.* *27*, 157–84.
165. Aguilar-Cuenca, R., Juanes-García, A., and Vicente-Manzanares, M. (2013). Myosin II in mechanotransduction: master and commander of cell migration, morphogenesis, and cancer. *Cell. Mol. Life Sci.*
166. Esue, O., Tseng, Y., and Wirtz, D. (2009). Alpha-actinin and filamin cooperatively enhance the stiffness of actin filament networks. *PLoS One* *4*, e4411.
167. Wachsstock, D. H., Schwarz, W. H., and Pollard, T. D. (1994). Cross-linker dynamics determine the mechanical properties of actin gels. *Biophys. J.* *66*, 801–809.
168. Yonemura, S., Wada, Y., Watanabe, T., Nagafuchi, A., and Shibata, M. (2010). alpha-Catenin as a tension transducer that induces adherens junction development. *Nat. Cell Biol.* *12*, 533–542.
169. Dufour, S., Mège, R.-M., and Thiery, J. P. (2013). catenin, vinculin, and F-actin in strengthening E-cadherin cell-cell adhesions and mechanosensing. *Cell Adhes. Migr.* *7*, -1.
170. Le Duc, Q., Shi, Q., Blonk, I., Sonnenberg, A., Wang, N., Leckband, D., and De Rooij, J. (2010). Vinculin potentiates E-cadherin mechanosensing and is recruited to actin-anchored sites within adherens junctions in a myosin II-dependent manner. *J. Cell Biol.* *189*, 1107–1115.
171. Weiss, E. E., Kroemker, M., Rüdiger, A. H., Jockusch, B. M., and Rüdiger, M. (1998). Vinculin is part of the cadherin-catenin junctional complex: complex formation between alpha-catenin and vinculin. *J. Cell Biol.* *141*, 755–764.

172. Abe, K., and Takeichi, M. (2008). EPLIN mediates linkage of the cadherin catenin complex to F-actin and stabilizes the circumferential actin belt. *Proc. Natl. Acad. Sci. U. S. A.* *105*, 13–19.
173. Borghi, N., Sorokina, M., Shcherbakova, O. G., Weis, W. I., Pruitt, B. L., Nelson, W. J., and Dunn, A. R. (2012). E-cadherin is under constitutive actomyosin-generated tension that is increased at cell-cell contacts upon externally applied stretch. *Proc. Natl. Acad. Sci. U. S. A.* *109*, 12568–73.
174. Leckband, D. E., de Rooij, J., le Duc, Q., and Wang, N. (2011). Mechanotransduction at cadherin-mediated adhesions. *Curr. Opin. Cell Biol.* *23*, 523–530.
175. Papusheva, E., and Heisenberg, C.-P. (2010). Spatial organization of adhesion: force-dependent regulation and function in tissue morphogenesis. *EMBO J.* *29*, 2753–68.
176. Marsden, M., and DeSimone, D. W. (2001). Regulation of cell polarity, radial intercalation and epiboly in *Xenopus*: novel roles for integrin and fibronectin. *Development* *128*, 3635–47.
177. Mammoto, T., Mammoto, A., and Ingber, D. E. (2013). Mechanobiology and Developmental Control. *Annu. Rev. Cell Dev. Biol.* *29*, 27–61.
178. Sawyer, J. M., Harrell, J. R., Shemer, G., Sullivan-Brown, J., Roh-Johnson, M., and Goldstein, B. (2010). Apical constriction: a cell shape change that can drive morphogenesis. *Dev. Biol.* *341*, 5–19.
179. Martin, A. C., Kaschube, M., and Wieschaus, E. F. (2009). Pulsed contractions of an actin-myosin network drive apical constriction. *Nature* *457*, 495–499.
180. Fernandez-Gonzalez, R., Simoes, S. D. M., Röper, J.-C., Eaton, S., and Zallen, J. A. (2009). Myosin II dynamics are regulated by tension in intercalating cells. *Dev. Cell* *17*, 736–743.
181. Walters, J. W., Dilks, S. A., and DiNardo, S. (2006). Planar polarization of the denticle field in the *Drosophila* embryo: roles for Myosin II (zipper) and fringe. *Dev. Biol.* *297*, 323–339.
182. Olguin, P., and Mlodzik, M. (2010). A new spin on planar cell polarity. *Cell* *142*, 674–6.
183. Rida, P. C. G., and Chen, P. (2009). Line up and listen: Planar cell polarity regulation in the mammalian inner ear. *Semin. Cell Dev. Biol.* *20*, 978–985.

184. Adler, P. N. (2002). Planar Signaling and Morphogenesis in *Drosophila*. *Dev. Cell* 2, 525–535.
185. Axelrod, J. D. (2001). Unipolar membrane association of Dishevelled mediates Frizzled planar cell polarity signaling. *Genes Dev.* 15, 1182–1187.
186. Hébert, J. M., and McConnell, S. K. (2000). Targeting of cre to the Foxg1 (BF-1) Locus Mediates loxP Recombination in the Telencephalon and Other Developing Head Structures. *Dev. Biol.* 222, 296–306.
187. Lakso, M., Pichel, J. G., Gorman, J. R., Sauer, B., Okamoto, Y., Lee, E., Alt, F. W., and Westphal, H. (1996). Efficient in vivo manipulation of mouse genomic sequences at the zygote stage. *Proc. Natl. Acad. Sci. U. S. A.* 93, 5860–5.
188. Dong, C., Yang, D. D., Wysk, M., Whitmarsh, A. J., Davis, R. J., and Flavell, R. A. (1998). Defective T Cell Differentiation in the Absence of Jnk1. *Science* (80- ). 282, 2092–2095.
189. Kuan, C. Y., Yang, D. D., Samanta Roy, D. R., Davis, R. J., Rakic, P., and Flavell, R. A. (1999). The Jnk1 and Jnk2 protein kinases are required for regional specific apoptosis during early brain development. *Neuron* 22, 667–676.
190. Davis, R. J. (2000). Signal transduction by the JNK group of MAP kinases. *Cell* 103, 239–52.
191. Winter, C. G., Wang, B., Ballew, A., Royou, A., Karess, R., Axelrod, J. D., and Luo, L. (2001). *Drosophila* Rho-associated kinase (Drok) links Frizzled-mediated planar cell polarity signaling to the actin cytoskeleton. *Cell* 105, 81–91.
192. Lee, J.-Y., Marston, D. J., Walston, T., Hardin, J., Halberstadt, A., and Goldstein, B. (2006). Wnt/Frizzled signaling controls *C. elegans* gastrulation by activating actomyosin contractility. *Curr. Biol.* 16, 1986–1997.
193. Skoglund, P., Rolo, A., Chen, X., Gumbiner, B. M., and Keller, R. (2008). Convergence and extension at gastrulation require a myosin IIB-dependent cortical actin network. *Dev. Cambridge Engl.* 135, 2435–2444.
194. Rolo, A., Skoglund, P., and Keller, R. (2009). Morphogenetic movements driving neural tube closure in *Xenopus* require myosin IIB. *Dev. Biol.* 327, 327–338.

195. Ma, X., Bao, J., and Adelstein, R. S. (2007). Loss of Cell Adhesion Causes Hydrocephalus in Nonmuscle Myosin II-B–ablated and Mutated Mice. *Mol. Biol. Cell* 18, 2305–2312.
196. Peng, X., Nelson, E. S., Maiers, J. L., and DeMali, K. A. (2011). New insights into vinculin function and regulation. *Int. Rev. Cell Mol. Biol.* 287, 191–231.
197. Hoffman, B. D., Grashoff, C., and Schwartz, M. A. (2011). Dynamic molecular processes mediate cellular mechanotransduction. *Nature* 475, 316–323.
198. Gomez, G. A., McLachlan, R. W., and Yap, A. S. (2011). Productive tension: force-sensing and homeostasis of cell-cell junctions. *Trends Cell Biol.* 21, 499–505.
199. Pasapera, A. M., Schneider, I. C., Rericha, E., Schlaepfer, D. D., and Waterman, C. M. (2010). Myosin II activity regulates vinculin recruitment to focal adhesions through FAK-mediated paxillin phosphorylation. *J. Cell Biol.* 188, 877–890.
200. Grashoff, C., Hoffman, B. D., Brenner, M. D., Zhou, R., Parsons, M., Yang, M. T., McLean, M. A., Sligar, S. G., Chen, C. S., Ha, T., et al. (2010). Measuring mechanical tension across vinculin reveals regulation of focal adhesion dynamics. *Nature* 466, 263–266.
201. Kibar, Z., Salem, S., Bosoi, C. M., Pauwels, E., De Marco, P., Merello, E., Bassuk, A. G., Capra, V., and Gros, P. (2011). Contribution of VANGL2 mutations to isolated neural tube defects. *Clin. Genet.* 80, 76–82.
202. Guyot, M.-C., Bosoi, C. M., Kharfallah, F., Reynolds, A., Drapeau, P., Justice, M., Gros, P., and Kibar, Z. (2011). A novel hypomorphic Looptail allele at the planar cell polarity Vangl2 gene. *Dev. Dyn. an Off. Publ. Am. Assoc. Anat.* 240, 839–849.
203. Yin, H., Copley, C. O., Goodrich, L. V., and Deans, M. R. (2012). Comparison of phenotypes between different vangl2 mutants demonstrates dominant effects of the Looptail mutation during hair cell development. *PLoS One* 7, e31988.
204. Wong, H.-C., Bourdelas, A., Krauss, A., Lee, H.-J., Shao, Y., Wu, D., Mlodzik, M., Shi, D.-L., and Zheng, J. (2003). Direct binding of the PDZ domain of Dishevelled to a conserved internal sequence in the C-terminal region of Frizzled. *Mol. Cell* 12, 1251–1260.

205. Martin, A. C., Gelbart, M., Fernandez-Gonzalez, R., Kaschube, M., and Wieschaus, E. F. (2010). Integration of contractile forces during tissue invagination. *J. Cell Biol.* 188, 735–749.
206. Fernandez-Gonzalez, R., and Zallen, J. a (2011). Oscillatory behaviors and hierarchical assembly of contractile structures in intercalating cells. *Phys. Biol.* 8, 045005.
207. Sawyer, J. K., Choi, W., Jung, K.-C., He, L., Harris, N. J., and Peifer, M. (2011). A contractile actomyosin network linked to adherens junctions by Canoe/afadin helps drive convergent extension. *Mol. Biol. Cell* 22, 2491–508.
208. Smutny, M., Cox, H. L., Leerberg, J. M., Kovacs, E. M., Conti, M. A., Ferguson, C., Hamilton, N. A., Parton, R. G., Adelstein, R. S., and Yap, A. S. (2010). Myosin II isoforms identify distinct functional modules that support integrity of the epithelial zonula adherens. *Nat. Cell Biol.* 12, 696–702.
209. Katsumi, A., Milanini, J., Kiosses, W. B., Del Pozo, M. A., Kaunas, R., Chien, S., Hahn, K. M., and Schwartz, M. A. (2002). Effects of cell tension on the small GTPase Rac. *J. Cell Biol.* 158, 153–164.
210. Lee, C.-S., Choi, C.-K., Shin, E.-Y., Schwartz, M. A., and Kim, E.-G. (2010). Myosin II directly binds and inhibits Dbl family guanine nucleotide exchange factors: a possible link to Rho family GTPases. *J. Cell Biol.* 190, 663–674.
211. Even-Ram, S., Doyle, A. D., Conti, M. A., Matsumoto, K., Adelstein, R. S., and Yamada, K. M. (2007). Myosin IIA regulates cell motility and actomyosin-microtubule crosstalk. *Nat Cell Biol* 9, 299–309.
212. Ehrlicher, A. J., Nakamura, F., Hartwig, J. H., Weitz, D. A., and Stossel, T. P. (2011). Mechanical strain in actin networks regulates FilGAP and integrin binding to filamin A. *Nature* 478, 260–263.
213. Skoglund, P., Rolo, A., Chen, X., Gumbiner, B. M., and Keller, R. (2008). Convergence and extension at gastrulation require a myosin IIB-dependent cortical actin network. *Development* 135, 2435–2444.
214. Lee, J., Andreeva, A., Sipe, C. W., Liu, L., Cheng, A., and Lu, X. (2012). PTK7 regulates myosin II activity to orient planar polarity in the mammalian auditory epithelium. *Curr. Biol.* 22, 956–66.

215. Thomas, S. M., Soriano, P., and Imamoto, A. (1995). Specific and redundant roles of Src and Fyn in organizing the cytoskeleton. *Nature* 376, 267–271.
216. Blake, R. A., Broome, M. A., Liu, X., Wu, J., Gishizky, M., Sun, L., and Courtneidge, S. A. (2000). SU6656, a selective src family kinase inhibitor, used to probe growth factor signaling. *Mol. Cell. Biol.* 20, 9018–9027.
217. Schmedt, C., Saijo, K., Niidome, T., Kühn, R., Aizawa, S., and Tarakhovsky, A. (1998). Csk controls antigen receptor-mediated development and selection of T-lineage cells. *Nature* 394, 901–904.
218. Imamoto, A., and Soriano, P. (1993). Disruption of the csk gene, encoding a negative regulator of Src family tyrosine kinases, leads to neural tube defects and embryonic lethality in mice. *Cell* 73, 1117–1124.
219. Ohyama, T., and Groves, A. K. (2004). Generation of Pax2-Cre mice by modification of a Pax2 bacterial artificial chromosome. *Genes*. New York NY 2000 38, 195–199.
220. Amsberg, G. K., and Schafhausen, P. (2013). Bosutinib in the management of chronic myelogenous leukemia. *Biologics* 7, 115–122.
221. Verma, S., Han, S. P., Michael, M., Gomez, G. A., Yang, Z., Teasdale, R. D., Ratheesh, A., Kovacs, E. M., Ali, R. G., and Yap, A. S. (2012). A WAVE2-Arp2/3 actin nucleator apparatus supports junctional tension at the epithelial zonula adherens. *Mol. Biol. Cell* 23, 4601–10.
222. Tehrani, S., Tomasevic, N., Weed, S., Sakowicz, R., and Cooper, J. A. (2007). Src phosphorylation of cortactin enhances actin assembly. *Proc. Natl. Acad. Sci. U. S. A.* 104, 11933–8.
223. Just, W., Thompson, P. M., Tolbert, C. E., and Campbell, S. L. (2013). Vinculin and metavinculin: Oligomerization and interactions with F-actin. *FEBS Lett.* 587, 1220–1229.
224. Wen, K.-K., Rubenstein, P. A., and DeMali, K. A. (2009). Vinculin nucleates actin polymerization and modifies actin filament structure. *J. Biol. Chem.* 284, 30463–30473.
225. DeMali, K. A., Barlow, C. A., and Burrridge, K. (2002). Recruitment of the Arp2/3 complex to vinculin: coupling membrane protrusion to matrix adhesion. *J. Cell Biol.* 159, 881–891.

226. Sefton, B. M., Hunter, T., Ball, E. H., and Singer, S. J. (1981). Vinculin: a cytoskeletal target of the transforming protein of Rous sarcoma virus. *Cell* 24, 165–174.
227. Zhang, Z., Izaguirre, G., Lin, S.-Y., Lee, H. Y., Schaefer, E., and Haimovich, B. (2004). The phosphorylation of vinculin on tyrosine residues 100 and 1065, mediated by SRC kinases, affects cell spreading. *Mol. Biol. Cell* 15, 4234–47.
228. Diez, G., Kollmannsberger, P., Mierke, C. T., Koch, T. M., Vali, H., Fabry, B., and Goldmann, W. H. (2009). Anchorage of vinculin to lipid membranes influences cell mechanical properties. *Biophys. J.* 97, 3105–12.
229. Xu, W., Baribault, H., and Adamson, E. D. (1998). Vinculin knockout results in heart and brain defects during embryonic development. *Development* 125, 327–337.
230. Zemljic-Harpf, A. E., Miller, J. C., Henderson, S. A., Wright, A. T., Manso, A. M., Elsherif, L., Dalton, N. D., Thor, A. K., Perkins, G. A., McCulloch, A. D., et al. (2007). Cardiac-myocyte-specific excision of the vinculin gene disrupts cellular junctions, causing sudden death or dilated cardiomyopathy. *Mol. Cell. Biol.* 27, 7522–7537.
231. Nakajima, H., and Tanoue, T. (2011). Lulu2 regulates the circumferential actomyosin tensile system in epithelial cells through p114RhoGEF. *J. Cell Biol.* 195, 245–261.
232. Nishimura, T., Takeichi, M., and Honda, H. (2012). Planar Cell Polarity Links Axes of Spatial Dynamics in Neural-Tube Closure. *Cell* 149, 1084–1097.
233. Ratheesh, A., Gomez, G. A., Akhmanova, A., Priya, R., Kovacs, E. M., Jiang, K., Brown, N. H., Stehbens, S. J., Verma, S., and Yap, A. S. (2012). Centralspindlin and  $\alpha$ -catenin regulate Rho signalling at the epithelial zonula adherens. *Nat. Cell Biol.* 14, 818–828.
234. Terry, S. J., Zihni, C., Elbediwy, A., Vitiello, E., Leefa Chong San, I. V., Balda, M. S., and Matter, K. (2011). Spatially restricted activation of RhoA signalling at epithelial junctions by p114RhoGEF drives junction formation and morphogenesis. *Nat. Cell Biol.* 13, 159–166.
235. Bardet, P.-L., Guirao, B., Paoletti, C., Serman, F., Léopold, V., Bosveld, F., Goya, Y., Mirouse, V., Graner, F., and Bellaïche, Y. (2013). PTEN Controls Junction Lengthening and Stability during Cell Rearrangement in Epithelial Tissue. *Dev. Cell* 25, 534–546.

236. Lee, H.-H., Tien, S.-C., Jou, T.-S., Chang, Y.-C., Jhong, J.-G., and Chang, Z.-F. (2010). Src-dependent phosphorylation of ROCK participates in regulation of focal adhesion dynamics. *J. Cell Sci.* *123*, 3368–77.
237. Lee, H.-H., and Chang, Z.-F. (2008). Regulation of RhoA-dependent ROCKII activation by Shp2. *J. Cell Biol.* *181*, 999–1012.
238. Parsons, S. J., and Parsons, J. T. (2004). Src family kinases, key regulators of signal transduction. *Oncogene* *23*, 7906–7909.
239. Wang, Y., Botvinick, E. L., Zhao, Y., Berns, M. W., Usami, S., Tsien, R. Y., and Chien, S. (2005). Visualizing the mechanical activation of Src. *Nature* *434*, 1040–1045.
240. McLachlan, R. W., Kraemer, A., Helwani, F. M., Kovacs, E. M., and Yap, A. S. (2007). E-cadherin adhesion activates c-Src signaling at cell-cell contacts. *Mol. Biol. Cell* *18*, 3214–3223.
241. Warrington, S. J., Strutt, H., and Strutt, D. (2013). The Frizzled-dependent planar polarity pathway locally promotes E-cadherin turnover via recruitment of RhoGEF2. *Development* *140*, 1045–54.
242. Arvanitis, D., and Davy, A. (2008). Eph/ephrin signaling: networks. *Genes Dev.* *22*, 416–429.
243. Pasquale, E. B. (2005). Eph receptor signalling casts a wide net on cell behaviour. *Nat. Rev. Mol. Cell Biol.* *6*, 462–75.
244. Pasquale, E. B. (2008). Eph-Ephrin Bidirectional Signaling in Physiology and Disease. *Cell* *133*, 38–52.
245. Brückner, K., Pasquale, E. B., and Klein, R. (1997). Tyrosine phosphorylation of transmembrane ligands for Eph receptors. *Science* *275*, 1640–1643.
246. Kullander, K., and Klein, R. (2002). Mechanisms and functions of Eph and ephrin signalling. *Nat. Rev. Mol. Cell Biol.* *3*, 475–486.
247. Palmer, A., Zimmer, M., Erdmann, K. S., Eulenburg, V., Porthin, A., Heumann, R., Deutsch, U., and Klein, R. (2002). EphrinB phosphorylation and reverse signaling: regulation by Src kinases and PTP-BL phosphatase. *Mol. Cell* *9*, 725–737.
248. Cowan, C. A., and Henkemeyer, M. (2001). The SH2/SH3 adaptor Grb4 transduces B-ephrin reverse signals. *Nature* *413*, 174–9.

249. Georgakopoulos, A., Litterst, C., Ghersi, E., Baki, L., Xu, C., Serban, G., and Robakis, N. K. (2006). Metalloproteinase/Presenilin1 processing of ephrinB regulates EphB-induced Src phosphorylation and signaling. *EMBO J.* *25*, 1242–52.
250. Davy, A., Aubin, J., and Soriano, P. (2004). Ephrin-B1 forward and reverse signaling are required during mouse development. *Genes Dev.* *18*, 572–583.
251. Lee, H.-S., Bong, Y.-S., Moore, K. B., Soria, K., Moody, S. A., and Daar, I. O. (2006). Dishevelled mediates ephrinB1 signalling in the eye field through the planar cell polarity pathway. *Nat. Cell Biol.* *8*, 55–63.
252. Chong, L. D., Park, E. K., Latimer, E., Friesel, R., and Daar, I. O. (2000). Fibroblast growth factor receptor-mediated rescue of x-ephrin B1- induced cell dissociation in *Xenopus* embryos. *Mol. Cell. Biol.* *20*, 724–34.
253. Lee, H.-S., Mood, K., Battu, G., Ji, Y. J., Singh, A., and Daar, I. O. (2009). Fibroblast growth factor receptor-induced phosphorylation of ephrinB1 modulates its interaction with Dishevelled. *Mol. Biol. Cell* *20*, 124–33.
254. Wei, S., Xu, G., Bridges, L. C., Williams, P., White, J. M., and DeSimone, D. W. (2010). ADAM13 induces cranial neural crest by cleaving class B Ephrins and regulating Wnt signaling. *Dev. Cell* *19*, 345–352.
255. Pickles, J. O., Claxton, C., and Van Heumen, W. R. A. (2002). Complementary and layered expression of Ephs and ephrins in developing mouse inner ear. *J. Comp. Neurol.* *449*, 207–16.
256. Pickles, J. O. (2003). Expression of Ephs and ephrins in developing mouse inner ear. *Hear. Res.* *178*, 44–51.
257. Miko, I. J., Henkemeyer, M., and Cramer, K. S. (2008). Auditory brainstem responses are impaired in EphA4 and ephrin-B2 deficient mice. *Hear. Res.* *235*, 39–46.
258. Gerety, S. S., and Anderson, D. J. (2002). Cardiovascular ephrinB2 function is essential for embryonic angiogenesis. *Development* *129*, 1397–1410.
259. Kelly, M., and Chen, P. (2007). Shaping the mammalian auditory sensory organ by the planar cell polarity pathway. *Int. J. Dev. Biol.* *51*, 535–547.
260. Nikolov, D. B., Li, C., Barton, W. A., and Himanen, J.-P. (2005). Crystal structure of the ephrin-B1 ectodomain: implications for receptor recognition and signaling. *Biochemistry* *44*, 10947–10953.

261. Himanen, J.-P., Saha, N., and Nikolov, D. B. (2007). Cell-cell signaling via Eph receptors and ephrins. *Curr. Opin. Cell Biol.* *19*, 534–542.
262. Gorfinkiel, N., and Blanchard, G. B. (2011). Dynamics of actomyosin contractile activity during epithelial morphogenesis. *Curr. Opin. Cell Biol.*, 1–9.
263. Kasza, K. E., and Zallen, J. A. (2011). Dynamics and regulation of contractile actin-myosin networks in morphogenesis. *Curr. Opin. Cell Biol.* *23*, 30–38.
264. Bao, J., Ma, X., Liu, C., and Adelstein, R. S. (2007). Replacement of nonmuscle myosin II-B with II-A rescues brain but not cardiac defects in mice. *J. Biol. Chem.* *282*, 22102–22111.
265. Levayer, R., and Lecuit, T. (2012). Biomechanical regulation of contractility: spatial control and dynamics. *Trends Cell Biol.* *22*, 61–81.
266. Solon, J., Kaya-Copur, A., Colombelli, J., and Brunner, D. (2009). Pulsed forces timed by a ratchet-like mechanism drive directed tissue movement during dorsal closure. *Cell* *137*, 1331–42.
267. Higginbotham, H., Bielas, S., Tanaka, T., and Gleeson, J. G. (2004). Transgenic mouse line with green-fluorescent protein-labeled Centrin 2 allows visualization of the centrosome in living cells. *Transgenic Res.* *13*, 155–164.
268. Simões, S. de M., Blankenship, J. T., Weitz, O., Farrell, D. L., Tamada, M., Fernandez-Gonzalez, R., and Zallen, J. A. (2010). Rho-kinase directs Bazooka/Par-3 planar polarity during *Drosophila* axis elongation. *Dev. Cell* *19*, 377–388.
269. Nishimura, T., Yamaguchi, T., Kato, K., Yoshizawa, M., Nabeshima, Y., Ohno, S., Hoshino, M., and Kaibuchi, K. (2005). PAR-6-PAR-3 mediates Cdc42-induced Rac activation through the Rac GEFs STEF/Tiam1. *Nat. Cell Biol.* *7*, 270–7.
270. Chen, X., and Macara, I. G. (2005). Par-3 controls tight junction assembly through the Rac exchange factor Tiam1. *Nat. Cell Biol.* *7*, 262–269.
271. Nance, J., and Zallen, J. A. (2011). Elaborating polarity: PAR proteins and the cytoskeleton. *Development* *138*, 799–809.
272. Siller, K. H., and Doe, C. Q. (2009). Spindle orientation during asymmetric cell division. *Nat. Cell Biol.* *11*, 365–374.

273. Ezan, J., Lasvaux, L., Gezer, A., Novakovic, A., May-Simera, H., Belotti, E., Lhoumeau, A.-C., Birnbaumer, L., Beer-Hammer, S., Borg, J.-P., et al. (2013). Primary cilium migration depends on G-protein signalling control of subapical cytoskeleton. *Nat. Cell Biol.* *15*, 1107–1115.
274. Katsumi, A., Milanini, J., Kiosses, W. B., del Pozo, M. A., Kaunas, R., Chien, S., Hahn, K. M., and Schwartz, M. A. (2002). Effects of cell tension on the small GTPase Rac. *J. Cell Biol.* *158*, 153–164.
275. Houk, A. R., Wu, L. F., Weiner, O. D., Mejean, C. O., Altschuler, S. J., Dufresne, E. R., Jilkine, A., Angenent, S. B., and Boltyanskiy, R. (2012). Membrane Tension Maintains Cell Polarity by Confining Signals to the Leading Edge during Neutrophil Migration. *Cell* *148*, 175–188.
276. Xu, J., Wang, F., Van Keymeulen, A., Herzmark, P., Straight, A., Kelly, K., Takuwa, Y., Sugimoto, N., Mitchison, T., and Bourne, H. R. (2003). Divergent signals and cytoskeletal assemblies regulate self-organizing polarity in neutrophils. *Cell* *114*, 201–214.
277. Kuo, J.-C., Han, X., Hsiao, C.-T., Yates, J. R., and Waterman, C. M. (2011). Analysis of the myosin-II-responsive focal adhesion proteome reveals a role for  $\beta$ -Pix in negative regulation of focal adhesion maturation. *Nat. Cell Biol.* *13*, 383–393.
278. Ohta, Y., Hartwig, J. H., and Stossel, T. P. (2006). FilGAP, a Rho- and ROCK-regulated GAP for Rac binds filamin A to control actin remodelling. *Nat. Cell Biol.* *8*, 803–814.
279. Guerrier, S., Coutinho-Budd, J., Sassa, T., Gresset, A., Jordan, N. V., Chen, K., Jin, W.-L., Frost, A., and Polleux, F. (2009). The F-BAR domain of srGAP2 induces membrane protrusions required for neuronal migration and morphogenesis. *Cell* *138*, 990–1004.
280. Soderling, S. H., Binns, K. L., Wayman, G. A., Davee, S. M., Ong, S. H., Pawson, T., and Scott, J. D. (2002). The WRP component of the WAVE-1 complex attenuates Rac-mediated signalling. *Nat. Cell Biol.* *4*, 970–975.
281. Peter, B. J., Kent, H. M., Mills, I. G., Vallis, Y., Butler, P. J. G., Evans, P. R., and McMahon, H. T. (2004). BAR domains as sensors of membrane curvature: the amphiphysin BAR structure. *Science* *303*, 495–499.
282. Fricke, R., Gohl, C., and Bogdan, S. (2010). The F-BAR protein family Actin' on the membrane. *Commun. Integr. Biol.* *3*, 89–94.

283. Ypsilanti, A. R., Zagar, Y., and Chédotal, A. (2010). Moving away from the midline: new developments for Slit and Robo. *Development* 137, 1939–1952.
284. Wang, Y., Du, D., Fang, L., Yang, G., Zhang, C., Zeng, R., Ullrich, A., Lottspeich, F., and Chen, Z. (2006). Tyrosine phosphorylated Par3 regulates epithelial tight junction assembly promoted by EGFR signaling. *EMBO J.* 25, 5058–5070.
285. Siller, K. H., Cabernard, C., and Doe, C. Q. (2006). The NuMA-related Mud protein binds Pins and regulates spindle orientation in *Drosophila* neuroblasts. *Nat. Cell Biol.* 8, 594–600.
286. Walsh, T., Shahin, H., Elkan-Miller, T., Lee, M. K., Thornton, A. M., Roeb, W., Abu Rayyan, A., Loulus, S., Avraham, K. B., King, M.-C., et al. (2010). Whole exome sequencing and homozygosity mapping identify mutation in the cell polarity protein GPSM2 as the cause of nonsyndromic hearing loss DFNB82. *Am. J. Hum. Genet.* 87, 90–4.
287. Zhan, S. H., Fejes, A. P., Coghlan, G., Triggs-Raine, B., Tekin, M., Kanaan, M., Doherty, D., Phelps, I. G., Mhanni, A. A., Chudley, A. E., et al. (2012). GPSM2 Mutations Cause the Brain Malformations and Hearing Loss in Chudley-McCullough Syndrome. *Am. J. Hum. Genet.* 90, 1088–1093.
288. Ren, G., Helwani, F. M., Verma, S., McLachlan, R. W., Weed, S. A., and Yap, A. S. (2009). Cortactin is a functional target of E-cadherin-activated Src family kinases in MCF7 epithelial monolayers. *J. Biol. Chem.* 284, 18913–22.
289. Na, H.-W., Shin, W.-S., Ludwig, A., and Lee, S.-T. (2012). The cytosolic domain of PTK7, generated from sequential cleavage by ADAM17 and  $\gamma$ -secretase, enhances cell proliferation and migration in colon cancer cells. *J. Biol. Chem.* 287, M112.348904–.
290. Ma, Y. C., Huang, J., Ali, S., Lowry, W., and Huang, X. Y. (2000). Src tyrosine kinase is a novel direct effector of G proteins. *Cell* 102, 635–646.
291. Luttrell, D. K., and Luttrell, L. M. (2004). Not so strange bedfellows: G-protein-coupled receptors and Src family kinases. *Oncogene* 23, 7969–7978.
292. Nichols, A. S., Floyd, D. H., Bruinsma, S. P., Narzinski, K., and Baranski, T. J. (2013). Frizzled receptors signal through G proteins. *Cell. Signal.* 25, 1468–75.

293. Skarnes, W. C., Rosen, B., West, A. P., Koutsourakis, M., Bushell, W., Iyer, V., Mujica, A. O., Thomas, M., Harrow, J., Cox, T., et al. (2011). A conditional knockout resource for the genome-wide study of mouse gene function. *Nature* *474*, 337–342.
294. Friedel, R. H., Plump, A., Lu, X., Spilker, K., Jolicoeur, C., Wong, K., Venkatesh, T. R., Yaron, A., Hynes, M., Chen, B., et al. (2005). Gene targeting using a promoterless gene trap vector (“targeted trapping”) is an efficient method to mutate a large fraction of genes. *Proc. Natl. Acad. Sci. U. S. A.* *102*, 13188–13193.